Postural Stability of Humans

by

Joel Martin

A Thesis submitted to
the Faculty of Graduate Studies and Research
in partial fulfilment of
the requirements for the degree of
Master of Applied Science

Ottawa-Carleton Institute for
Mechanical and Aerospace Engineering

Department of Mechanical and Aerospace Engineering
Carleton University
Ottawa, Ontario, Canada
December 1, 2009

Your file Votre référence
ISBN: 978-0-494-63462-2
Our file Notre référence
ISBN: 978-0-494-63462-2

The undersigned recommend to

the Faculty of Graduate Studies and Research

acceptance of the Thesis

Postural Stability of Humans

Submitted by **Joel Martin**

in partial fulfilment of the requirements for the degree of

Master of Applied Science

M. Ahmadi, Supervisor

A. Chan, Supervisor

R. Langlois, Supervisor

M. Yaras, Department Chair

Carleton University

2010

Abstract

This thesis investigates the interrelationships between various parameters involved in shipboard postural stability, such as muscle force, centre of pressure, and centre of mass. A series of tasks, including quiet standing on a steady deck, sagittal manual materials handling consisting of lifting and lowering a rigid load, ascending and descending stationary ship stairs, and balancing on a motion platform simulating unsteady deck motion representative of quiescent periods aboard a frigate operating in high sea state were performed by six fit subjects. Each subject was instrumented such that synchronized time-varying foot pressure distributions, postural configuration as sensed optically using 34 passive retro-reflective markers and eight infra-red cameras, and EMG signals of twelve muscle groups potentially relevant to postural stability were collected. Post-processing techniques were implemented and refined to extract relevant data as well as to compute derived data including centre of mass position and muscle activation. A comprehensive correlation analysis was performed illuminating the relationships that exist between individual muscle activation signals, centre of pressure movement, and centre of mass movement.

The results support many previous observations in shipboard postural stability literature and provide additional insight that directly supports understanding of postural stability and the development of biodynamic postural stability models. The results show the importance of taking a systems engineering approach to the study of postural stability, rather than the approach that has typically been taken; which has been to study one or two parameters in isolation. The results also show that centre of pressure is maintained within only a small fraction of the base of support during the tasks performed. This may imply that motion induced interruptions will occur prior to centre of pressure reaching the actual physical

boundary of the base of support as well. This would support recent findings by Langlois *et al.* [1] where motion induced interruptions were observed in cases where traditional models did not predict them. The results also strongly suggest the need for articulated postural stability models with variable stiffness, actuated joints in order to model complex tasks and accommodate the substantial changes to centre of mass and mass moment of inertia that are possible in the human body.

Acknowledgments

This thesis would not have been possible without the assistance and efforts of many people. I would like to thank Prof. Chris Joslin for allowing the use of the Vicon motion capture system. I would like to thank Mr. Jason Grammenos for his technical expertise in helping to use the Vicon system during data capture sessions. I would like to thank Scott MacKinnon and Carolyn Duncan, of Memorial University, for the loan of their F-Scan Mobile system. I would also like to thank my thesis supervisors, Profs. Mojtaba Amahdi, Adrian Chan, and Rob Langlois; whose various areas of expertise and wealth of knowledge allowed the success of an extremely broad and ambitious thesis project, and who have had the patience to deal with many unusual circumstances encountered along the way. I would especially like to thank my many friends and family for "listening" on the many occasions I found myself in need of a sympathetic ear.

Table of Contents

List of Tables

List of Figures

Nomenclature

Units

This thesis uses S.I. units.

Abbreviation	Description
BoS	Base of Support
CMP	Centroidal Moment Pivot
CoG	Centre of Gravity
CoM	Centre of Mass
CoP	Centre of Pressure
CSV	Comma Separated Value
DoF	Degrees of Freedom
ECG	Electrocardiogram
EHP	Extreme High-pass Filtering
EMG	Electromyogram
ES	Equilibrium Score
FRI	Foot Rotation Indicator
FSB	Functional Stability Boundary
GCoM	Ground projection of Centre of Mass
GRF	Ground Reaction Force
IEMG	Integrated Electromyogram
IPSB	Index of Proximity to Stability Boundary
MFRI	Modified Foot Rotation Indicator
MII	Motion Induced Interruption
MUAP	Muscle Unit Activation Potential
NaN	Not a Number
PSI	Postural Stability Index
RMS	Root Mean Square
SAR	Stability Area Ratio
sEMG	Surface Electromyogram
SOT	Sensory Organization Test
WRTI	Weighted Residence Time Index
ZMP	Zero Moment Point
ZRAM	Zero Rate of change of Angular Momentum

Table 0.1: Abbreviations

Chapter 1

Introduction

1.1 Motivation

An elderly gentleman is recovering from a series of small strokes. He has battled diabetes for most of his adult life, he has battled cancer and won, he has fought in a World War and returned home. Although he needs to be in long term care for rehabilitation and for oversight of the treatment of his diabetes, the man is ambulatory and helps with odd-jobs in the care facility. He speaks with pride to his son and his grandson about the work that he does while recovering; it gives him a sense of fulfillment despite the impact of the strokes. Months later, the man falls and breaks his hip. He is unable to leave his bed unassisted and his health, his zeal for rehabilitation, and his zest for life deteriorate. Within a year my grandfather died.

Between 35% and 40% of all generally healthy individuals, living outside of care facilities, aged 65 or older suffer falls each year. This statistic increases further in the over 75 population and increases by a factor of three when considering individuals who reside in long term care facilities. Of those residing in long term care, the severity of injuries associated with falls also increases, with 10% to 25% of falls resulting in the need for hospital care. Care for fall-related injuries represents six percent of total medical expenditures on the over 65 population in the United States. Injuries are the fifth leading cause of death in the elderly, and two thirds of those injuries resulting in death are fall related injuries. In fact, 75% of the deaths associted with injuries incurred in falling are suffered by the 13%

of the population that is aged 65 or older [6, 7].

A young man, a son, patrols a small and dusty village along with his friends and comrades. As they follow their patrol route a cyclist passes them by and they pay him little heed. For most of the small group, their lives end in a blinding flash of fire and shrapnel as the cyclist sets off the bomb strapped to him. For my friend's son, his life begins anew in many aspects. He finds himself in an allied hospital, both of his legs lost to the blast. Now he must begin the fight to relearn how to walk, aided by simple prosthetics that do little to mimic the natural gait that he has always taken for granted on his patrols. Stairs will prove especially challenging, as will uneven or loose terrain.

One study, performed in Hong Kong, showed that 15% of lower limb amputees die within thirty days of the amputation and that only 55% of amputees survive beyond 4 years after amputation. While 44% of amputees were able to return home, only 11% of those could walk unassisted and only half of those given prostheses were able to regain independant locomotion [8].

These are just two of many situations that expose the fact that we take too much for granted in our ability to maintain our balance, the second nature of bipedal locomotion, and the freedom of ambulation. For the sake of those who lose these abilities and freedoms it is vital to increase our understanding of postural stability of humans.

"Postural stability is classically based upon the centre of mass (CoM) position and its displacements within the base of support (BoS)" [9]. The CoM normally exhibits continuous shifting over the base of support. Postural stability, therefore, is the ability to maintain this shifting within the limits of stability [10]. Understanding postural stability, and the strategies employed by humans to maintain it, is important to a wide array of industries and health-related fields. Applications for postural stability research include biped robotics [3, 2, 11], active prosthetics [12], neurological implants [13], rehabilitation therapy [10], falling tendencies in the elderly [14, 15, 9, 16, 17, 18], and motion induced interruptions (MII) [4, 19, 20, 21, 22, 23].

In the field of rehabilitation therapy, the focus is placed upon understanding the different strategies that can be employed to maintain postural stability. Three main strategies

have been identified as the ankle strategy, the hip strategy, and the stepping strategy [10]. Each successive strategy tends to be employed for further increased perturbations from the stability limits. However, the selection of a strategy has also been shown to be dependent upon the sensory inputs and posture at the time of the disruption. The ankle strategy tends to be used for small perturbations and simply shifts the CoM through ankle joint rotation. The hip strategy is used when either ankle motion is limited or ineffective, or when the perturbation is too large to be countered by the ankle strategy. This strategy can produce much faster changes in CoM position, making it a better option for countering perturbations that move CoM either rapidly or very close to stability limits. If the perturbation is large enough to move the CoM beyond the limits of stability, then the step strategy is employed [10].

In the fields of biped robotics and, by extension, active prosthetics, postural stability becomes important in determining control strategies and algorithms. Strategies for biped postural control tend to utilize ground reference points such as Centre of Pressure (CoP), Ground projection of the Centre of Mass (GCoM) [2], Zero Moment Point (ZMP) [2], and Zero Rate of change of Angular Momentum (ZRAM) point [3] as stability criteria. In general, these ground reference points are physical points on the ground plane where reaction forces act (or, in some cases, theoretical points for reaction forces to act). The details of what forces and moments are considered in the calculation of the various ground reference points result in the differences in definition of the different points and in robustness and general applicability of the points to various tasks. Regardless of which ground reference point is used, the goal is for the control system to use these stability criteria and plan paths that ensure postural stability is maintained. In the case of active prosthetics, there is the added complexity of having to match the natural gait and control system of the human leg (at least in the case of single amputees) [12].

In the case of neurological implants, the actual nervous and motor signals become important. The intent is to bridge the human system with technology and enable the two to work in conjunction to produce natural movements and maintain postural stability. The

Victhom (Quebec City, Canada) NeuroStep is an excellent example of the type of technologies becoming available due to research into the biological control systems involved in postural stability [13]. This device, which recently entered clinical trials in Canada, is fully implantable and is designed to help combat a condition known as foot drop. Foot drop is a condition that presents with an inability to lift the toes during swing phase, just before heel strike. The NeuroStep connects to the peroneal and tibial nerves and can integrate with the body's sensing and stimulation nervous networks through these connections. The controller, powered by a pacemaker battery, is implanted in the upper thigh. Once the patient has recovered from the surgery to implant the device, their natural gait is analyzed and the device programmed via a wireless connection to customize the control unit to the patient's gait. The device then acts as a control interface to bridge damaged nervous and motor connections that have resulted from injury or disease and present as foot drop [13].

Postural stability is of particular concern in the elderly. There is a definite decrease in postural stability associated with aging [14, 9, 16, 17, 18]. This increase has been attributed to a decline in vibratory sensation, a decline in the number of vestibular hair cells, and a loss of visual acuity [14]. As well, there is evidence of reductions in nerve conduction velocity, number of motor units, and muscle mass associated with aging [14]. An understanding of the factors that increase the risk of falling in the elderly is vital to reducing the incidence of falls and designing care facilities that minimize these risks.

The concept of MII, first introduced by Baitis and Applebee [21], is important to shipboard industries such as the fishing [4] and shipping industries, as well as to the Navy [19]. An MII is an incident where the accelerations due to external perturbations (ship motion in this case) become sufficient to cause a person to slide or lose balance unless they temporarily abandon their allotted task to make a postural adjustment in order to remain upright [19]. Previous research has found a strong correlation between wave motion and MII frequency, as well as CoP and thoraco-lumbar kinematics of both uninterrupted tasks and tasks that experience MII [4].

To date, the majority of studies of postural stability have either concentrated on static tasks or have investigated the contributions of isolated parts of the postural control system

of humans such as motion of CoP, motion of CoM, muscle forces, or the effects of loss of one or more sensory inputs. From a systems engineering standpoint, it is important to evaluate the interactions and interrelations of all of these aspects of postural stability in order to understand the function of the system as a whole; for, as Aristotle stated, "the whole is more than the sum of its parts." The current work, therefore, was devised to begin to investigate some of these potential interactions and interrelations and to identify which show indications of being most important to postural stability and how best to further explore postural stability from a systems engineering standpoint.

1.2 Research Objectives

The objective of this research is to experimentally record subject body kinematics, ground interface forces, and muscle excitation during simple postural stability tasks and use these data to gain insight into appropriate postural stability modeling and quantitative stability parameters. In particular:

1. What are potential quantitative indices for evaluating aptitude for postural stability?
2. How do CoM and CoP move relative to one another in human postural stability?
3. What is the kinematic threshold within which CoP is maintained during the performance of typical ship-board postural stability tasks; and what might this imply regarding the kinematic threshold of MIIs?
4. What muscles are most active in human postural stability control?
5. What tools and research equipment are required to support this work and to develop a postural stability lab for use in future studies that require the concurrent measurement of electromyogram (EMG), CoP and CoM.

1.3 Development Contributions

1. Algorithms for the calculation of CoM from motion capture data collected using either the Vicon or NaturalPoint OptiTrack systems and anthropometric data and corresponding Matlab routines.

2. Postural stability research capability in the Applied Dynamics Lab at Carleton University.

1.4 Research Contributions

1. Showed that the index of postural stability (the standard deviation of CoP) introduced by [20] can be extended to some degree to roughly estimate relative performance of complex postural tasks.

2. Through the use of cross-correlation analysis of 18 postural stability parameters, showed the importance of a systems engineering approach to improving the understanding and modelling of postural stability. Specifically it was shown that the relationships between CoM, CoP, and estimated muscle force of 12 different muscles are highly dependent on the individual as well as the task being performed. This is contrary to the typical approach that considers CoM to be dependent on CoP.

3. Definition of kinematic thresholds of CoP during the performance of typical shipboard postural stability tasks. Traditional models have assumed MII to occur when CoP approaches the edge of the BoS. The current research shows strong indications that CoP is maintained within a much smaller fraction of the total area under the BoS. This implies that MII may occur when CoP is still well within the BoS, with as little as 28% of the area under the BoS being used.

4. Showed the profound effect of joint articulation on various postural stability parameters and the relationships between them during the performance of complex tasks. This strongly supports the need to develop articulated postural stability models.

5. Showed that two common postural stability strategies are joint stiffening and direct control of CoM through joint articulation. This indicates that it is important to include variable stiffness, actuated joints in any articulated postural stability model that is to be developed.

1.5 Outline

This section outlines the contents and organization of subsequent chapters in this thesis.

Chapter 2: Review of Literature A review of literature focusing on the field of postural stability. Specific focus on general postural stability, postural stability of the elderly, measures of balance aptitude, EMG processing techniques, and biped robotics control.

Chapter 3: Methodology The task procedures and equipment used for data collection are introduced. Data analysis techniques are described.

Chapter 4: Results and Discussion Results of the current study are reported and discussion of those results are provided.

Chapter 5: Conclusions and Recommendations The research conclusions are given and recommendations for future work are offered.

Chapter 2

Literature Review

2.1 Postural Stability

2.1.1 General Postural Stability

From a systems engineering viewpoint, postural stability encompasses a complex system comprised of sensory, motor, and processing subsystems as seen in Figure 2.1 [10]. The sensory subsystem provides inputs to the nervous system which acts as the processing subsystem (both the central and peripheral nervous systems are involved as is the cerebellum). The processing subsystem must evaluate the information from the sensory subsystem and select an appropriate motor response that is then passed as an input to the motor subsystem for execution.

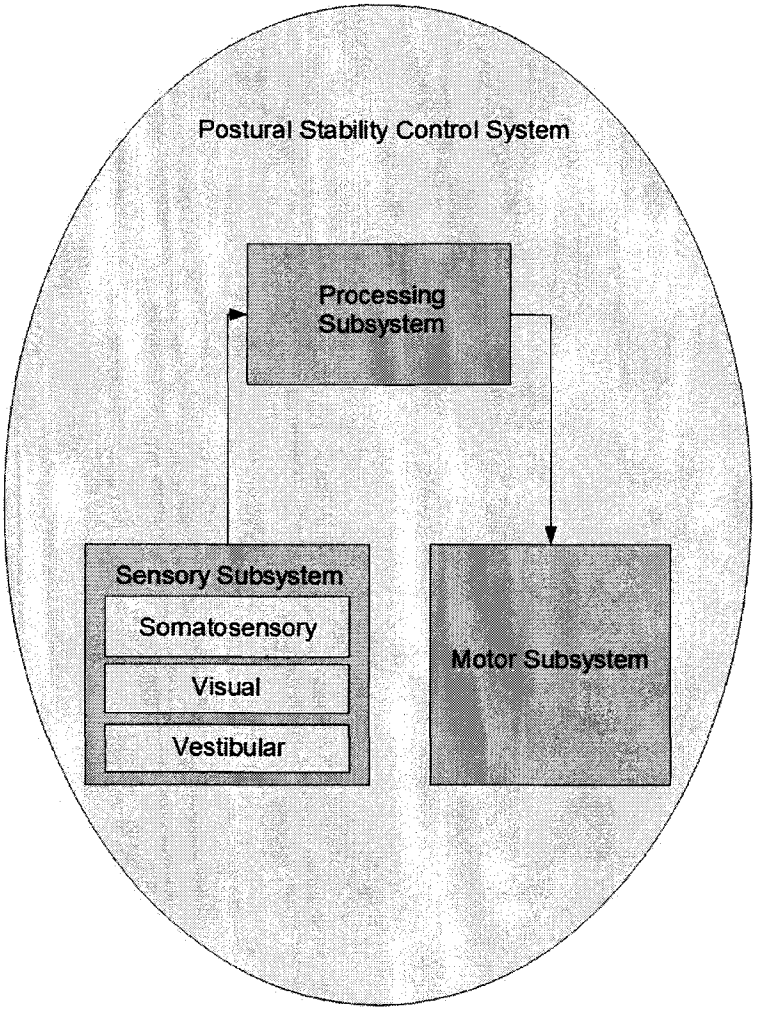

Figure 2.1: Block diagram of postural stability control system.

The sensory subsystem has three major components: visual, vestibular, and somatosensory. These components provide a feedback control loop and act in conjunction to improve postural stability. While all three are situation dependent and individual components may dominate in given situations, no single component singlehandedly controls the CoM at a given time. Of these components, the visual and somatosensory systems provide information from the external environment while the vestibular system provides information on the body's global orientation. The somatosensory system tracks the relative position of individual body segments. This is known as proprioception; though, in the case of dynamic movements, it is more accurately referred to as kinesthesia. The visual system tracks the position of the body relative to objects in its environment as well as movement of those objects relative to the environment. In this way, the visual system may help feed the equivalent of estimators and/or integrators in the processing subsystem that can be used to predict future positional information. The vestibular system tracks head orientation and acceleration. [10]

The processing subsystem integrates the information from the sensory subsystem and its various components. This processing is done in the cerebellum, basal ganglia, and supplementary motor area of the brain. Processing time can be critical, and the different components of the sensory subsystem can be processed at varying speeds; the somatosensory system being the fastest, followed by the visual, and vestibular systems [10].

The motor subsystem must act to produce the response selected by the processing subsystem. The actual response may vary depending upon the movement itself and it is this subsystem that tends to be exploited in treatment and therapy. Although there can be many potential responses to any given change in postural stability, there are three autonomous responses that are common. These responses take advantage of reflex arcs in the nervous system, such that coordinated muscle control does not need to be planned by the processing subsystem. Rather, the processing subsystem selects from the options of autonomous responses and activates the desired reflex arc and intensity of the response in the motor subsystem [10].

While many different perturbations can affect postural stability, the effect of oscillatory motion is of vital importance to maritime industries such as fishing, shipping, and the Navy. As such, a great deal of research has been focused upon the prediction of MII [1, 24, 4, 19, 21, 22, 20]. An investigation into the effects of frequency, magnitude, and direction of oscillation on postural stability in standing was conducted by Nawayseh and Griffin [20]. This study used electro-hydraulic vibrators attached to a rigid plate to produce translational and rotational oscillations. The frequency, velocity, and accelerations associated with these motions were varied across a range of values for both types of motion. This setup was in contrast to previous studies [18, 22, 25, 26, 27, 28] that had used either a pull force, visual cue, or transient fore-and-aft motions to unbalance participants. Unfortunately, only subjective means were used to determine stability; the participants were asked whether they felt they had lost balance and what, if subjected to the same motion again, the probability of losing their balance again was. The study found that increased amplitude of horizontal oscillations increased instability, the worst case being at a frequency of oscillation of 0.5 Hz. In the case of fore-and-aft oscillations, instability was increased even further than in lateral oscillations. However, changes in CoP were similar in both lateral and fore-and-aft oscillations. Instability increased with increases in frequency of oscillation in the cases of both roll and pitch. One final point of significance was the discovery that translational oscillation had the greatest negative effect at low frequencies while rotational oscillation had the greatest negative effect at high frequencies. Nawayseh and Griffin [20] also mention previous work that attempted to use CoP as a parameter for predicting CoM [29, 30]. However, as these studies dealt only with passive models they are inadequate for dynamic motions where active control (internal muscle forces, etc.) must be accounted for.

In a study by Crossland, a series of tipping coefficients (Equation (2.1)) proposed by Graham *et al.* [23] were calculated to help predict MII during various tasks with various

orientations relative to the ship [19].

$$\left(\frac{1}{3}h\ddot{\eta}_4 - \ddot{D}_2 - g\eta_4\right) - \frac{l}{h}\ddot{D}_3 > \frac{l}{h}g \; OR \; \left(-\frac{1}{3}h\ddot{\eta}_4 + \ddot{D}_2 + g\eta_4\right) - \frac{l}{h}\ddot{D}_3 > \frac{l}{h}g \tag{2.1}$$

where $\ddot{D}_3$ is the vertical acceleration, $\ddot{D}_2$ is the lateral acceleration, η_4 is the instantaneous roll angle, $\ddot{\eta}_4$ is the instantaneous roll acceleration, h is the height of the CoM, and l is half of the length of the BoS. The value $\frac{l}{h}$ is defined as the theoretical tipping coefficient. If the inequality is true, an MII is predicted. This research found that the proposed model was capable of predicting the frequency of MII in all task types and two different ship types. The model, as well as the experimental data, also showed that MII were much more likely to occur when facing laterally than while facing longitudinally.

Finally, a recent study by Duncan [4] investigates the effect of sea conditions on the motion of CoP and thoraco-lumbar kinematics during execution of typical shipboard tasks. While most such studies use simulated motion for repeatability of test conditions, the simulated motions can not typically reproduce the same range of motion as would be experienced at sea. In particular, the translational components of the motion are not reproduceable. Duncan's study was performed during a series of sea trials on the Quest research vessel in order to explore the full range of motions. This study found that the frequency of MII was highly dependent upon the type and degree of wave motion. Facing starboard during significant wave heights of five meters (Sea State 5) produced the highest frequency of MII of all of the conditions investigated; further validating the conclusions from Crossland. This increase was attributed to the larger amplitude of perturbation in the roll axis. As stated by Duncan, this is due to the relatively small BoS in the anterior-posterior direction under these conditions requiring a change-in-support strategy. In addition, this study found that CoP velocities and thoraco-lumbar velocities were greatly increased even in uninterrupted tasks under these conditions. These velocities were yet further increased when MII occurred. Additional analysis was performed on the data from [4], and an articulated postural stability model was proposed and evaluated against both the empirical data from the Quest sea trial and against the non-articulated model described in Equation (2.1) [1]. This additional

study found that the non-articulated model tends to under predict MII frequency, but has a higher correlation coefficient than the articulated model. Even more importantly, it was found that observed MIIs could occur when no physical instability was imminent. This introduces the possibility that non-physical parameters, perceived motion or imbalance, can affect MII frequency.

2.1.2 Postural Stability of the Elderly

Degradation of performance of any of the subsystems involved in postural stability control can reduce the ability to maintain stability. Damaged proprioceptors can impair balance and injury or pathology of the muscles and joints involved in postural stability can result in increased postural sway as well as a loss of balance. In particular, degenerative diseases affecting the knee have been shown to have a negative impact on postural stability [10, 14]. In particular, previous research has shown that postural stability is negatively impacted by age-related deterioration of the sensory subsystems, slowing of nerve conduction velocities, reduction in the number of motor units, reduction in overall muscle mass [14]. In addition, the processing subsystem is negatively affected by aging [14].

Studies have shown that the maintenance of postural stability requires a certain amount of cognitive attention [14]. These studies have shown a significant decrease in postural stability when performing a primary static postural task while also performing a secondary cognitive task. While most such studies have focused on the external indicators of postural stability, a study by Rankin *et al.* [14] explored "the effects of secondary cognitive tasks on the neuromuscular response characteristics underlying reactive balance control in young versus older adults". This study had subjects perform a primary standing balance task on a perturbing platform both in isolation and while performing a secondary cognitive math task. The platform was hydraulically actuated and had a 15 cm range of motion fore-and-aft at velocities from 20-60 cm/s. The study investigated the surface EMG (sEMG) signals of the gastrocnemius, tibialis anterior, biceps femoris, rectus femoris, erector spinae, and rectus abdominis. For the purposes of this study, EMG onset was defined to be the point at which signal amplitude rose to be greater than three standard deviations above the baseline

signal. The sEMG was then integrated over a window from 36-500 ms following EMG onset and binned in order to separate monosynaptic and supraspinal responses. It was found that both young and old adults experienced a decrease in amplitude of the EMG signals when the cognitive task was being performed. This decrease was observed to be significantly greater in the elderly.

In the majority of postural stability research, motion of the CoM and CoP has been analyzed in the time and frequency domains. However, due to significant nonlinear properties of muscle and tissue, and to the nonlinear nature of the feedback control system of the nervous system, these may not be the most suitable domains to use [9]. One study evaluated the potential of using fractal analysis upon the CoM and CoP of a group of elderly subjects [9]. This study found a significant difference in fractal dimension[1] between antero-posterior and mediolateral directions in both eyes open and eyes closed experiments. It was also found that CoM fractal dimension was smaller than that of CoP in both directions. Fractal dimension was also found to increase in the eyes closed experiment compared to the eyes open experiment.

2.2 Balance Aptitude

In 1975 a study was conducted to determine "sensitive means to measure postural steadiness and stability" [32]. This study published standards for CoP during standing and sustained weight shifting of normal men, partitioned into three age groups. The study found that two characteristics were common for upright posture. First, there is a large area over which an individual's weight can be shifted while maintaining postural stability; and second, that CoP will fluctuate continuously about a mean value. It is important to note that this study also found that the younger groups showed much greater stability than the oldest group.

One classical measure of postural stability is the NeuroCom International Sensory Organization Test (SOT). This test evaluates the coordination of the visual, proprioceptive, and vestibular systems with respect to postural stability by the use of dynamic posturography.

[1] "The fractal dimension is introduced as the index for describing the irregularity of a time series" [31]

The outcome of the SOT is a measure called the equilibrium score (ES) [33]. The ES is calculated as

$$ES = 12.5 - [\theta_{max}(ant) - \theta_{max}(post)]/12.5 \tag{2.2}$$

where $\theta_{max}(ant)$ is the maximum sway angle in the anterior direction and $theta_{max}(post)$ is the maximum sway angle in the posterior direction, both measured in degrees. ES, therefore, is dependent upon the maximum sway angles in both the anterior and posterior directions. An additional measure of postural stability that has been proposed is the Postural Stability Index (PSI) [33]. This index accounts for shear force and anthropometric measures and is calculated as

$$PSI = \Sigma|Mgh\theta|/\Sigma|\tau| \tag{2.3}$$

where M is the mass of the subject, g is the acceleration due to gravity, h is based upon anthropometric data of the average height of the CoM above the ground plane (0.55 times the subject's height), τ is the stabilizing torque at the ankle, and θ is the sway angle.

The spread and length of a stabilogram, the trace of the CoP motion, has been used to describe and quantify postural stability [34, 35]. Three additional indices for quantifying postural stability are presented by Bagchee *et al.* [15]. This study introduces the concept of a Functional Stability Boundary (FSB). This is a slight departure from the BoS, in that the FSB is a smaller subset of the contact area (area under the foot) defined as the region within the BoS in which "a person can balance while performing a task without the possibility of loss of balance" [15]. In the study, the stability boundary was constructed using the maximum CoP displacements that occurred without falling. The proposed indices were evaluated across four tasks, including quiet standing, reaching, bending, and sudden loading. These three indices were the Index of Proximity to Stability Boundary (IPSB)

$$IPSB = p/\lambda \tag{2.4}$$

where p is the minimum distance between the stabilogram and the FSB and λ is the normalizing length; Stability Area Ratio (SAR)

$$SAR = A_t/A_{sb} \tag{2.5}$$

where A_t is the area of the envelope around the stabilogram and A_{sb} is the area of the FSB, and Proximity Zones and Weighted Residence Time Index (WRTI)

$$WRTI = \kappa(\alpha_3 e^3 + \alpha_4 e^4 + \alpha_5 e^5) \tag{2.6}$$

where κ is a scaling constant ($\kappa = e^{-4}$) used to scale the WRTI to be within a convenient range; α_3, α_4, and α_5 are non-dimensional fractions of time spent in each of the corresponding proximity zones of the FSB - where zones one and two are the zones that the CoP would normally reside in during stability. Nawayseh and Griffin [20] also proposed a simple index for evaluating postural stability. They proposed using the standard deviation of the displacement of CoP as a measure of postural sway.

2.3 EMG Processing

Depending upon the derived parameters that are desired, there are a number of common types of processing that can be performed on raw EMG signals. These include full wave rectification, linear envelope detection, integration of the full wave rectified signal over the entire period of muscle contraction, and various methods of integrating the full wave rectified signal [36]. Examples of these processed signals are shown in Figure 2.2. Typically, the raw EMG signal is first high-pass and then low-pass filtered (also known as band-pass filtering) to eliminate low frequency motion artifacts and high frequency noise prior to further processing. Typically, it is accepted that EMG frequency content will range between 20-500 Hz. Full wave rectification simply calculates the absolute value of the EMG. This derived signal is mainly used as an input to further processing techniques [36]. Linear envelope is the result of a low-pass filter being applied to the full wave rectified signal. The linear envelope approximates the second order response of the muscle impulses and

produces a phase lag in the resulting signal that accounts for electromechanical delay in the system [37]. While the linear envelope is often referred to as the integrated EMG (IEMG), this terminology is confusing as the processing does not perform a mathematical integration of the signal [36].

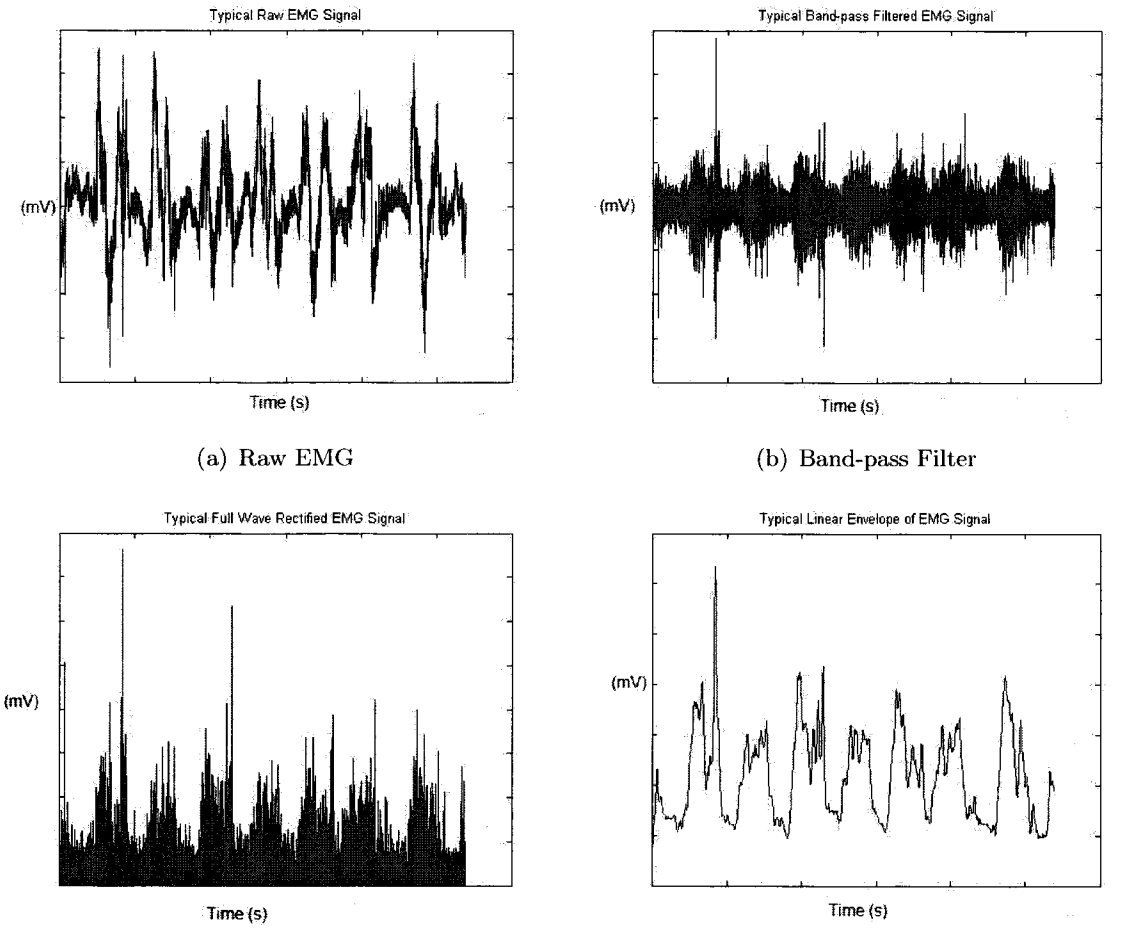

(a) Raw EMG

(b) Band-pass Filter

(c) Full Wave Rectified

(d) Linear Envelope

Figure 2.2: Signals resulting from common EMG processing techniques.

Until recently, it has been generally accepted that sEMG signals should be high pass filtered with cutoffs of 20 to 30 Hz in order to remove motion artifacts prior to being further processed to estimate muscle force. It was assumed that the entirety of the frequency content in the sEMG signals from this frequency up to 500 Hz or so held valid information on muscle force. However, recent studies have shown strong evidence to the contrary. One

well known phenomenon that contradicts this viewpoint is the fact that fatigued muscles will display a larger amplitude EMG signal without a corresponding increase in force output [36]. The physiology behind this phenomenon is explained by [36] as being a combination of several changes that occur in fatigued muscles. The conduction velocity of the muscle unit activation potentials (MUAPs) is reduced, larger and faster motor units with shorter MUAPs begin to drop out of recruitment, motor units begin to fire synchronously, and an 8-10 Hz tremor can be seen in the EMG. Of these, the synchronous firing of motor units is likely the single largest cause of observed increases in EMG amplitude in fatigued muscles [36]. As well, fatigued muscles show a significant shift in signal power towards the lower spectrum [37]. This would indicate that the lower frequency signals in the sEMG must not be associated with force. Potvin and Brown [37] go so far as to suggest that removing as much as 99% of sEMG signal power may substantially increase the accuracy (reduction of RMS error of 14%) of muscle force estimates. In their study, Potvin and Brown evaluated both first and sixth order Butterworth filters (two commonly used filters/orders in the EMG literature) and evaluated the RMS error of muscle force estimates using a variety of high-pass cutoff frequencies while recording EMG of the biceps brachii at 1024 Hz. It was found that for a first order filter, the optimum high-pass cutoff frequency was 410 Hz and for a sixth order filter it was 140 Hz. An important corollory of this discovery is that it may be important to record sEMG at sample rates in excess of 1000 Hz when using sEMG to predict muscle force.

Potvin and Brown's technique for muscle force estimation has come to be known as Extreme High Pass (EHP) Filtering. While the initial study [37] was specific to the biceps brachii and did not attempt to claim suitability in a generalized case, further work by several authors has validated this as an improved method for muscle force estimation [37, 38, 39]. In fact, an additional benefit has been discovered in that the EHP filtering also serves to remove electrocardiogram (ECG) noise from the EMG signals of muscles in the torso [39].

2.4 Biped Robotics Control

A focal point of biped robotics control has been the establishment of a general stability criterion. Such a criterion should be "simple, yet powerful enough to capture the essence of rotational stability" [3] and should also be based on the physical system. Given such a criterion, it is possible for a controller to continuously update the calculation of the criterion based on updated states and take action to keep it within established limits. Many concepts for such a criterion have been proposed but each has been limited in usefulness to very specific tasks/terrain and has suffered from certain shortcomings. The first such concept was the Zero Moment Point (ZMP), introduced by Elftman [40] in 1938. In 1999 Goswami proposed the Foot-Rotation Indicator (FRI) [2]. Most recently, the ZRAM point [3] (also known as Centroidal Moment Pivot (CMP) [11]) has been proposed as a ground reference point that is applicable in the general case. The CMP extends the applicability of these criteria to more complex movements than previously possible.

The ZMP has been shown by Goswami [3] to be equivalent to the CoP. While this point does still give some useful information regarding the postural stability of a subject, it has limited usefulness for biped robotics control as it is only defined in the convex hull of the contact surface (foot). As such, the first of the proposed ground reference points to be discussed will be the FRI. The FRI is defined as "the point on the foot/ground contact surface, within or outside the convex hull of the foot-support area, at which the resultant moment of the force/torque impressed on the foot is normal to the surface" [2] (note that the terminology "impressed force/torque" implies that ground reaction forces (GRF) are ignored). Mathematically, FRI is defined using (2.7) and Figure 2.3 shows a schematic representation of the system and FRI.

$$\left(\tau_1 + \vec{FO_1} \times \vec{R_1} - \vec{FG_1} \times m_1\vec{g}\right)_t = 0 \tag{2.7}$$

where R_1 and τ_1 are the ankle force and torque imparted by the rest of the body when the stance foot is considered in isolation, O_1 is the origin of the local coordinate system of the foot, G_1 is the centre of gravity (CoG) of the foot, m_1 is the mass of the foot and g is

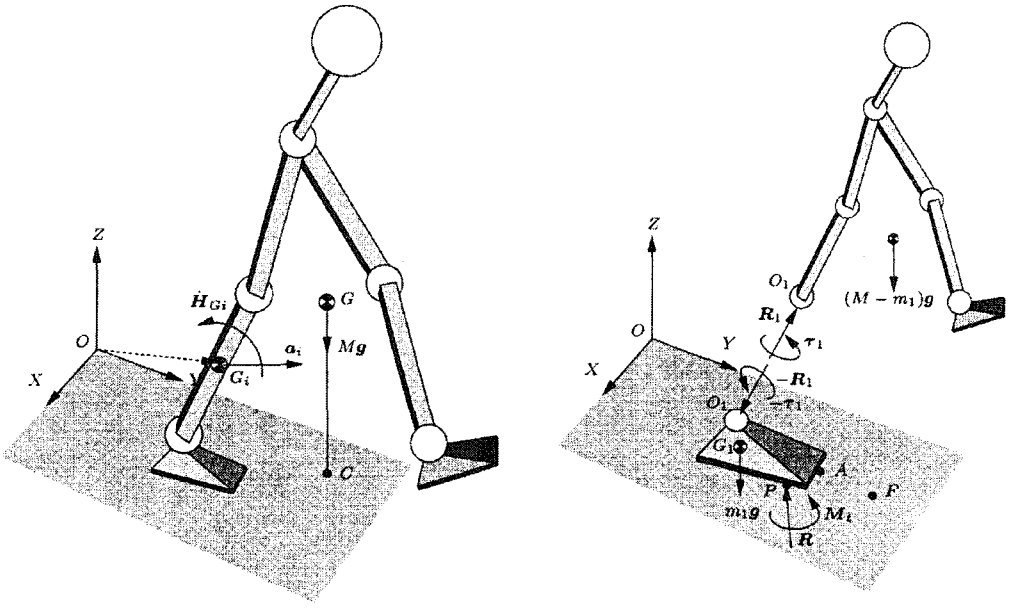

Figure 2.3: Schematic of FRI [2].

the acceleration due to gravity. F is the FRI point and is not constrained to be within the BoS. In fact, the distance of F from the BoS boundary is a measure of the instability of the system [2]. To ensure no foot rotation the controller must maintain FRI within the BoS. In the case of a stationary task, FRI reduces to the ground projection of the CoM (GCoM) [2].

ZRAM proposes an extremely simple and robust criterion for stability that is based solely upon the physical properties and dynamics of the system. Simply stated, ZRAM is based upon the concept that if the rate of change of the angular momentum, $\dot{\vec{H}}_G$, of the system about its CoM is zero, the system is stable. Therefore, to be stable, the GRF must act through the CoM. If the GRF does not act through the CoM, Goswami and Kallem propose that there is a theoretical point (A) that, were the GRF shifted to act parallel to its original direction and through A, the GRF would then act through the CoM and $\dot{\vec{H}}_G$ would be zero. This point, A, is the ZRAM point [3]. Mathematically, ZRAM is represented by (2.8) or (2.9), and is depicted in Figure 2.4.

$$\vec{GP} \times \vec{R} = \dot{\vec{H}}_G \neq \vec{0} \tag{2.8}$$

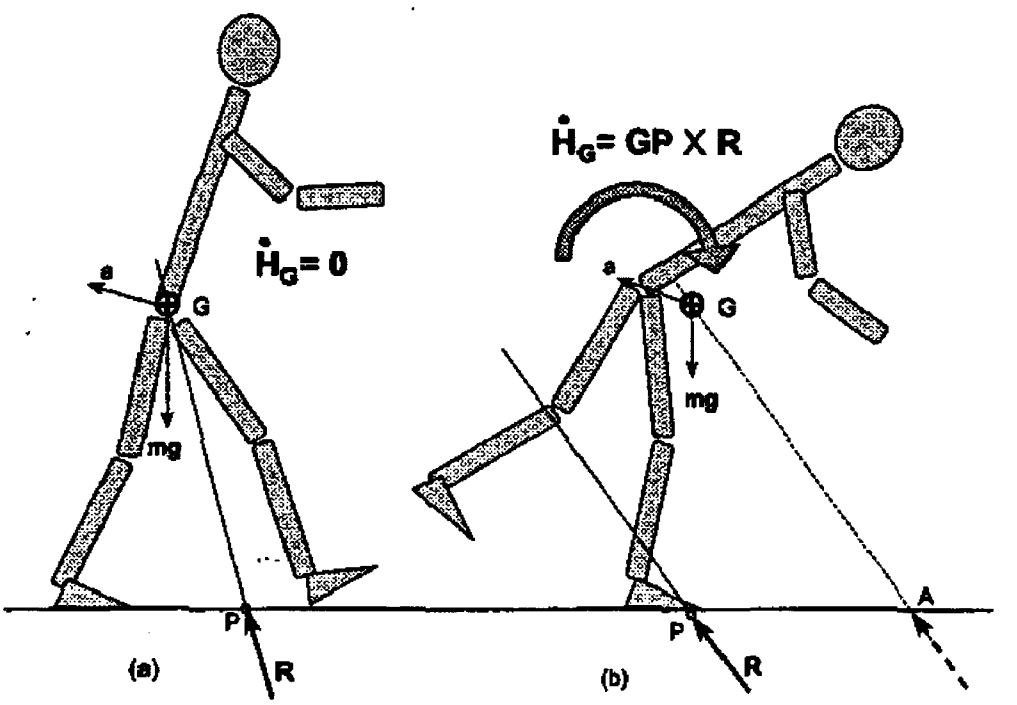

Figure 2.4: Schematic of ZRAM [3].

$$\vec{GA} \times \vec{R} = \vec{0} \tag{2.9}$$

where G is the CoM, P is the CoP, R is the GRF, and A is the ZRAM point. It is important to note that, given this definition, $\vec{GA}$ is parallel to $\vec{R}$ and $\vec{AP} \times \vec{R} = \dot{\vec{H}}_G$. ZRAM offers a number of advantages that have not been available with previously proposed criteria. First, it is well established in stability theory that $\dot{\vec{H}}_G$ contains stability information and ZRAM is derived from $\dot{\vec{H}}_G$. Second, controllers can directly manipulate $\dot{\vec{H}}_G$ and/or act on parameters derived from $\dot{\vec{H}}_G$ such as the ZRAM point. Goswami and Kallem propose three strategies that a controller could use to manipulate the ZRAM point to prevent loss of stability. First, it is possible to act to enlarge the support polygon such that, in its new configuration, it encompasses the ZRAM point. Second, it is possible to move the CoM with respect to the CoP such that the GRF acts through the new location of the CoM. Third, it is possible to alter the direction of the GRF such that it acts through the CoM by changing the centroidal

acceleration.

Popovic *et al.* provide an excellent overview of the historical development of ground reference points as stability criteria [11]. In addition they explore how each of these points behave relative to one another through a standard walking gait cycle of human subjects. A number of conclusions are made regarding this relative motion. First, it is found that FRI and ZMP do not vary relative to one another during normal gait; therefore implying that FRI is not a sufficient measure of foot rotational acceleration. This first conclusion lead to the development of a modified FRI which is introduced below. Second, it was found that ZRAM (CMP) and ZMP vary at most by 14% of the foot length. This is taken as an indication of the accuracy with which angular momentum is controlled by humans. Third, it is shown that when ZRAM (CMP) is coincident with ZMP the GRF passes through the CoM. It is proposed, therefore, that the departure of ZRAM from ZMP could be used as a possible indicator of impending instability. Finally, it is proposed that while in robotics controller design one must accurately track joint trajectories, humans and animals appear to directly control limb impedance which provides more robust handling of unexpected disturbances.

The modified FRI (MFRI) point proposed by Popovic *et al.* [11] is defined mathematically using Equation (2.10),

$$(\vec{r}_{MFRI} - \vec{r}_{ZMP}) \times (m_{foot}\vec{g})\,|_{horizontal} = \left[\frac{d\vec{L}^{foot}\,(\vec{r}_{MFRI})}{dt}\right] \tag{2.10}$$

where $\vec{r}_{MFRI}$ is the modified foot rotation indicator point, $\vec{r}_{ZMP}$ is the zero moment point m_{foot} is the mass of the foot, g is the acceleration due to gravity, and $\vec{L}^{foot}$ is the length of the foot. The MFRI examines the moment caused by the weight of the foot rather than GRF and thus MFRI-ZMP separation will be substantially greater than FRI-ZMP given that $GRF >> m_{foot}g$.

Chapter 3

Methodology

As discussed, many aspects of postural stability have been studied in varying detail and in isolation. In particular, most studies have focused on one of three areas: displacements of body segments, movement of CoP, and EMG [32]. However, very few studies have been conducted to establish the effects of the interactions of the various aspects of postural stability. The current research attempts to apply systems engineering concepts to postural stability and explore the interaction of the sensory, processing, and motor subsystems. There are three sets of data that are pertinent to such an investigation.

EMG provides information on the electrical signals driving the motor subsystem and can therefore be considered as output from the processing subsystem and input to the motor subsystem. EMG can also be used to estimate muscle force, and thus output from the motor subsystem. Recording EMG signals is a relatively simple task requiring, at the most basic level, surface electrodes to be placed on the skin over the muscle and an amplifier to provide signals with usable amplitudes for further analysis. There are many commercial systems available that provide this basic capability along with more advanced and/or convenient features.

CoP provides information about the output of the motor subsystem; specifically, indicating where the GRF occurs. CoP is also very easily recorded and be collected with something as simple as a force plate with sensors on each of the four corners of the plate. As with EMG, there are many commercially available systems for recording CoP. Some of these systems are little more than the simple force plate, requiring relatively stationary

subjects, while others provide more versatile solutions along with additional related data that can be recorded.

CoM, which is the quantity of interest in studying the displacements of body segments in postural stability, provides additional information about the output of the motor subsystem, and how the body is moving on the whole. It can also be considered as an input to a feedback loop to the sensory subsystem. CoM is significantly more difficult to record than the other two sets of data as it is not directly measurable during normal activity. Instead, one must rely on a more directly measurable type of data such as the position and orientation of individual body segments. When used in conjunction with anthropometric data acquired through the study of human physiology, the position and orientation of the body segments can be used to calculate CoM of the entire body. To the author's knowledge, there are no commercially available systems for measuring CoM of the human body during normal activity. To that end, the current research uses a method of calculating overall CoM of the human body during normal activity as specified in Section 3.2.3.

Given means by which to record such data, it is possible to evaluate the various thesis objectives identified in Section 1.2 for any given task(s) one wishes to evaluate postural stability for. As those few studies that have explored a broader range of aspects of postural stability have tended to focus on normal walking, and as an interest in further understanding MII has been identified, this study will explore more complex motions associated with common ship-board tasks. The four primary tasks that were selected include a quiet standing task, a sagittal lift/lower task, a stair climbing task, and a balancing task on a simulated ship-deck. These tasks give a range of interesting postural movements including reaching, bending, external loading, single support phase, and external perturbation of the support surface.

These four tasks and three sets of data provide the means with which to investigate each of the thesis objectives. It is possible to get empirical data for postural stability criteria such as the position of the CoM and CoP, to track the motion of these criteria relative to each other as in Popovic *et al.* [11], and to directly measure how close to the boundaries of the BoS humans typically get before experiencing an MII. Given the EMG signals of various

muscles of interest, it is possible to estimate the relative force produced by each, and their relative levels of activity during the performance of these tasks.

The remainder of this chapter will outline the specific tasks to be evaluated, along with the equipment selected for recording CoP, CoM, and EMG data. As well, analysis techniques for each type of data will be developed. This study was reviewed and approved by the Carleton University Research Ethics Committee.

3.1 Task Performance Procedures

3.1.1 Quiet Standing Task

The participants were asked to stand with feet shoulder width apart and remain as still as possible in a relaxed, upright posture for 30 seconds. While the data collected during the performance of this task can be evaluated in the same manner as the rest of the tasks described below, this particular task has an additional purpose. As described in [20], the standard deviation of the displacement of the CoP from its mean value over a 30 second quiet standing task can be used as a measure of aptitude for postural stability.

3.1.2 Sagittal Lift/Lower Task

This task was based upon the sagittal lift/lower task in [4]. Participants were asked to lift a 10 kg mass to and from a table approximately 72 cm high and 60 cm in front of them (Figure 3.1). A line was placed on the floor, 60 cm from the table to direct participants where their toes should be placed and the task was performed with feet shoulder width apart. Target zones on both the floor and the table were outlined with masking tape to allow for consistency between lifts/lowers. The task (lift plus lower) was repeated three times over a period of 60 seconds and participants were asked to return to a resting state for a ten-count between each lift or lower.

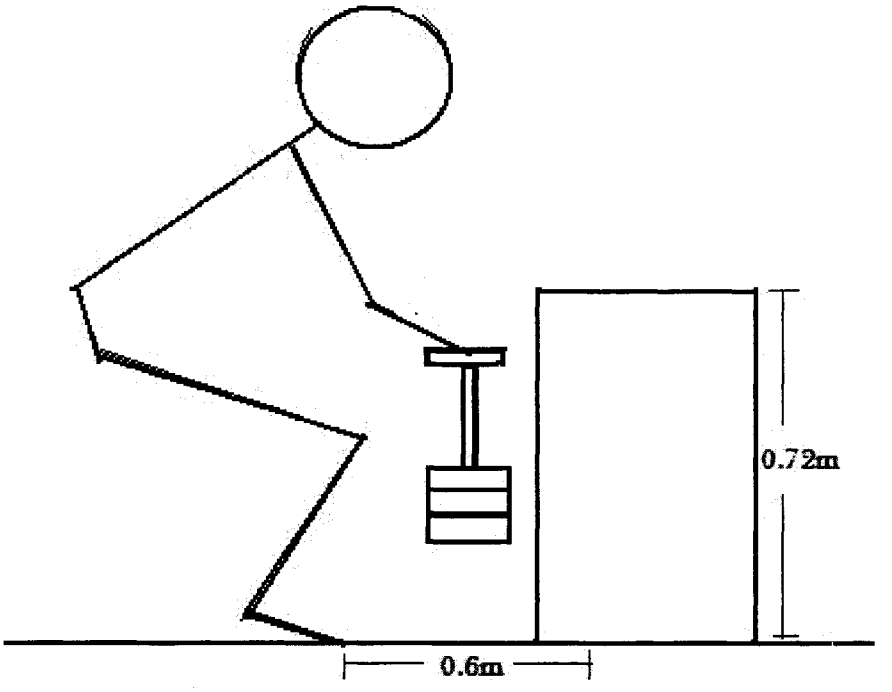

Figure 3.1: A schematic of sagittal lifting/lower task from [4].

3.1.3 Stair Climbing Task

Participants were asked to walk up a flight of four to five steps (depending on participant's height, in order to keep all markers within the motion capture volume) and then to descend them again backwards. This task was to be repeated for a duration of 60 seconds at whatever pace was comfortable for the participant. While hand rails were available for safety, participants were instructed to hover their hands above the rails and only use them if they felt they were at risk of falling. This meant that all of their body weight was being supported through the contact of their feet on the steps.

3.1.4 Motion Platform Task

A MOOG 6DOF2000E Model 170-131 Electric Motion Platform [41] (Figure 3.2) was used for the motion platform task. A custom built safety railing was affixed to the platform to prevent participants from falling off.

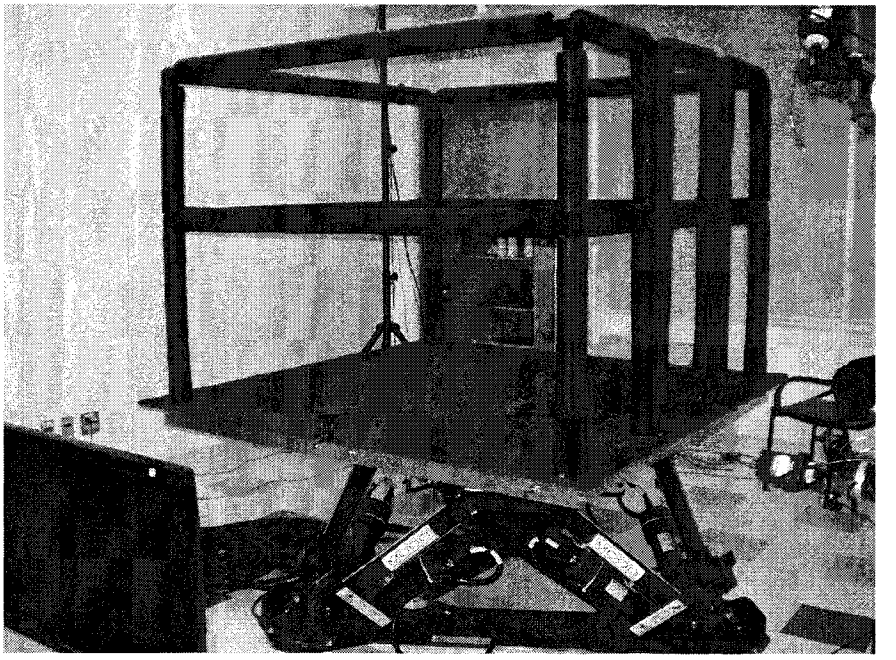

Figure 3.2: MOOG 6DOF Motion Platform - minus boom for fall arrest harness.

In order to simulate standing on a ship-deck on the open sea, participants were asked to stand on a six degree of freedom (6 DoF) motion platform and maintain their balance

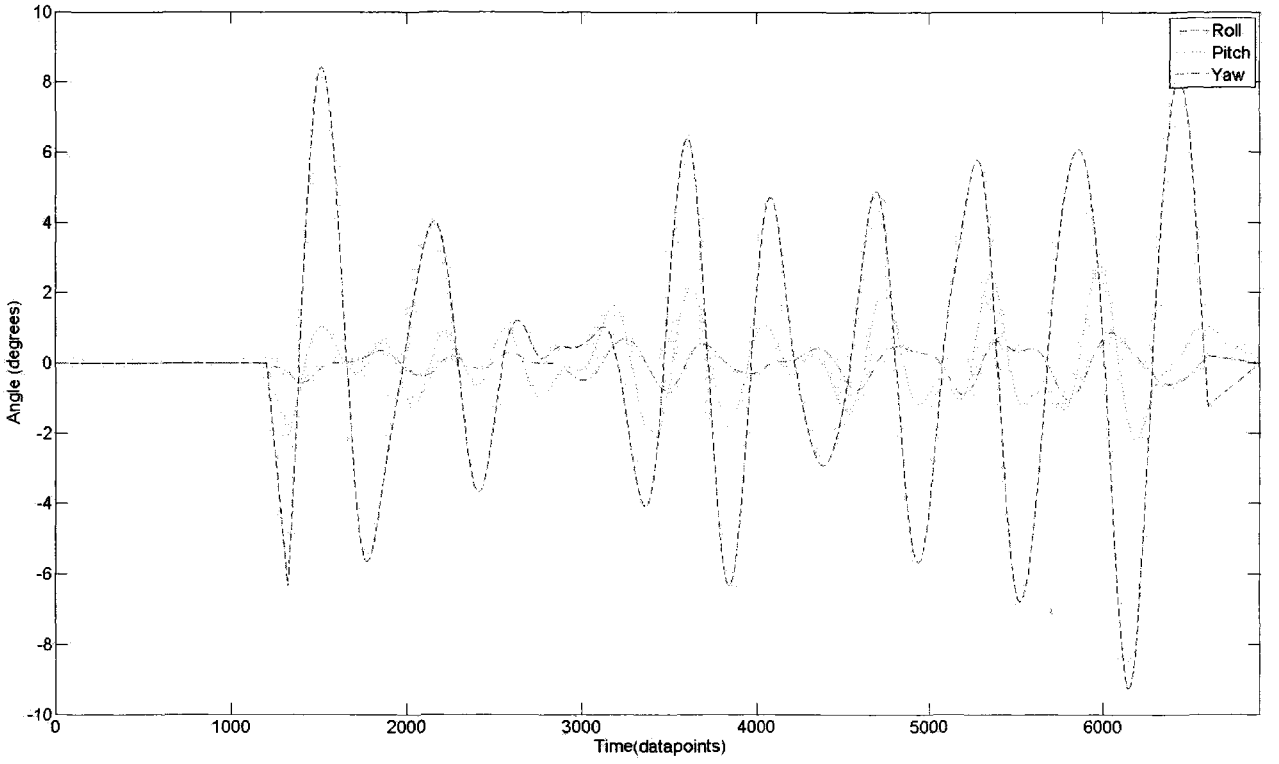

Figure 3.3: Motion profile for the MOOG 6DoF platform.

for 90 seconds. During this time, the platform went through a series of predetermined, pseudo-random, ship-like motions consisting of roll, pitch, and yaw movements (rotations about the longitudinal, lateral, and vertical axes respectively). Figure 3.3 shows a plot of this motion. This motion is representative of a quiescent period for a frigate operating in sea state 5 (characterized by a significant wave height of 2.5-4 m). In particular, the motion profile corresponds to a ship traveling 10 knots at an angle of 45 degrees to four meter high waves.

3.2 Instruments and Apparatus

3.2.1 CoP Data

The Tekscan F-Scan system [42] was used to capture the CoP under the feet of the participants during all tasks. The system consists of two thin insole inserts (Figure 3.4) that are placed in the participants' shoes. These inserts contain 960 pressure sensitive sensels and attach to an ankle cuff that transmits the pressure data to the F-Scan Research software via Ethernet cables. These sensels are composed of pressure sensitive ink whose electrical resistance is proportional to the compressive force applied to it. The inserts can be trimmed to fit the participant's shoes (note that this reduces the total number of sensels; however, the sensel density remains the same). The system provides pressure data for each sensel point of each foot, as well as calculates the CoP. The F-Scan system is capable of sample rates up to 750 Hz and the spacing between individual sensels is 5.08 mm. This provides ample sensitivity for CoP calculations even during quiet standing. Each sensel can take on a raw value from 0-255. Through the available calibration utility in the accompanying Research software, these raw data values can be converted to pressure values.

Pressure data were recorded using the Tekscan Research software along with the F-Scan system. For the quiet standing task and the motion platform task, described in Sections 3.1.1 and 3.1.4 respectively, an F-Scan system was used to record pressure data at sample rates of 500 Hz and 375 Hz respectively, using kPa as the unit of measure and a precision of five decimal points. For the sagittal lift/lower task and stair climbing task, described in Sections 3.1.2 and 3.1.3 respectively, an F-Scan Mobile system was used. Due to limitations of available memory on the mobile system, the sample rate was limited to 150 Hz for these two tasks. Dynamic pressure and centre of pressure data were individually exported to comma separated value (CSV) files for each foot of each participant.

Each participant spent several minutes with the insoles in their shoes prior to calibration and sensitivity being set in order to acclimate the insoles to the temperature and moisture levels inside the shoes. Calibration was performed using the Research software and sensitivity was set such that the participants' own body weight did not quite place any of the

sensels at a raw reading of 255. This was to accommodate the fact that additional force would be placed on the feet in some of the tests and avoided sensel saturation in those cases.

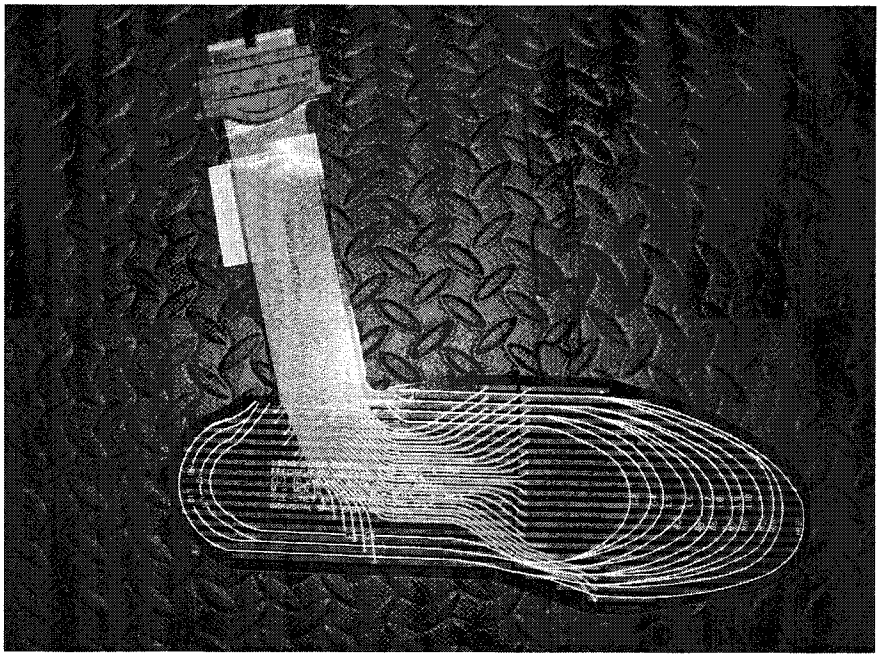

Figure 3.4: F-Scan insole.

Data Reduction and Analysis

Centre of pressure data were imported into Matlab using the script shown in Appendix A.3.1. In order to determine how close to the boundaries of the contact surface (sole of the foot) centre of pressure came before an MII occurred, it was necessary to establish what those boundaries were. Due to the nature of the F-Scan sensors and software, this information was not readily available. Therefore, an algorithm was developed to estimate the convex hull of the foot from the pressure data. This algorithm, shown in Appendix A.3.2, evaluated each frame of pressure data and marked those positions in the sensel grid that contained non-zero values (NaNs were converted to zeros as they represent grid positions that do not contain sensels even in the untrimmed insole). The result, after evaluating all frames, is a data mask representing which grid positions contained valid pressure data in at least one frame of data. Those grid positions outside of this mask can be considered to be outside of the boundary of the foot.

As the Tekscan Research software measures CoP relative to a fixed point at the top-left of the insole sensor grid, which does not correspond to a point on the physical foot, the CoP data were converted to a coordinate system with the origin at the leftmost point of the heel as seen in Figure 3.5. For measurements in the lateral direction, this means that lower values are closer to the outer edge of the left foot but closer to the inner edge of the right foot. For measurements in the sagittal direction, lower values are closer to the heel for both feet.

The CoP was then normalized against these boundaries and plotted over time.

3.2.2 EMG Data

The CleveMed BioCapture system [43] (Figure 3.6), consisting of the BioRadio 150 and BioRadio Lite software, was used to record EMG signals of various muscle groups of the participants during all tasks. Two BioCapture systems were used, one for the left side of the body and one for the right. Each system can accommodate a maximum of eight EMG channels, of which six were attached to electrodes placed on the muscle groups of interest,

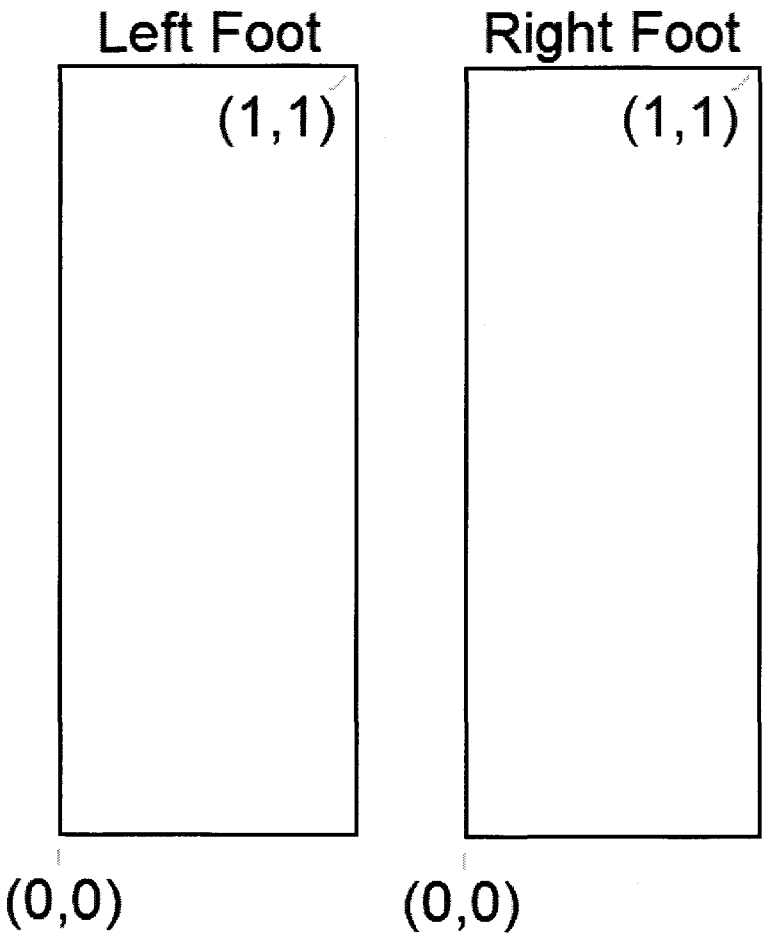

Figure 3.5: Converted reference frame for CoP data.

one was attached to a data synchronization circuit (Section 3.2.5), and one was allowed to record with no electrodes attached to provide a baseline noise signal in case adaptive filtering was required to remove any power line interference. The last channel was used to connect the synchronization circuit described in Section 3.2.5.

Ideally, EMG data would have been recorded at 1024 Hz to allow the use of the EHP Filtering technique for estimating muscle force [37]. However, the BioCapture system had to be set to record at a maximum of 800 Hz and 12 bit data resolution in order to minimize dropped data packets over the wireless connection. While the BioCapture system supported hardware filtering, this was disabled so that a record of the raw EMG signal was available. The raw signal data were saved as a CSV file using the BioRadio Lite software.

Figure 3.6: CleveMed BioCapture system.

Table 3.1 lists the muscles groups of interest to the current research, as well as a brief description of the general form and function of each muscle according to Gray's Anatomy [5].

Muscle	Short	Description	Primary Function	Secondary Function
Rectus abdominus	RA		Bending thorax forward.	Draw pelvis upwards when thorx fixed or during climbing.
Erector spinae	ES	Attaches at posterior pelvis and follows side of spine attaching through various tendons to the ribs.	Keeps spine erect.	Bends trunk backwards.
Rectus femoris	RF	Middle muscle of anterior thigh (quadriceps).	Extensor of lower leg.	Flexor of pelvis when thigh fixed.
Biceps femoris	BF	One muscle within hamstring, extending from top of femur to fibula.	Acts with rest of hamstring as flexor of lower leg.	Helps to arch trunk backwards when in stooped posture.
Tibialis anterior	TA	Lateral muscle of the shin, attaching proximally to upper tibia and distally to first metatarsal of foot.	Flexor of foot.	Stabilizes and stiffens ankle joint.
Gastrocnemius	G	Major muscle of the calf, attaching proximally at the knee and distally to the heel at the achilles tendon.	Extensor of foot.	Can assist in flexing femur relative to tibia.

Table 3.1: Muscle groups of interest.

Myotronics Ag/AgCl DuoTrode electrodes, coupled with snap-on, insulated leads were used to connect to the muscles that were monitored for EMG. These electrodes are provided in pairs, mounted on a single adhesive backing at a fixed separation and with conductive gel pre-applied to the contact surfaces of the electrodes. Figures 3.7 and 3.8 identify the muscle groups of interest and show the placement of the electrodes. The electrodes and leads were applied to the participants prior to putting on a motion capture suit, associated with body segment motion tracking, in order to allow the tight fitting suit to help eliminate artifacts caused by motion of the wires during recording. Additional medical tape was used to help secure the electrodes and prevent their coming loose while putting on the suit or moving.

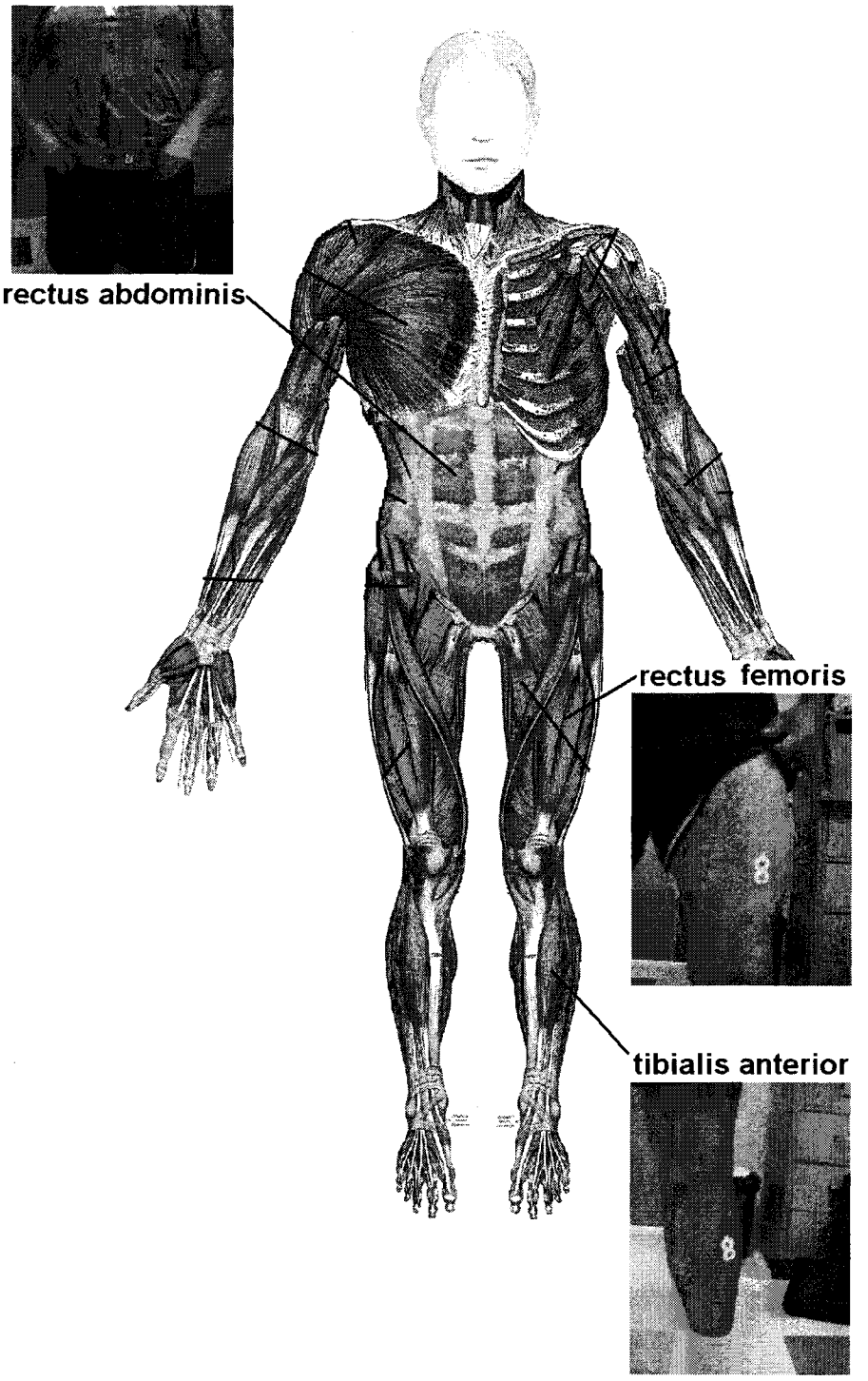

Figure 3.7: Anterior muscles of interest and electrode placement [5].

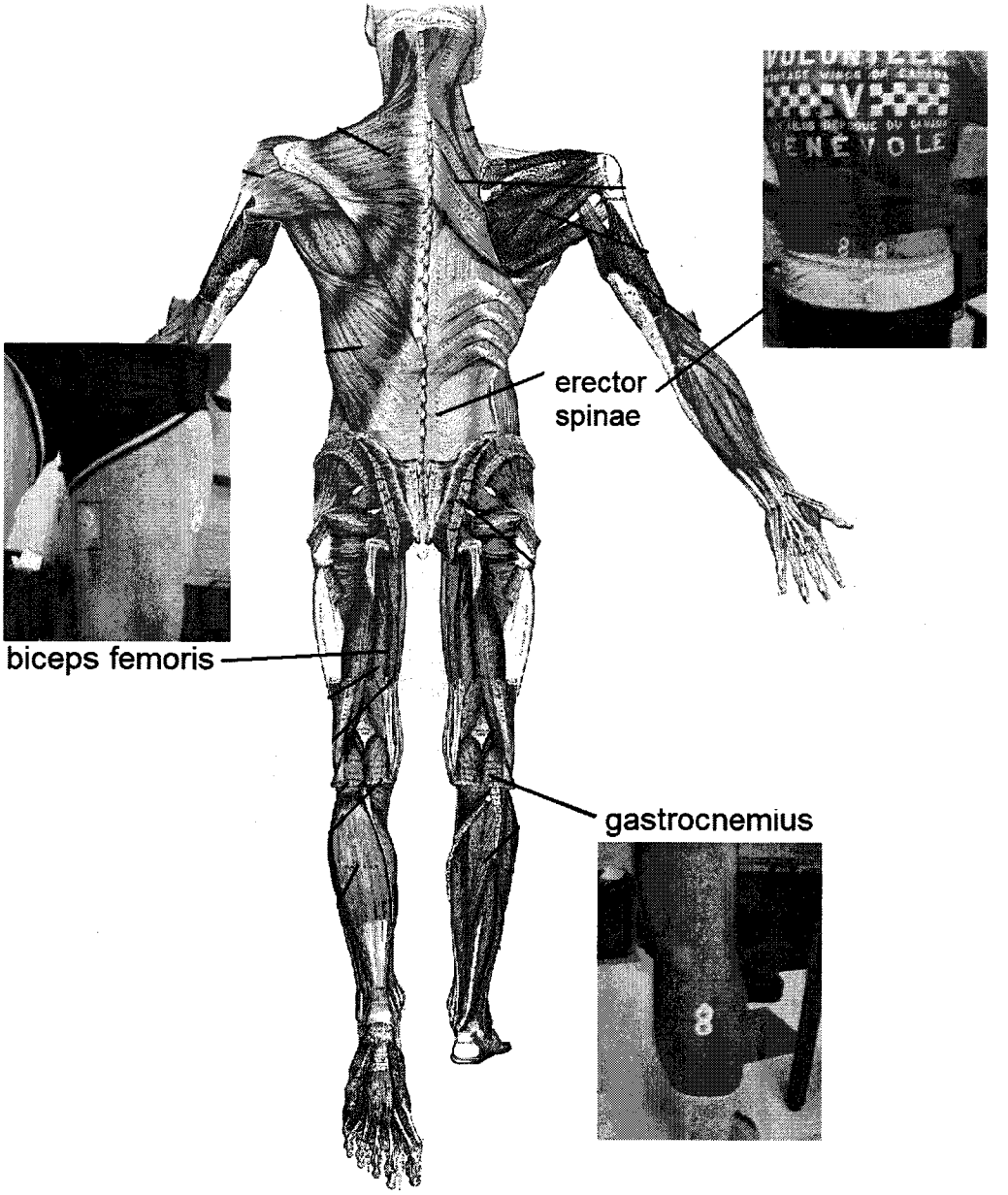

Figure 3.8: Posterior muscles of interest and electrode placement [5].

Data Reduction and Analysis

The CSV files containing EMG data were loaded into Matlab. As the CleveMed system operates wirelessly, and as it is possible for the participant's movements to occasionally cause electrodes to lose contact, it is possible that the raw data recorded with the CleveMed system has some dropped data points. The software was set up to record a value of 10,000 mV in place of dropped data points. This value is an impossible EMG amplitude and was therefore able to be used to identify dropped data points programatically. The script shown in Appendix A.2.4 was used to fill in the dropped data points before any EMG analysis was performed. It was necessary to assume that the muscle force immediately prior to and immediately following any dropped data points would be reasonably similar to the missing data. For small gaps this should be a reasonable assumption, even in the worst case scenario where the data gap occurs during a transitory period in the participant's muscle activity. A cursory evaluation of the dropped data points indicated that the vast majority of gaps were only 29 ms long, with the largest gap encountered being 249 ms. To fill the gaps, the gap length was divided in two, with the first half of the gap being filled with a copy of the data preceding the gap and the latter half of the gap being filled with a copy of the data following the gap.

After missing data points were filled, the next step in the analysis of the EMG data was to perform typical filtering techniques to remove extraneous signals that tend to get superimposed onto the EMG signal when recording with surface electrodes. The filtering technique used is based upon [36] (chapter on Kinesiological Electromyography). Specifically, a sixth order Butterworth filter (using the built in *butter* routine in Matlab) was used with stop bands below 10 Hz and above 400 Hz. The stop band below 10 Hz removes low frequency motion artifacts that can result from movement of the electrodes on the skin or of the electrode leads during performance of the tasks. Generally, as discussed in [36], EMG signals can vary in frequency content from about 10 Hz to 500 Hz (sometimes as much as 1000 Hz); however, the majority of the signal power tends to be well below 400 Hz.

In addition to the bandpass Butterworth filter, an algorithm for adaptive filtering to remove 60 Hz hum was available. An additional, empty channel was allowed to record on the CleveMed systems and could be used as the noise signal to be passed to this adaptive filter. However, since the data recording was done in a darkened room to accommodate the infrared motion capture cameras, inspection of the Welch power spectrum graphs (see Figure 3.9 for an example) indicated that no 60 Hz hum was present in the signals so the adaptive filter proved unnecessary. Appendix A.4.1 shows the script used to produce these power spectra.

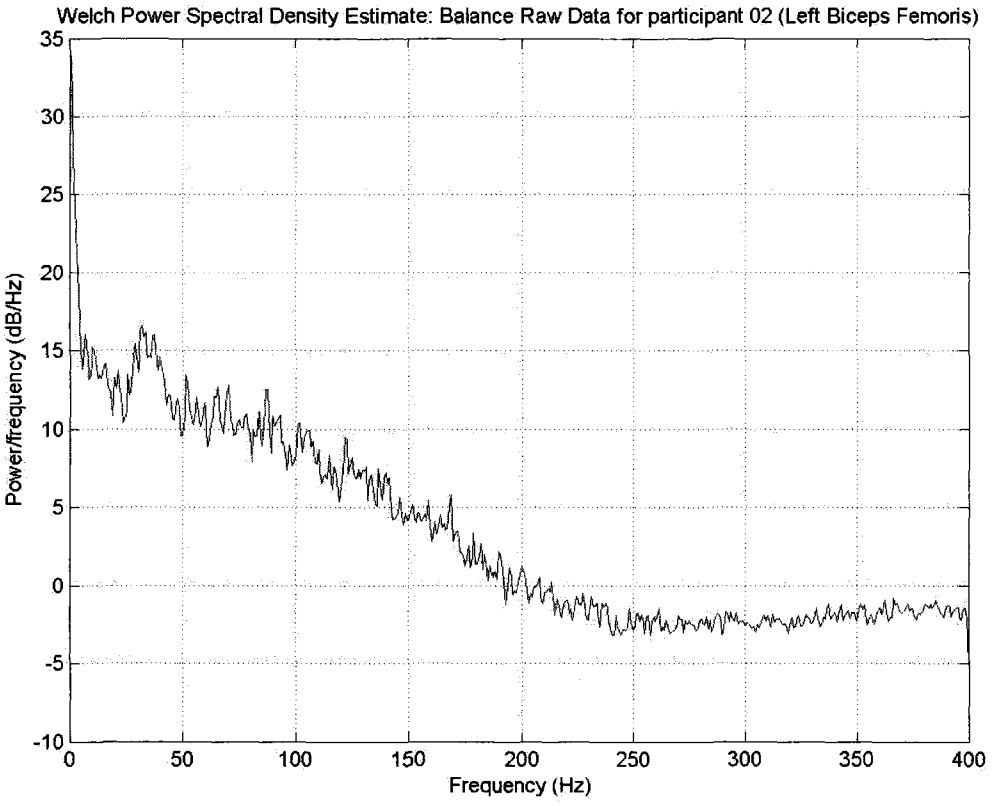

Figure 3.9: Sample Welch power spectrum plot.

The final piece of analysis for the EMG data was to use the EMG signal to get an estimate of the relative muscle force exerted by each muscle being monitored. A typical linear envelope estimation of force was performed on the EMG data [36, 37]. The basic algorithm is summarized below and the Matlab script used to perform the force estimation

is shown in Appendix A.4.2.

1. Low pass filter the raw signal at 400 Hz (typically this would be 500 Hz, the upper bound on EMG signal content, however, 400 Hz is the maximum cutoff possible when using the butter routine with the sample rate of 800 Hz).

2. High pass filter the resulting signal at 20 Hz to eliminate motion artifacts.

3. Full wave rectify the resulting signal.

4. Calculate the linear envelope of the resulting signal.

3.2.3 CoM Data

In order to calculate CoM, motion capture was used to record the position and orientation of the participant's body throughout the execution of the tasks. Due to equipment availability, two different motion capture systems were used in this research. The OptiTrack system was used for the quiet standing task and the motion platform task, described in Sections 3.1.1 and 3.1.4 respectively. The Vicon system was used for the sagittal lift/lower task and the stair climbing task, described in Sections 3.1.2 and 3.1.3 respectively.

OptiTrack Camera System

A Full Body Motion Capture OptiTrack system [44] by Naturalpoint was used for motion capture of the participants. This system uses 34 retro-reflective markers placed upon the participant's body and eight infrared cameras (Figures 3.10 and 3.11) to track those markers during the performance of the tasks. The cameras used were the OptiTrack FLEX:V100R2, which offer a 100 fps capture rate, shutter times from 20 μs to 1 ms, a resolution of 640x480 pixels, operate with 850 nm IR, and have a 46.2 degree field of view. While the accuracy of marker position is dependent upon marker size and distance to the camera, these cameras are capable of sub-millimeter precision. The ARENA software (Figure 3.12) that is coupled with the camera system resolves the position of the markers within each camera's field of view into 3D spatial coordinates and is capable (after calibration) of tracking the individual markers,

as well as rigid body segments, and providing real-time and post-processed visualizations of the captured motion. Calibration of the system was done prior to each capture session using the calibration functionality in the ARENA software as described in the user tutorials found in [44]. The ARENA software was used to export the capture sessions for each task to C3D files for further data reduction and analysis.

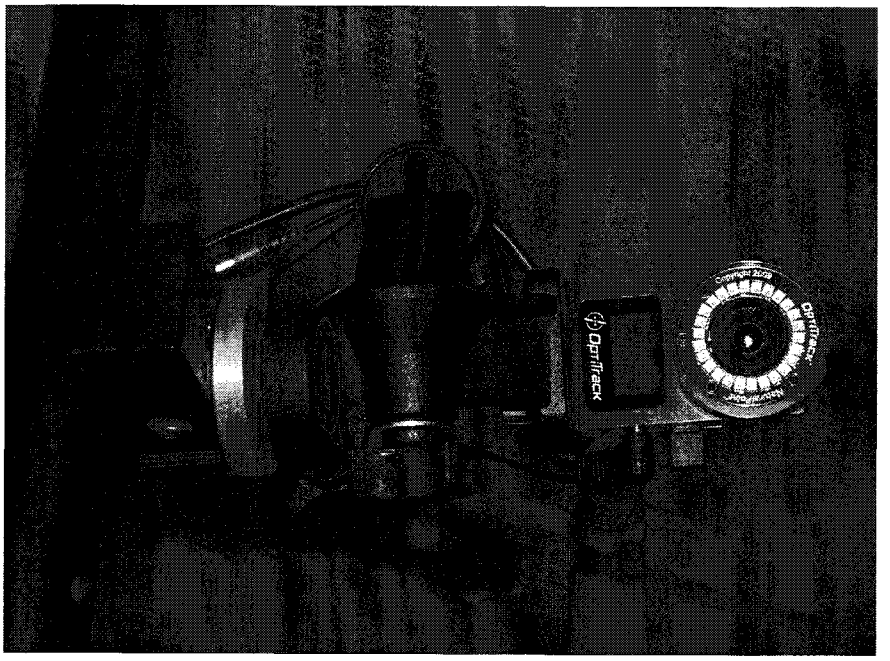

Figure 3.10: OptiTrack cameras.

Figure 3.11: Representative camera setup.

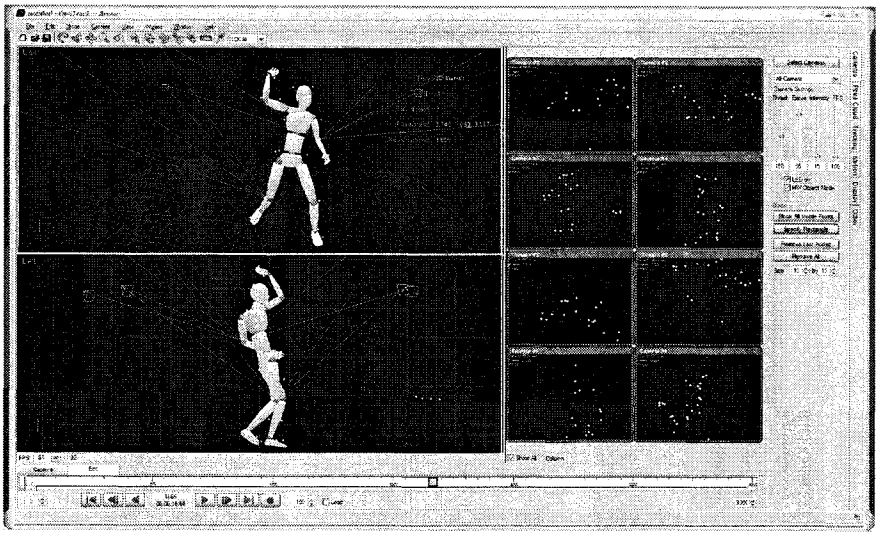

Figure 3.12: ARENA screenshot.

Vicon Camera System

The Vicon system [45] was very similar to the OptiTrack system in many respects. The most notable differences being higher resolution cameras, and 120 fps capture rate. The layout of the markers and the global coordinate system were also slightly different, however, other than accounting for these differences in the algorithms described in Section 3.2.3, this had no bearing on the research.

Data Reduction and Analysis

The motion capture data were exported to C3D file format. C3D.org's C3Dserver software and their C3D Matlab Toolkit were then used to import the C3D data into Matlab. Using the anthropometric data published by Winter [36], markers were chosen to represent the proximal and distal ends of each of the body segments described. Table 3.2 summarizes the pertinent information from Winter and associates markers with the distal and proximal ends of those body segments. The motion capture data were then used to determine the position and orientation of each body segment (by calculating the vector from the proximal to distal marker) and the antrhopomentric data were used to calculate the position of the CoM for each segment. Once the individual segment CoMs were calculated, a weighted sum of those CoMs was calculated (using the antrhopometric data for fraction of total body weight) in order to obtain the overall CoM of the body. The implementation of this algorithm is shown in Appendix A.5.1.

It should be noted that, due to occluded markers in the sagittal lift/lower task and stair climbing task, the motion capture data had to be run through a cubic spline interpolation routine in Matlab in order to fill in missing data points prior to calculating CoM. It should also be noted that there were problems with occluded markers in the quiet standing task and motion platform task. However, as the Arena software was available and had support for data scrubbing it was used to fix these issues. The Arena software offers three methods for gap filling; linear, cubic, and angle interpolation. The first two methods are recommended to be used for gaps no larger than 1-5 frames. For larger gaps, the angle method is suggested.

Segment	Definition	Proximal Marker	Distal Marker	Weight*	CoM**
Hand	Wrist axis/knuckle II middle finger	Wrist	Base of Pinky	0.0060	0.506
Forearm	Elbow axis/ulnar styloid	Elbow	Wrist	0.0160	0.430
Upper arm	Glenohumeral axis/elbow axis	Shoulder	Elbow	0.0280	0.436
Foot	Lateral malleolus/head metatarsal II	Heel	Toe	0.01450	0.500
Leg	Femoral condyles/medial malleolus	Knee	Ankle	0.0465	0.433
Thigh	Greater trochanter/femoral condyles	Hip	Knee	0.1000	0.433
Trunk, head, neck	Greater trochanter/glenohumeral joint	Hip	Top of Spine	0.5780	0.660

Table 3.2: Anthropometric data (*: as fraction total body weight, **: as fraction of segment length measured from proximal head).

According to Naturalpoint, this method involves "interpolating the rigid body angles at the start and end of the gap and taking [into account] the expected marker positions."

As well, a number of issues surrounding coordinate reference frames had to be surmounted for this analysis. The camera systems have the origins of their respective coordinate systems at the centre of the capture volumes. However each system uses a different orientation of the x, y, and z-axes. Finally, in the case of the sagittal lift/lower task the participants were facing a positive 45 degree rotation about the vertical axis and in the case of the stair climbing task they were facing a negative 135 degree rotation about the vertical axis of the Vicon camera reference frame. The Vicon data were rotated using a transformation matrix to orient it with the sagittal and lateral directions of the participants' bodies. To remove the translation of this body coordinate system with respect to the origin of the

Vicon camera system's reference frame, the mean value of the CoM was removed from the CoM data. This effectively puts the origin of the body coordinate system at the "resting" position of the participant when they are in place to perform the respective task. In the case of the quiet standing task and motion platform task, the participants stood at the origin of the OptiTrack camera system's reference frame and aligned with its axes so no further coordinate conversion was required.

3.2.4 Cross-correlation Analysis

A detailed cross-correlation analysis was performed between the various parameters being measured (CoP, CoM, muscle force) for the purposes of determining what level of dependence there was between these parameters as well as what, if any, delays exist between them. This cross-correlation analysis explored the covariance between pairs of parameters at various lags. A correlation was defined as being significant if it passed a $p < 0.01$ significance test. The algorithm was based on the Matlab *xcov* routine, and can be seen in Appendix A.5.3. It should be noted that, due to the different sample rates used by each of the data recording systems, it was necessary to first convert all data to the same sample rate. As well, the maximum lag allowed in the *xcov* routine was set to approximately half of the periodicity of the task in order to prevent the correlation analysis from mistakenly correlating values from different cycles in the repetition of the tasks.

3.2.5 Data Synchronization

Data from the various equipment were time-synchronized, to an accuracy on the order of a hundredth of a second, through a simple electrical circuit. The circuit was powered by a 1.5 V battery and controlled by a momentary-on switch. The outputs of the circuit were connected to an 850 nm LED, and to a free channel on the BioRadios. The participants were instructed to step forcefully on the switch at the start of their capture sessions, resulting in a synchronization signal being picked up by the BioRadios and motion capture cameras while a pressure spike would be recorded by the F-Scan system. The data were visually inspected to find the frame where the synchronization signal went from "on" to "off" and

those frames were used as the starting frames for each type of data. This synchronization was only available in the quiet standing and motion platform tasks.

3.3 Participants

Six participants (4 male, 2 female) were recruited through word of mouth for this study. Ages ranged from 26 to 46, with the mean age being 36.7. All participants were free of mobility and/or balance problems. Two participants did have conditions that might manifest in the results: Participant 03 suffered from foot drop in her left foot and Participant 02 had his vastus lateralis removed in his right leg. Participants were asked to state their dominant foot. Table 3.3 shows the demographics of the participants. Note that participant IDs were auto-incremented within the Tekscan Research software and that Participant 01 is not included in the study as that ID was assigned to the researcher during setup and trials.

In accordance with Carleton University's ethics policy, all participants were supplied with an initial Letter of Information describing the study and what would be expected of them. Prior to commencement of the study, participants were given the opportunity to ask questions and clarify the process and procedures. Finally, an Informed Consent form was signed by each participant. All participants were free to request withdrawal from the study at any time.

Participant	Gender	Age	Mass (kg)	Dominiant Foot	Notes
02	M	46	124.74	Right	vastus lateralis removed
03	F	46	83.91	Right	foot drop in left foot, no EMG for stair climbing
04	M	40	90.26	Right	no CoM data for sagittal lift/lower or stair climbing
05	F	26	77.11	Right	
06	M	31	82.55	Right	no CoM data for quiet standing or motion platform
07	M	31	118.39	Right	

Table 3.3: Participant demographics

Chapter 4

Results and Discussion

4.1 Quantitative Index for Evaluating Aptitude for Postural Stability

4.1.1 Motivation

The ability to predict the relative performance of individuals at postural stability tasks is very important for establishing individual risk levels associated with the performance of those tasks under adverse conditions, such as shipboard operations in heavy seas. The use of a quantitative index to represent such relative performance levels would provide an easy means for tuning models (such as MII models) to the ability of specific individuals.

Various measures for evaluating the natural aptitude for postural stability of an individual were introduced in Section 2.2. For the purposes of the current research, the measure introduced by Nawayseh and Griffin [20] will be used due the simplicity of its implementation using the same equipment necessary for the other components of the research.

While previous research has focused mainly on predicting the performance of individuals at simple postural tasks based solely on CoP and postural sway angles, the current research will investigate whether or not this measure can be extended to predicting performance of more complex postural tasks. In order to evaluate the applicability of the index of postural stability to these tasks, the index will be calculated for each participant based on their performance of the quiet standing task. The participants' relative indices will then be

compared to their performance of the other tasks. Specifically, the standard deviation of the CoP and CoM while performing those tasks. The expectation, assuming that the index can be extended to predicting performance of more complex tasks, is that the ranking of the standard deviation of the CoP and CoM across participants will remain constant across tasks; indicating that their relative performance remains constant.

4.1.2 Results and Discussion

The quiet standing task was performed by each participant. The recording session for each participant lasted for 60 seconds in order to allow time for performing the data synchronization. However, in order to eliminate transient effects at the beginning of the recording, only the final 30 seconds of recorded centre of pressure data were used in calculating the index of postural stability aptitude. Table 4.1 summarizes the participants' indices. These values are slightly smaller than the approximate value of 10 mm reported in [20]; however, the closest case to quiet standing in that study was a fore-and-aft oscillation with frequency of 0.125 Hz and velocity of 0.04 m/s. Accounting for these differences, the values from the current research are reasonable for quiet standing.

Participant	Left Foot (Rank)	Right Foot (Rank)
02	6.8965 (6)	6.6497 (5)
03	3.0236 (3)	1.8980 (2)
04	4.0481 (4)	3.7902 (4)
05	2.0668 (2)	2.7629 (3)
06	1.7150 (1)	1.6878 (1)
07	5.9178 (5)	9.0539 (6)

Table 4.1: Postural stability aptitude (Standard deviation of CoP in mm).

Evaluating these indices, one would expect that participants 02 and 07 would have the poorest performance in the remaining tasks and that Participant 06 would show substantially better performance than all others. These indices will be compared to the individual participant's actual performance of the other tasks.

Sagittal Lift/Lower Task

Table 4.2 shows the ranked indices of postural stability aptitude for each of the participants, as well as the standard deviation of their CoP and CoM (as measures of performance) while performing the sagittal lift/lower task. As expected due to the dynamic nature of the task, the standard deviations are much larger than those in the quiet standing task. Figure 4.1 shows a graphical representation of this data, along with trend lines. While it can be seen that there is not a 1:1 relationship between the postural stability index and the performance of the sagittal lift/lower task, the data do show a linear relation. Participant 02, who was ranked very low on his postural stability index, ranked first or second for all measures of performance in this task. Participant 05 experienced a similar discrepancy between postural stability index and performance in the sagittal lift/lower task. The remaining participants, however, ranked very similarly in performance based on both CoP and CoM when compared to their indices of postural stability.

Participant	Left Foot (Rank)		Right Foot (Rank)		CoM (Rank)
	Index	CoP	Index	CoP	
02	(6)	42.4700 (1)	(5)	40.5432 (2)	27.3275 (1)
03	(3)	47.8916 (2)	(2)	51.9294 (3)	35.3939 (2)
04	(4)	61.5430 (5)	(4)	56.6917 (4)	N/A
05	(2)	67.2261 (6)	(3)	62.8037 (6)	65.8764 (3)
06	(1)	53.1356 (3)	(1)	39.0086 (1)	N/A
07	(5)	61.2845 (4)	(6)	62.3940 (5)	N/A

Table 4.2: Performance of sagittal lift/lower task versus postural stability index (Standard deviation of CoM and CoP in mm).

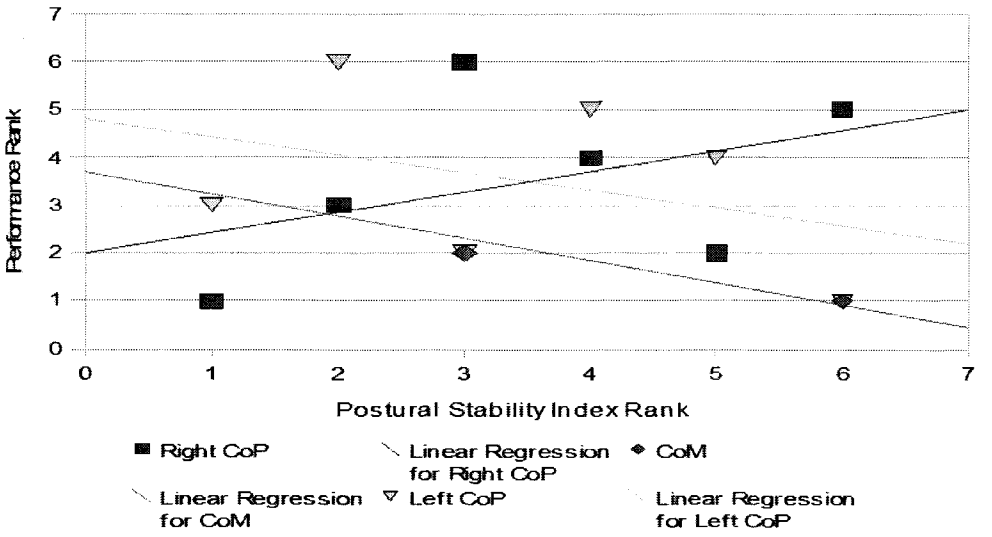

Figure 4.1: Performance indices for sagittal lift/lower task.

Motion Platform Task

Table 4.3 shows the ranked indices of postural stability aptitude for each of the participants, as well as the standard deviation of their CoP and CoM (as measures of performance) while performing the motion platform task. Figure 4.2 shows a graphical representation of this data, along with trend lines. While it can be seen that there is not a 1:1 relationship between the postural stability index and the performance of the motion platform task, the data do show a linear relation. Participant 02 shows similar performance, with regards to CoP, as his ranked index of postural stability. However, he shows a significant increase in rank when considering performance based on CoM. Participant 03, on average, ranked similarly in performance of the motion platform task compared to her index of postural stability; performing slightly better in CoP, but slightly worse in CoM. Participant 04 shows much better performance in CoP of the left foot, as well as CoM, compared to his index; however, he shows much worse performance in CoP of the right foot. Participant 05 performs much worse with regards to left foot CoP, but on par with the rank of her index for the other measures of performance. Participant 06 performs about equally to what would be expected based on his index. Participant 07 shows an improvement in performance based on left foot CoP, but is otherwise about on par with his index.

Participant	Left Foot (Rank)		Right Foot (Rank)		CoM
	Index	CoP	Index	CoP	
02	(6)	14.9790 (4)	(5)	18.2491 (5)	34.2329 (2)
03	(3)	10.6081 (1)	(2)	5.8265 (1)	41.0526 (4)
04	(4)	12.9038 (2)	(4)	20.3541 (6)	32.6901 (1)
05	(2)	18.2902 (6)	(3)	15.9885 (3)	38.6036 (3)
06	(1)	15.8367 (5)	(1)	11.6174 (2)	N/A
07	(5)	14.3333 (3)	(6)	18.0261 (4)	91.0535 (5)

Table 4.3: Performance of motion platform task versus postural stability index (Standard deviation of CoM and CoP in mm).

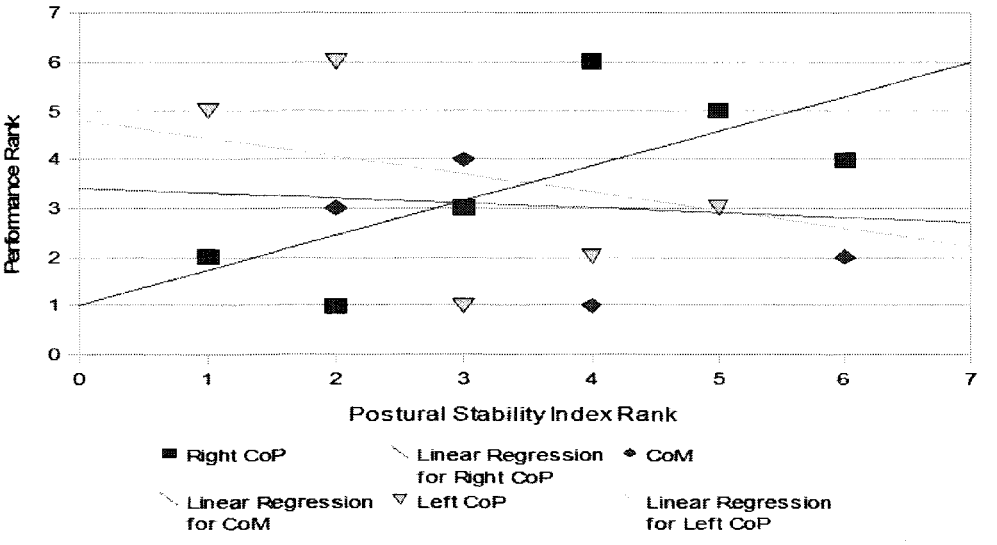

Figure 4.2: Performance indices for motion platform task.

4.1.3 Conclusions

While most participants show at least some sign of performing similarly to what could be expected based on their index of postural stability, there is a fair amount of variation seen in the results. This could easily be attributed to the differences in the tasks themselves, and it could be suggested that the index should be calculated for each type of task. However, even then there are still differences between the measure of performance based on CoP versus that based on CoM. The data show that some individuals keep tighter control of CoP while allowing CoM more freedom whereas others keep CoM under tight control while allowing CoP to move more freely. This is likely a result of employing different stability strategies, and neither is necessarily more or less inherently stable than the other. So, while an index of postural stability may prove useful as one of multiple tuning parameters, or as a quick estimation of how an individual will perform at postural tasks in general, it can not be used to predict accurately what an individual's performance of a specific task will be like.

4.2 Relative motion of CoM and CoP

4.2.1 Motivation

Two of the most important, and certainly the two most frequently studied, postural stability parameters are the CoM and CoP. As seen in Chapter 2, these two parameters are typically studied in isolation of one another. The question posed in the current research is whether or not this is sufficient for a proper understanding of postural stability of humans as they perform complex postural tasks?

As a human performs some arbitrary postural task they move individual body segments by articulating their joints resulting in continuous motion of their CoM throughout the performance of the task. What ultimately determines stability is whether the moments associated with these movements, the motion of CoM, and any additional forces acting on the human body are balanced such that stability is maintained. One way in which the postural control system can balance these moments is through the position of the CoP as

this directly impacts the magnitude of the moment caused by the GRF. What is of interest to the current research is the exact nature of the relationship between CoM and CoP. Is one entirely dependent upon the other? Is CoM allowed to move far from its most stable position before CoP is adjusted to help bring CoM back towards a more stable position? Exactly how similar is the motion of these two important postural stability parameters and how much delay is there in this aspect of the postural stability control system?

4.2.2 Results and Discussion

In Figures 4.3 through 4.15, values for the CoP are measured from the leftmost point of the heel of the foot (similar to the depiction in Figure 3.5) while the values for CoM are measured from the intersection of the sagittal and lateral planes of the body.

Quiet Standing Task

Figures 4.3 through 4.7 show the motion of the CoM and CoP of each foot for all participants during the quiet standing task (with the exception of Participant 06, whose motion capture file was unusable for this task). As expected based on observations in previous studies, as well as on the dynamics of the quiet standing task, it can be seen that all participants maintained very steady CoM and CoP in the lateral direction, with the exception of Participant 03 (Figure 4.4), who suffers from foot drop in her left foot as previously discussed, and an oscillation of CoM in Participant 07's data (Figure 4.7). This oscillation can be attributed to movement of the arms and possibly upper torso given that there is no corresponding motion of the CoP to indicate shifting of weight between the feet. In the sagittal direction, most participants show a very strong visual correlation between the CoM and CoP. It appears that Participant 03 is the most severe exception to this, and again this can likely be attributed to the degradation of neuromuscular pathways associated with her foot drop condition. The strongest correlation is seen in Participant 05 (Figure 4.6), where the plots of CoM and CoP of each foot can almost be superimposed upon one another. There are, however, some subtle differences that are of interest, and which are also present in the data from the other participants. The CoM has a slightly, but noticeably, steeper

slope when it moves; indicating that the velocity of the CoM is greater than that of the CoP. Also, some of the more minor changes in CoM are "washed out" in the CoP plot; indicating that the postural stability control system can accommodate small perturbations in CoM without effecting a change in GRF.

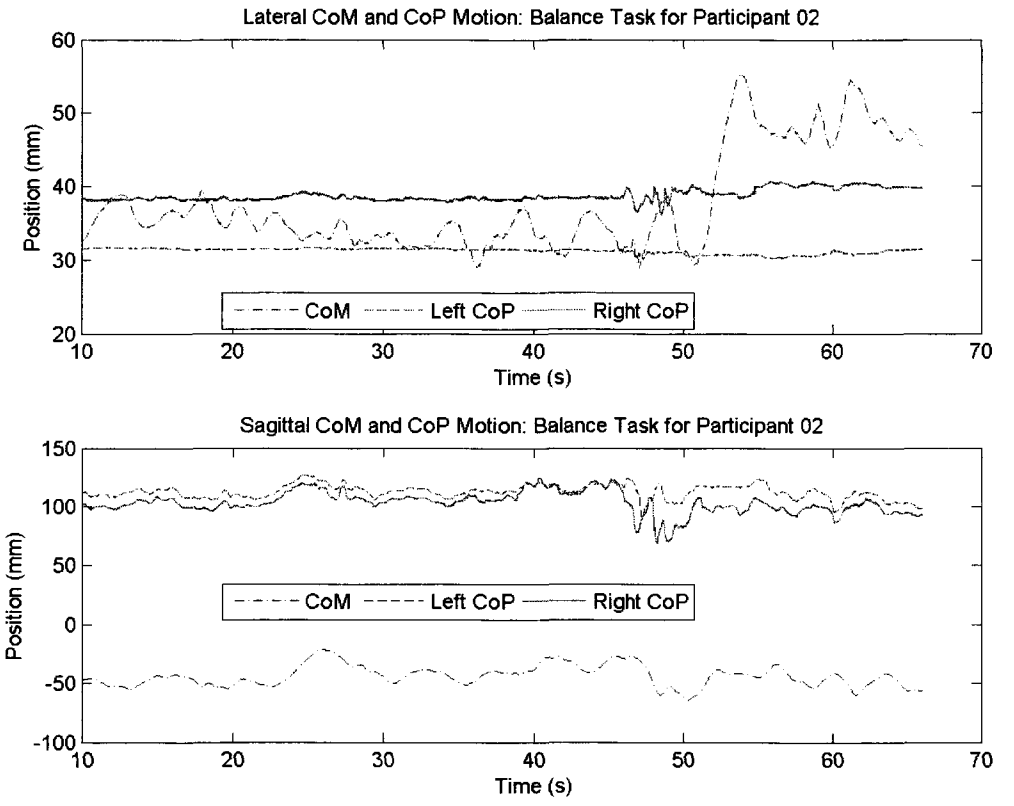

Figure 4.3: Motion of CoM vs CoP for quiet standing task - Participant 02.

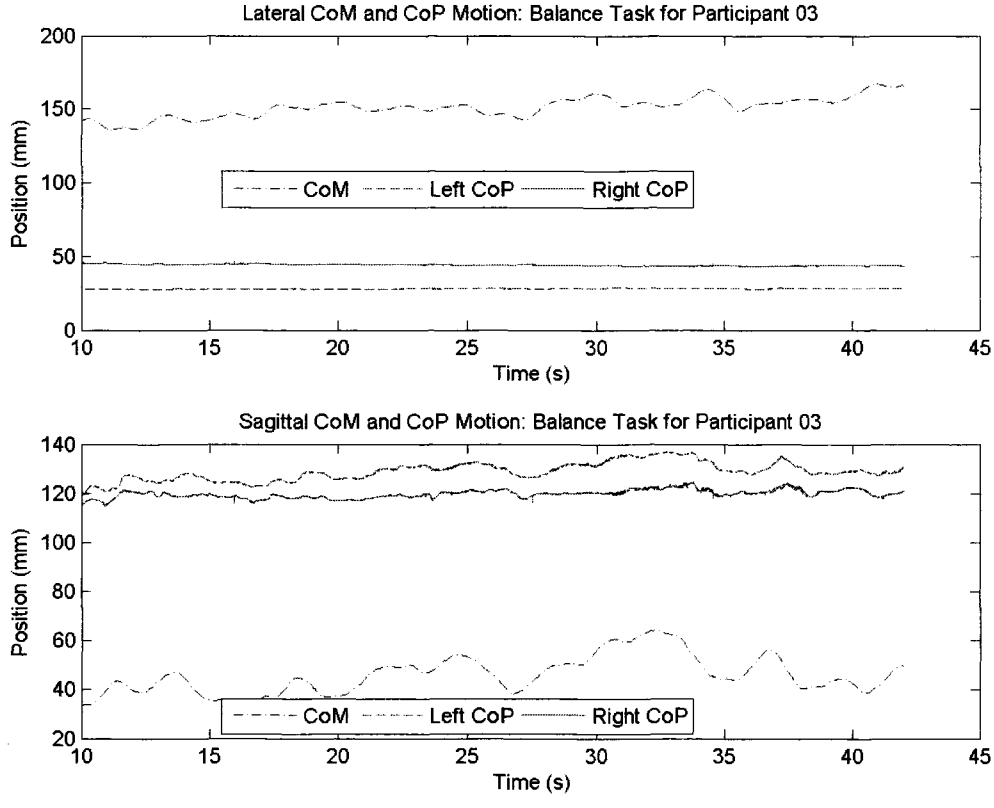

Figure 4.4: Motion of CoM vs CoP for quiet standing task - Participant 03.

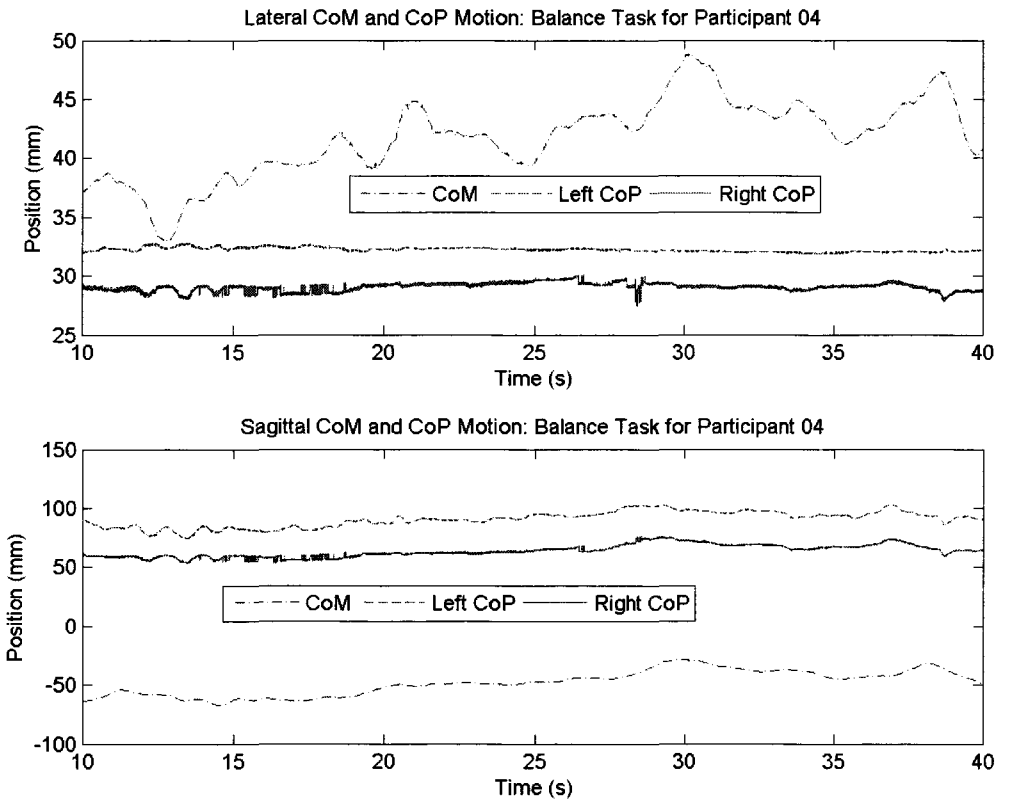

Figure 4.5: Motion of CoM vs CoP for quiet standing task - Participant 04.

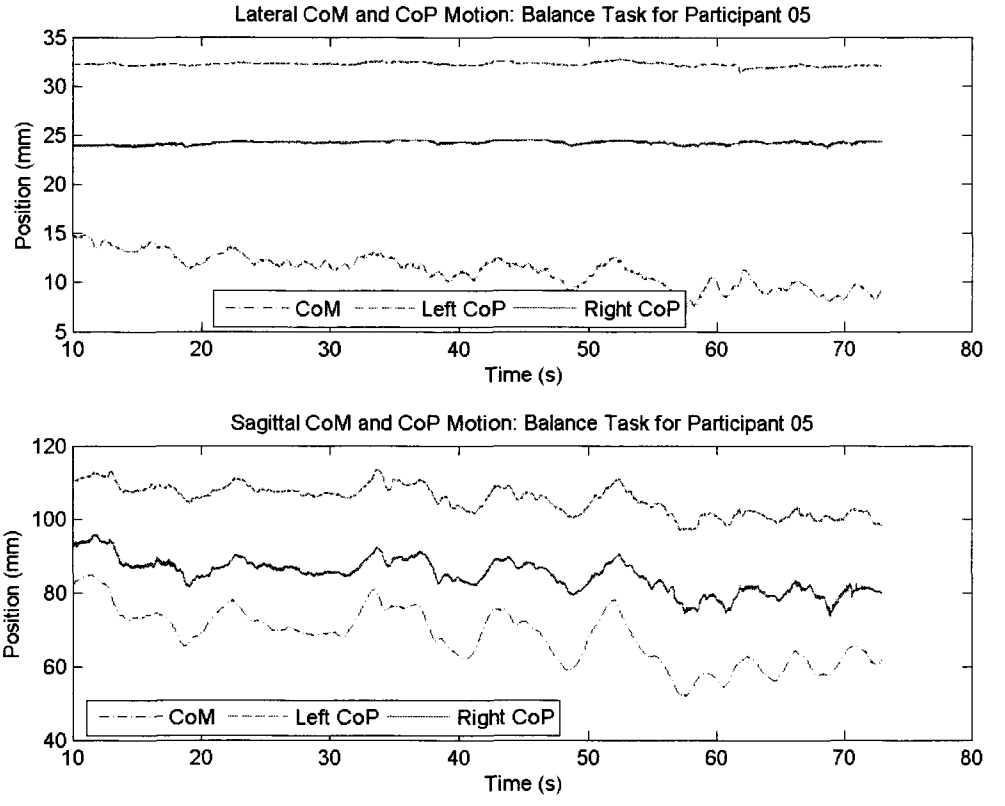

Figure 4.6: Motion of CoM vs CoP for quiet standing task - Participant 05.

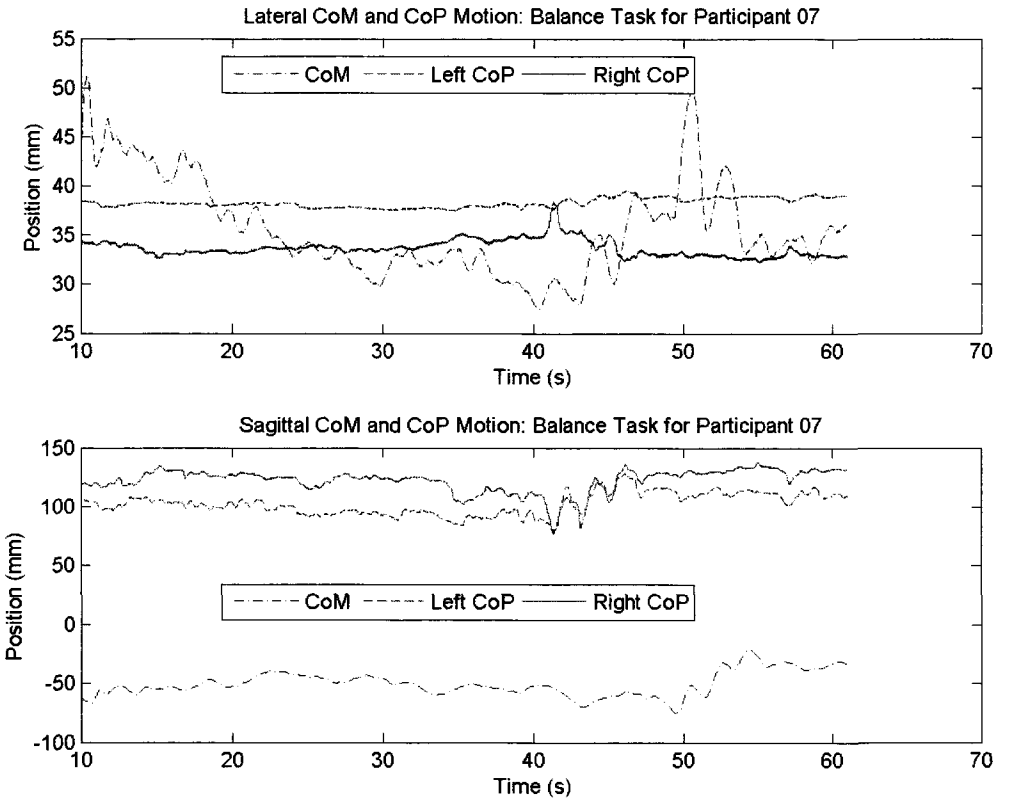

Figure 4.7: Motion of CoM vs CoP for quiet standing task - Participant 07.

Table 4.4 shows the results of the cross-correlation analysis on the CoM and CoP. All Pearson r-values meet or exceed a significance test of $p < 0.01$. With the exception of Participant 07, all participants show very high correlation between the sagittal components of CoM and CoP. This indicates that the majority of influence on the sagittal component of the CoM for the quiet standing task is related to the CoP. For the left feet, the magnitude of the lag between CoM and CoP is consistently between 1.0 and 1.4 seconds, excepting Participant 07. However, while CoM leads CoP for Participants 02 and 04, it lags CoP for the other participants. In the case of the right feet, in the sagittal direction, all participants except for 02 and 07 have lags with a magnitude of 0.32 seconds. Some participants have CoM leading CoP, while others have CoM lagging CoP. All participants were right foot dominant, which might account for the lag in the right feet being approximately one third of that in the left feet. In the lateral direction, the degree of correlation between CoM and CoP is much less, with the exception of the right foot of Participant 03. However, the lag associated with the correlation of lateral CoM and CoP for the right foot of Participant 03 represents such a large fraction of the overall data that the correlation can not be relied upon. The lower correlation coefficients for the lateral direction indicate that the majority of the influence on the lateral component of CoM comes from a source other than control of CoP. Finally, the relatively large magnitudes of the lag for this task indicate that continuous, fast control is not necessary. Instead, CoM may be allowed to drift freely towards the BoS until the gradual adjustment of CoP reverses the direction of CoM velocity. At this point CoM begins to drift in the opposite direction and is allowed to continue thus until the gradual adjustment of CoP again reverses the direction of CoM velocity. This strategy is similar to station keeping strategies used for geosynchronous satellites. This strategy is extremely efficient, but only effective for relatively low and predictable velocities of CoM.

Participant	Sagittal				Lateral			
	Left Foot		Right Foot		Left Foot		Right Foot	
	r-value	lag(s)	r-value	lag(s)	r-value	lag(s)	r-value	lag(s)
02	0.8860	1.09	0.8892	1.23	-0.2626	-2.71	0.4992	-0.75
03	0.7024	-1.39	0.8725	-0.32	0.2664	-0.60	-0.5536	5.00
04	0.5777	1.31	0.6949	0.32	-0.3080	0.22	-0.3867	-4.21
05	0.6848	-1.03	0.6407	-0.32	0.8246	-0.43	-0.5830	0.00
07	-0.2267	-0.15	-0.2705	-0.92	-0.0769	3.08	0.1378	0.00
mean	0.5248	-0.03	0.5654	0.00	0.0887	-0.09	-0.1773	0.01
std	0.4345	1.22	0.4797	0.82	0.4694	2.08	0.4762	3.29

Table 4.4: Cross-correlation analysis of motion of CoM vs CoP for quiet standing task.

Sagittal Lift/Lower Task

Analysis of the sagittal lift/lower task was only successful on three of the six participants. This was due to the large number of occluded markers, upwards of 80% of the frames for some markers, in the motion capture data. The nature of the task, bending down to pick up the weight, resulted in the participants' bodies occluding many of the markers important in defining the body segments for calculation of CoM. The table itself likely also contributed to occluded markers in the lower extremities.

Figures 4.8, 4.9, and 4.10 show the motion of the CoM and CoP in both the sagittal and lateral directions for participants 02, 03, and 05 respectively. In the lateral direction, Participants 02 and 03 (Figures 4.8 and 4.9 respectively) show a substantial amount of movement of the CoM. This is somewhat unexpected given the nature of the task; however, in the case of Participant 02 this motion is accompanied by a corresponding difference in CoP between the left and right feet and this difference is consistent with the direction of the CoM motion (shifting of the CoP of the right foot towards the outer edge of the foot appears to be associated with movement of the CoM towards the left).

In the sagittal direction there is a strong visual correlation in the shape of the CoM and CoP plots; both exhibit a characteristic double peak associated with each repetition of the task. The first peak can be associated with the participants bending forward to pick the mass off the ground, or reaching forward to pick it up from the table in the other half of the cycle. The valley can be associated with the participants returning to an upright posture while holding the mass. The second peak can be associated with the participants reaching forward to place the mass on the table, or bending down to put it on the floor in the second half of the cycle.

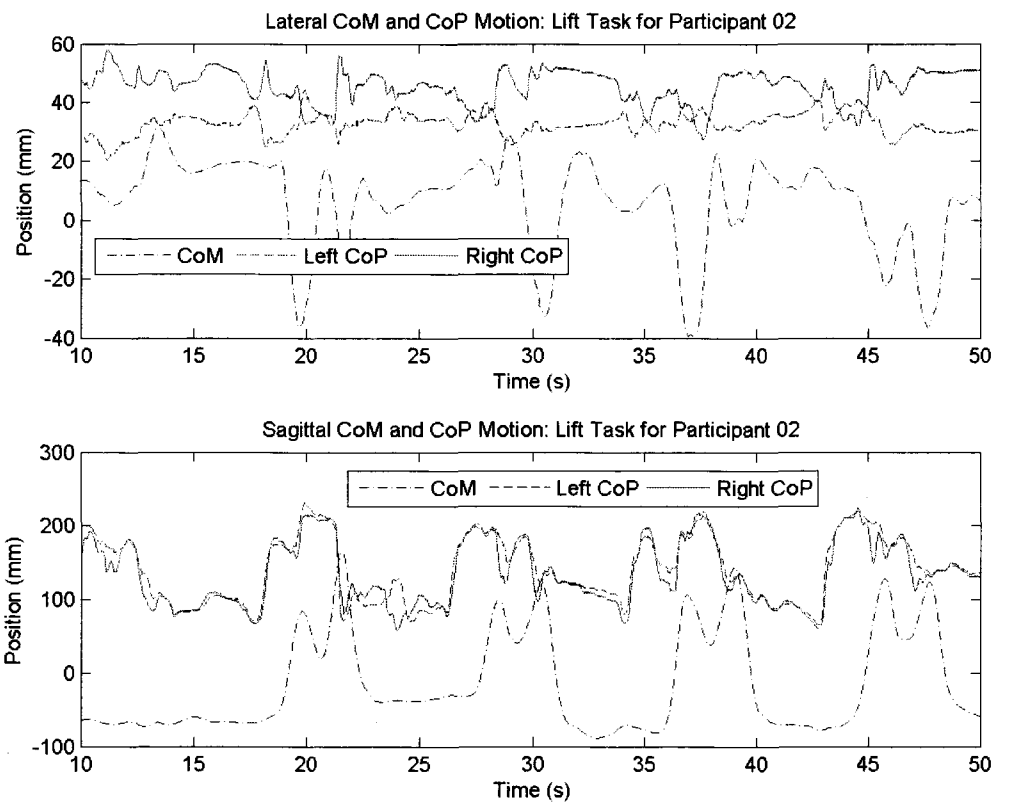

Figure 4.8: Motion of CoM vs CoP for sagittal lift/lower task - Participant 02.

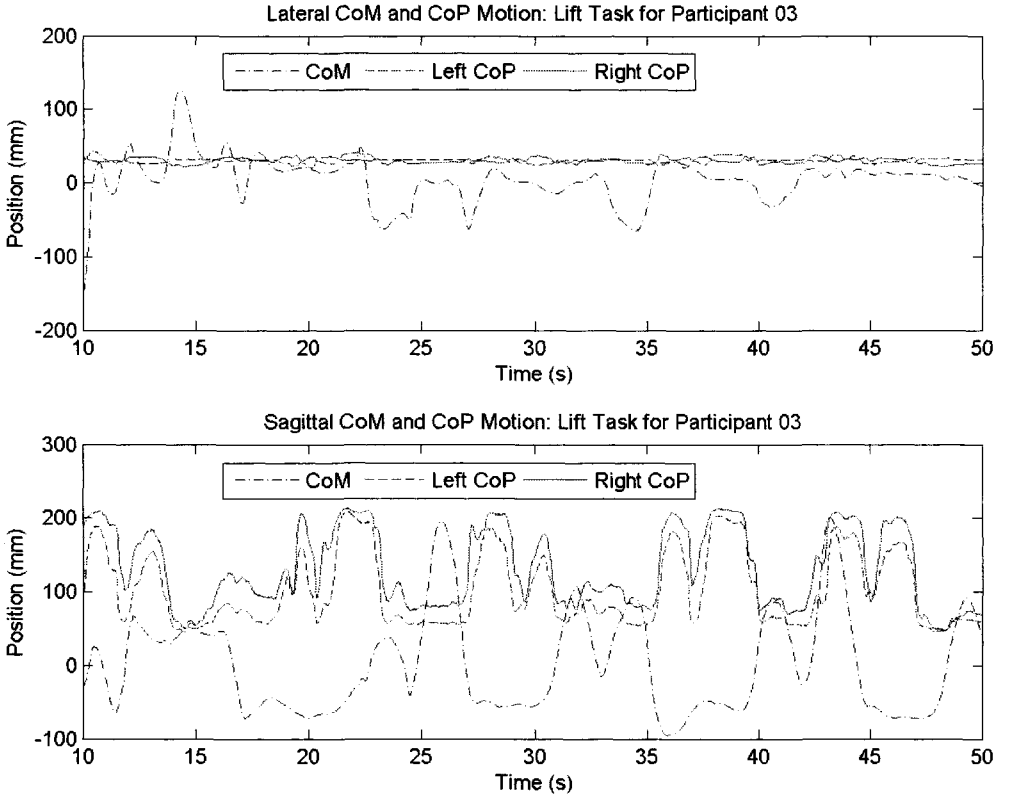

Figure 4.9: Motion of CoM vs CoP for sagittal lift/lower task - Participant 03.

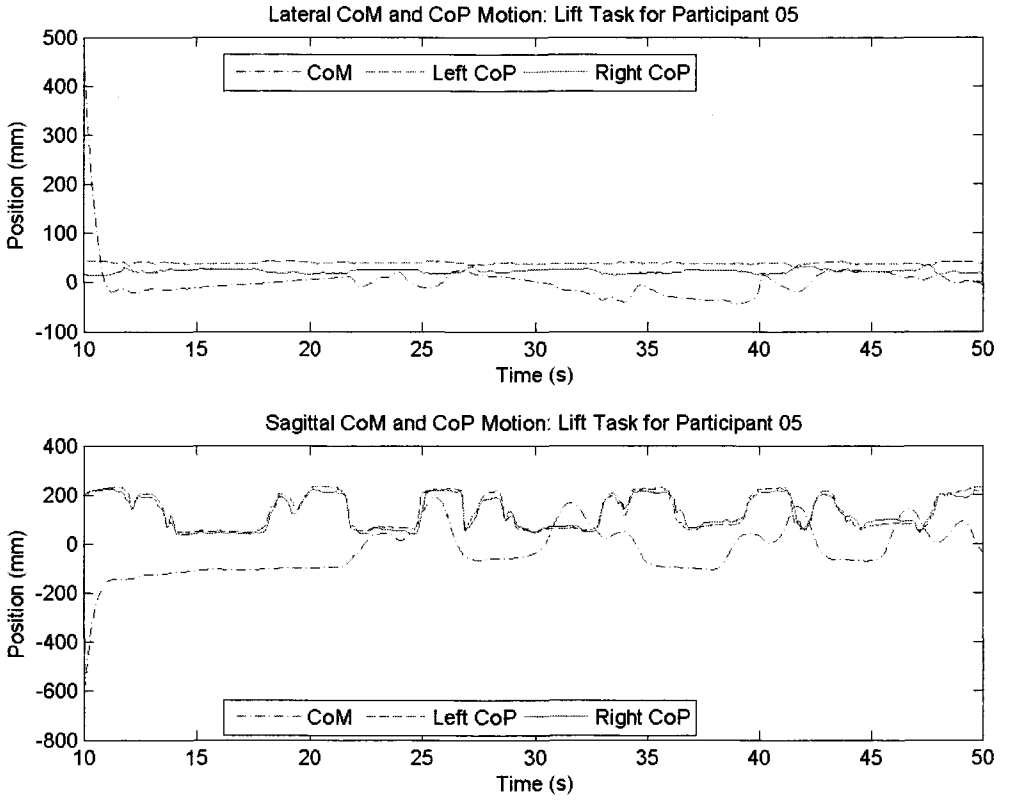

Figure 4.10: Motion of CoM vs CoP for sagittal lift/lower task - Participant 05.

Table 4.5 shows the results of the cross-correlation analysis on the CoM and CoP. All Pearson r-values meet or exceed a significance test of $p < 0.01$. While there is substantial correlation shown between CoM and CoP, it shows that the majority of influence on the CoM comes from sources independent of the CoP for the sagittal lift/lower task. Given that the task involves large articulations about the hips, knees, ankles, and also extension of the upper limbs, these results are not surprising. The level of independence between CoM and CoP can be attributed to the articulation of the joints allowing sudden changes in both the position of CoM as well as the mass moment of inertia of the body. This suggests that it is very important to consider articulated models for predicting MII as well as to discover and include those parameters that do have a larger influence on CoM in these types of dynamic tasks.

	Sagittal				Lateral			
Participant	Left Foot		Right Foot		Left Foot		Right Foot	
	r-value	lag(s)	r-value	lag(s)	r-value	lag(s)	r-value	lag(s)
02	0.1434	1.69	-0.2151	-2.56	0.1931	-6.00	-0.3793	-4.91
03	0.2667	-3.73	0.2004	-3.72	0.3078	-3.94	0.3010	-2.72
05	-0.2218	-1.97	-0.1873	-1.93	0.4335	-1.80	-0.2725	-1.71
mean	0.0628	-1.34	-0.0673	-2.74	0.3115	-3.91	-0.1169	-3.11
std	0.2540	2.77	0.2322	0.91	0.1203	2.10	0.3658	1.64

Table 4.5: Cross-correlation analysis of motion of CoM vs CoP for sagittal lift/lower task.

Stair Climbing Task

The nature of the stair climbing task, coupled with the use of the pressure insoles, resulted in unusable pressure data. When participants raised a foot to step up, a CoP was still recorded despite the fact that no weight (and thus no pressure) was on the foot. This was due to the fact that the tightness of the shoes worn by the participants was enough to register some small amount of pressure in the sensors. Even without that limitation, the CoP for the non-stance foot would be undefined. As well, due to a combination of limited stair depth and awkwardness caused by the equipment and cables attached to the participants, cases where the participant did have their foot on the ground tended to have only the ball of the foot in contact with the stair while pressures were still sensed near the heel of the sensor due, again, to the tightness of the shoes. Another problem arose from the fact that the cables attached to the pressure sensors at the participants' ankles and the narrowness of the stairs prevented them from turning around to walk down the stairs naturally. Instead, participants had to back down the stairs. There is evidence that at least two participants were uncomfortable enough with this movement that they instinctively grabbed the railings on the stairs to steady themselves. Finally, there is also evidence in the recorded pressure data that suggests that the cables that were connected to the pressure sensors at the participants' ankles were suffering from loose connections when the cables moved in response to the stepping motion. For these reasons analysis of the results of the stair climbing task was deemed to be futile. However, for the sake of completeness, the raw data are represented in the figures found in Appendix B.1.

Motion Platform Task

Figures 4.11 to 4.15 show the motion of the CoM and CoP for all participants for the motion platform task (with the exception of Participant 06, whose motion capture file was unusable for this task). The first item of interest in these results is that, despite the changes in roll angle of the motion platform (observable in the changes in CoM in the lateral direction), there is little motion of the CoP in the lateral direction for any of the

participants. In the sagittal direction, while most participants show substantially noisier CoP plots, the similarities between the motion of CoM and CoP are still evident. As with the quiet standing task, the overall shape of the CoM and CoP motion is similar, the CoM exhibits slightly steeper slopes, and the more subtle motions of CoM become washed out in the CoP plot.

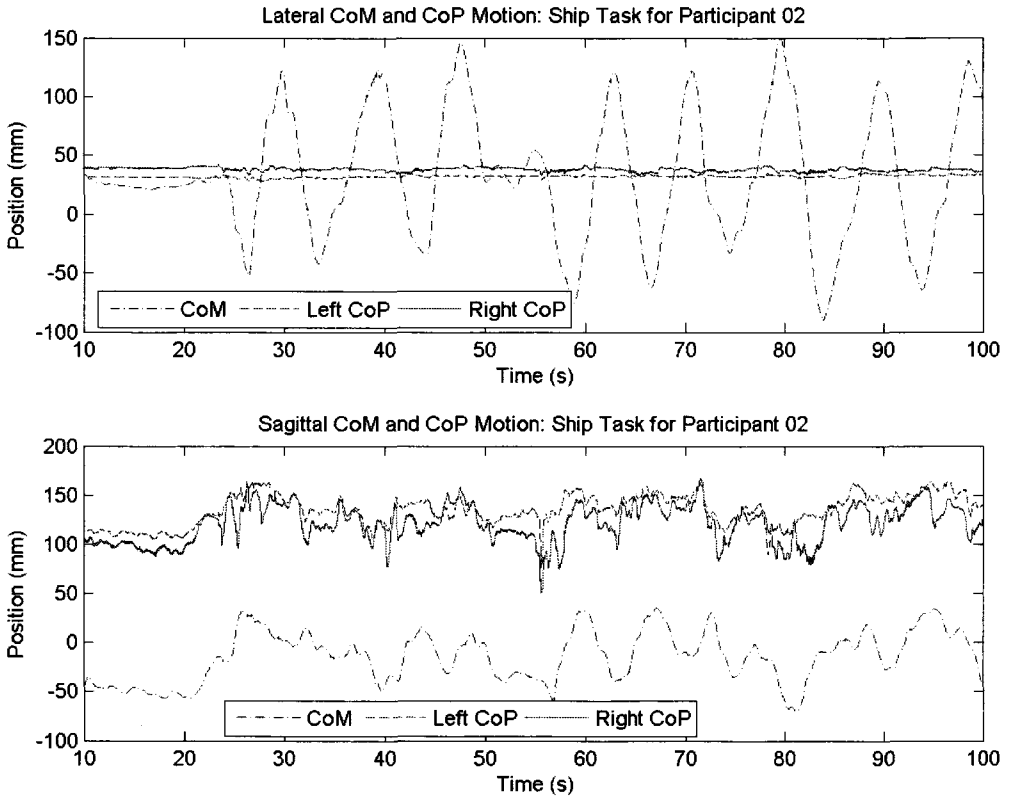

Figure 4.11: Motion of CoM vs CoP for motion platform task - Participant 02.

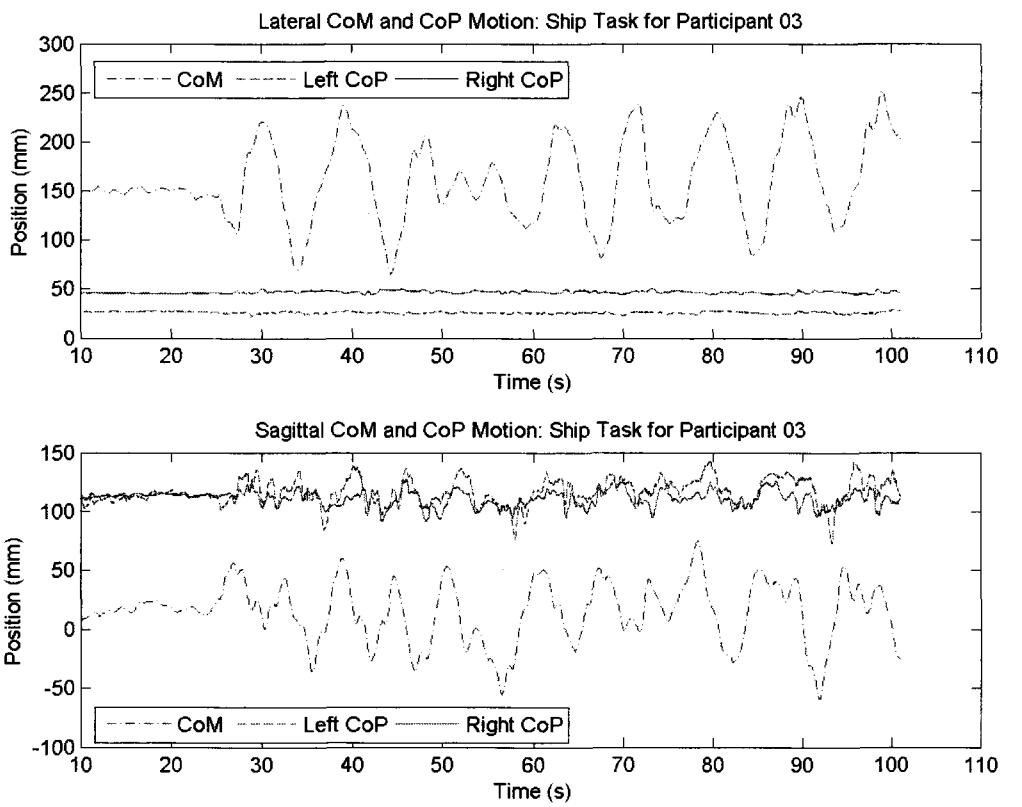

Figure 4.12: Motion of CoM vs CoP for motion platform task - Participant 03.

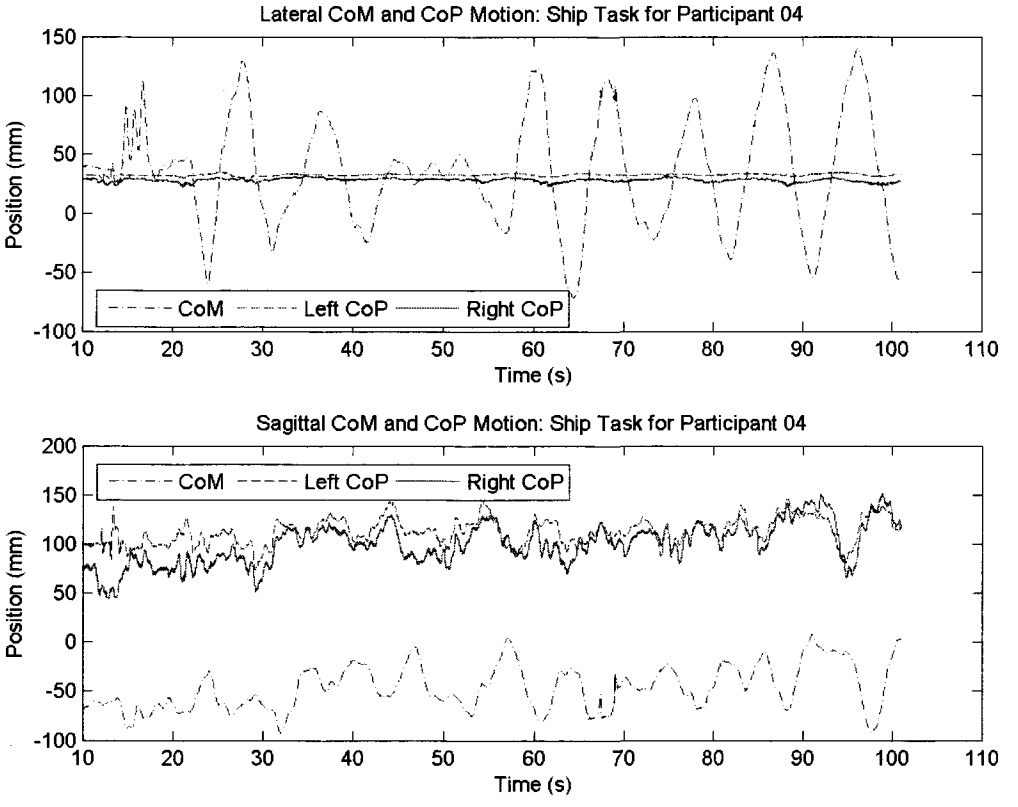

Figure 4.13: Motion of CoM vs CoP for motion platform task - Participant 04.

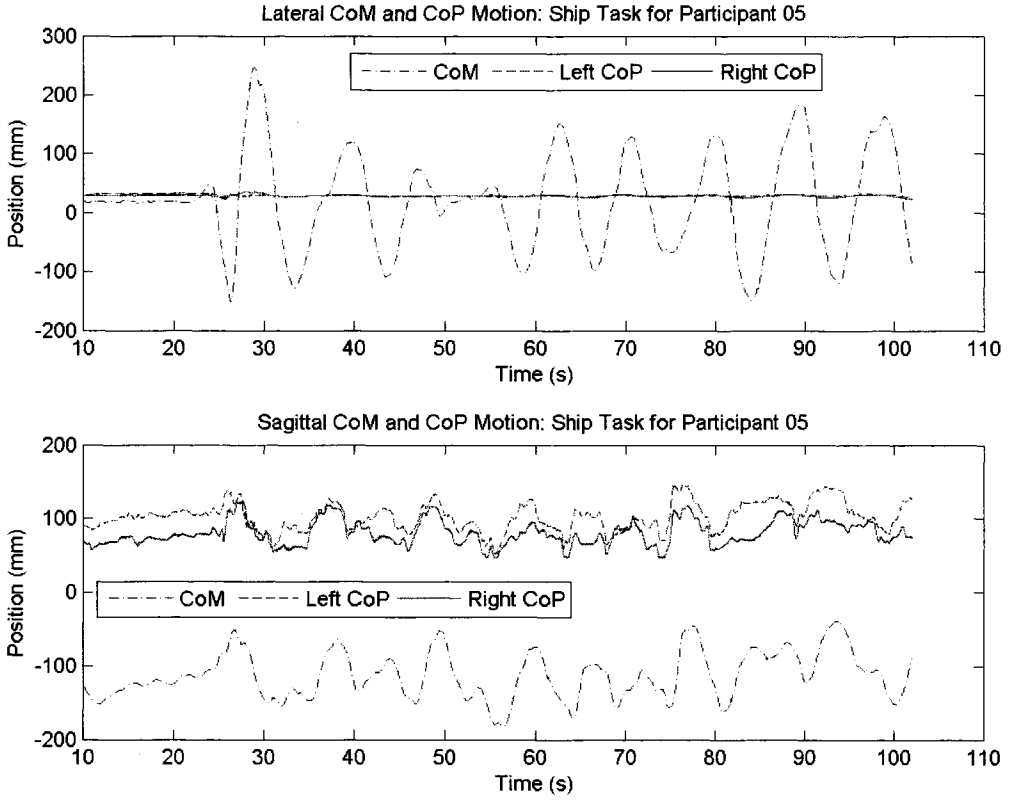

Figure 4.14: Motion of CoM vs CoP for motion platform task - Participant 05.

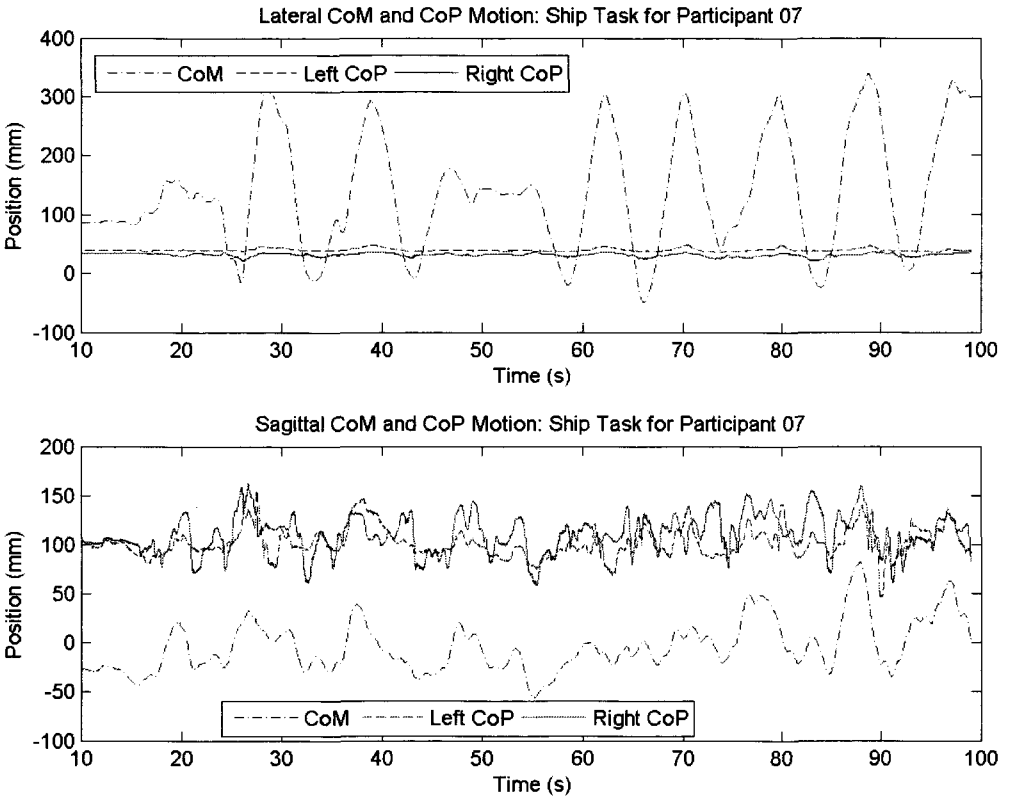

Figure 4.15: Motion of CoM vs CoP for motion platform task - Participant 07.

Table 4.6 shows the results of the cross-correlation analysis on the CoM and CoP. All Pearson r-values meet or exceed a significance test of $p < 0.01$. As with the quiet standing task, there is very high correlation between the sagittal components of CoM and CoP with the exception of Participant 07. While Participant 04 shows a substantially larger lag, the other participants show similar lags to the quiet standing task in the left foot. On the other hand, the difference in lags between the left and right feet that were seen in the quiet standing task are not present in the motion platform task. Rather, the lags in left and right feet are quite similar. There are larger correlations in the lateral direction than in the quiet standing task; most likely these can be attributed to the large roll angles involved in the platform motion as compared to the minimal sway angles in the lateral direction for the quiet standing task.

	Sagittal				Lateral			
Participant	Left Foot		Right Foot		Left Foot		Right Foot	
	r-value	lag(s)	r-value	lag(s)	r-value	lag(s)	r-value	lag(s)
02	0.8440	0.90	0.7551	0.90	-0.1421	-5.00	0.3689	1.65
03	0.8037	-1.42	0.7422	-1.34	0.4727	-1.76	-0.3399	1.28
04	0.8491	2.59	0.8001	2.47	0.5750	2.33	0.5756	2.03
05	0.9302	0.67	0.7589	0.59	0.4204	0.73	0.8379	0.57
07	-0.1448	-0.31	0.7257	-0.27	0.7214	-0.16	-0.6742	3.61
mean	0.8568	0.69	0.7641	0.65	0.3315	-0.93	0.3606	1.38
std	0.0530	1.64	0.0251	1.56	0.3222	3.19	0.5049	0.62

Table 4.6: Cross-correlation analysis of motion of CoM vs CoP for motion platform task.

4.2.3 Conclusions

In Section 4.2.1 several questions were posed regarding the relationship between the motion of CoM and CoP during postural stability tasks. The first question, whether either CoM or CoP are directly dependent on the other, can be answered in the negative. While all of the tasks performed in the current research showed some level of correlation between CoM and CoP, even the tasks with the strongest correlation showed that there are other parameters that influence the motion of CoM and CoP. As well, it was shown that there are significant differences in correlation and lag between the two values across participants. The second question, whether CoM is allowed to move far from its stable position prior to CoP being adjusted to help bring CoM back to a more stable position, can also be answered in the negative. In all of the tasks performed in the current research CoM and CoP were both in constant motion. The final question posed was to determine exactly how similar the motion of these two postural stability parameters is and how much delay exists in this aspect of the postural stability control system. While the level of correlation between CoM and CoP was shown to be highly dependent on the specific task being performed, significant correlation was seen in all of the tasks performed and the level of correlation for a given task was fairly constant between participants. The amount of delay between the motion of CoM and CoP (for those tasks for which the synchronization circuit was available) varied greatly between tasks, participants, direction (sagittal versus lateral), and dominant versus non-dominant feet. Some participants had CoM leading CoP while others showed the opposite trend.

These results indicate that it is very important to consider that the relationship between CoM and CoP is heavily dependent upon the specific task being performed; which in turn implies that the postural stability control system acts differently during various postural stability tasks. As well, the results indicate that studying only one or two postural stability parameters in isolation is not sufficient. Despite the strong correlation between CoM and CoP, there are other major influences on these parameters that are dependent on the task being performed and on the system as a whole.

4.3 Kinematic Threshold of CoP

4.3.1 Motivation

The ability to predict MIIs is important in evaluating ship designs, as well as for establishing workplace safety regulations for shipboard industries. As discussed in Section 2.1.1, there are existing models for the prediction of MII which have been tuned using experimental data and proven to have reliable accuracy for simple shipboard tasks. These models, specifically the model described by Graham [23], are based on rigid bodies and predict whether tipping would occur under a given set of conditions. As shown in Equation (2.1), the tipping coefficient is based on the length of the BoS (which in turn defines the maximum CoP) as well as the height of the CoM.

While these models have proven adequate, given tuning against experimental data, there are several potential deficiencies with such a simplified model. The use of a rigid body in the model is perhaps the most restricting aspect of Graham's model. Many shipboard tasks are very dynamic in nature, involving articulation of multiple joints through reaching and bending, changing external forces as loads are lifted or carried, and multiple postural positions may be involved in a single complex task. A single, rigid body representation can not account for the changes in CoM, mass moment of inertia, joint stiffness, and other physical properties that occur in the human body during complex tasks. Another deficiency with Graham's model is that it assumes the CoP is allowed to reach the full extent of the BoS prior to an MII. While tuning allows the model to overcome this deficiency, it would be preferable for the model to represent the actual bounds of CoP; which likely differ from task to task and person to person. These differences between individuals performing various tasks are another potential deficiency of the existing models.

If all of these deficiencies can be confirmed, it would provide strong support for the development of a more robust model which is a better analogue to human postural stability. As such, the current research will attempt to establish what the actual bounds of CoP are for the various tasks examined, as well as how the differences between individuals and the actual tasks themselves affect the various postural stability parameters.

4.3.2 Results and Discussion

Traditional models for predicting MII are based on tipping conditions for rigid bodies [23, 19] and, for the most part, assume that the threshold for CoP is defined by the boundaries of the BoS. The minima and maxima of Figures 4.16 through 4.27 represent the kinematic thresholds of CoP, the thresholds at which the postural stability control system takes action to move the CoP away from the edges of the BoS, for the tasks conducted in the current research. The data shows that the postural stability control system is maintaining CoP well within the BoS. While no MIIs were induced in the current research, this substantially reduced portion of the BoS in which the CoP is maintained may imply that an individual's comfort level, perceived stability, and other non-physical parameters may result in MIIs occurring prior to the CoP reaching the boundary of the full BoS. Similar observations have been made by Langlois *et al.* [1]. This, in turn, may imply that traditional MII models are not representative of the complete system. It is important to note, in the case where both feet are in contact with the support surface, that a CoP that approaches the inner edge of the side of the foot is not inherently unstable or likely to cause an MII, as it is possible to shift weight towards the opposite foot without inducing an MII or experiencing a fall. Due to the reference frame described in Section 3.2.1, this means that in the lateral direction we are interested in the minima of the CoP for the left feet and the maxima of the CoP for the right feet.

Sagittal Lift/Lower Task

The sagittal lift/lower task is a particularly good task for evaluating the kinematic threshold of CoP due to the large external moments caused by lifting the 10 kg mass. These moments, if not actively countered by postural stability control, would easily cause tipping. As seen in Figures 4.16 through 4.21, the sagittal component of the CoP is maintained between 0.2 and 0.9 of the length of the foot for all participants. The lateral component of CoP is maintained between 0.2 and 0.8 of the width of the foot when all participants are considered. However, several of the participants show signs of standing with their CoP shifted towards the inner

edge of at least one of their feet. If those cases are excluded due to the fact that they do not represent an approach toward a kinematic threshold of MII using the argument given above, the lateral component of CoP is maintained between approximately 0.2 and 0.6 of the width of the foot from the outer edge of the foot. Considering both the sagittal and lateral thresholds together this represents an area under the BoS that is only 28% of the total area under the BoS. This represents a substantial reduction in the observed kinematic thresholds of CoP compared to the overal area under the BoS. As traditional MII models allow CoP to reach the edge of the BoS before an MII is predicted this may also suggest that these models would have a tendency to underestimate the number of MIIs if the kinematic threshold for MII is similarly reduced in area.

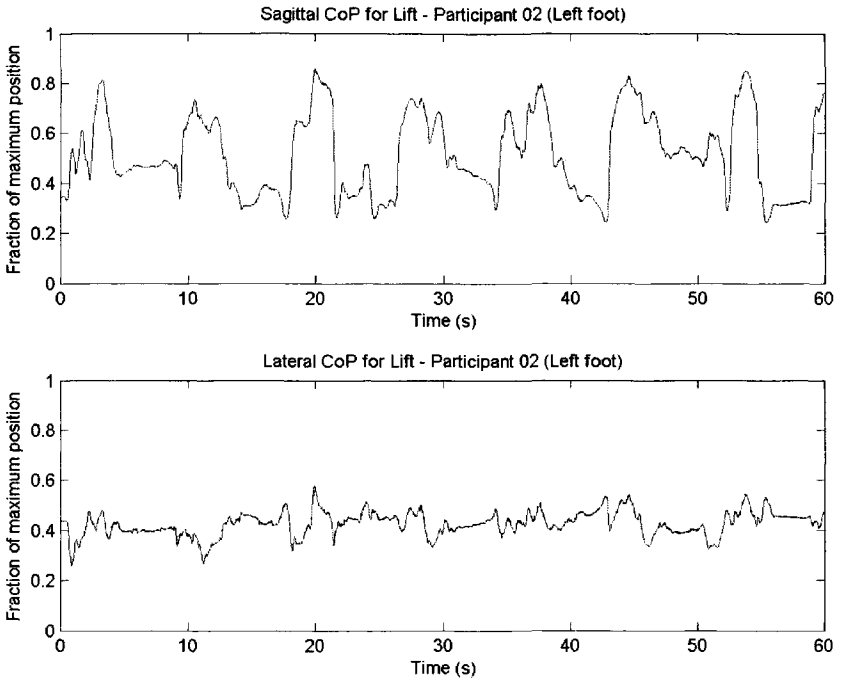

(a) Left Foot

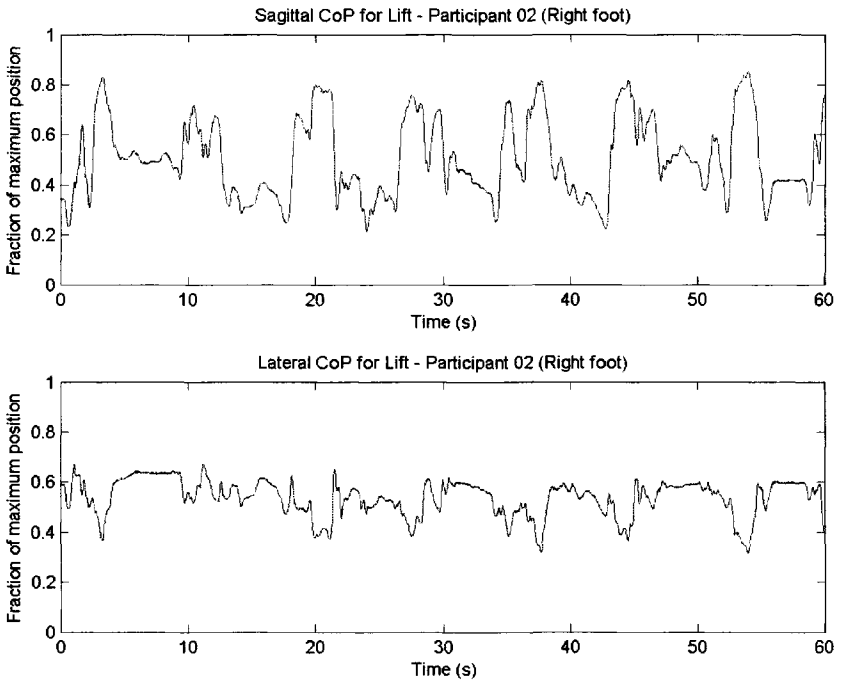

(b) Right Foot

Figure 4.16: CoP for lift task - Participant 02.

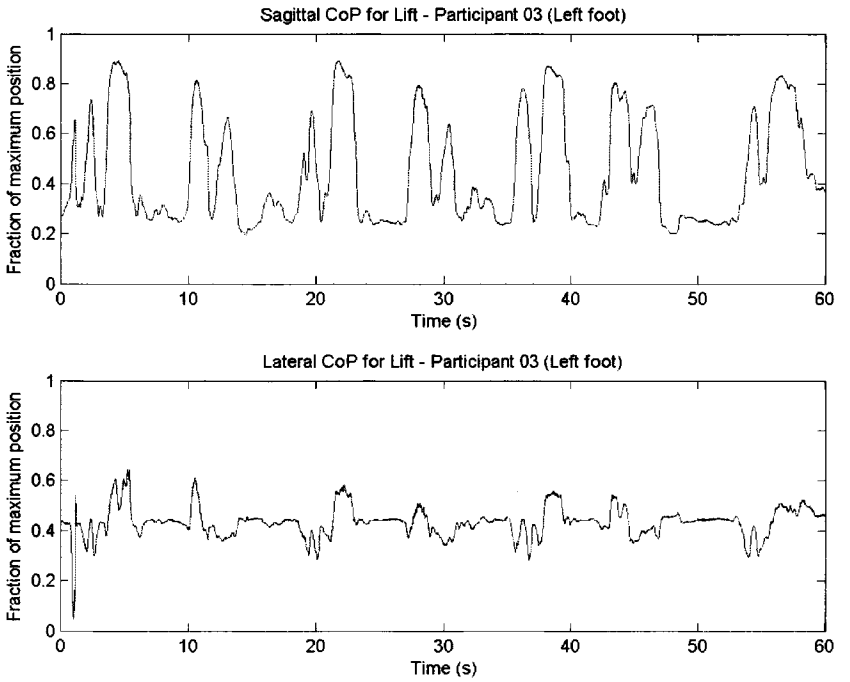

(a) Left Foot

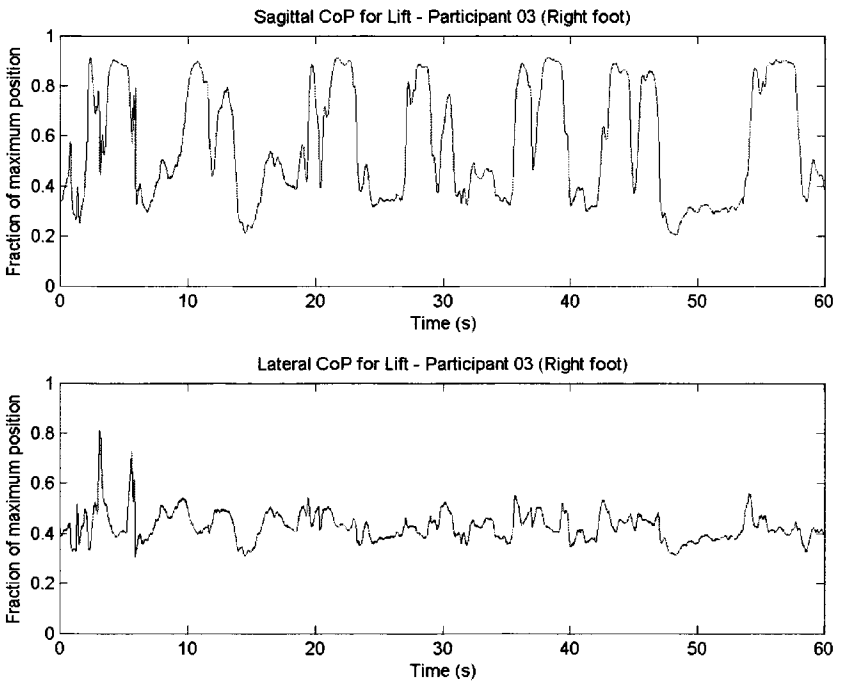

(b) Right Foot

Figure 4.17: CoP for lift task - Participant 03.

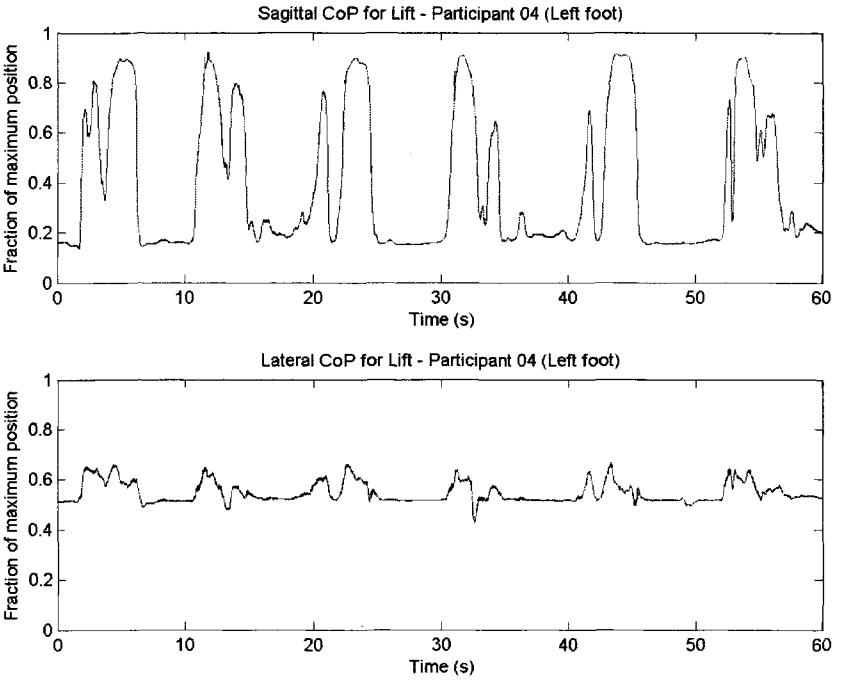

(a) Left Foot

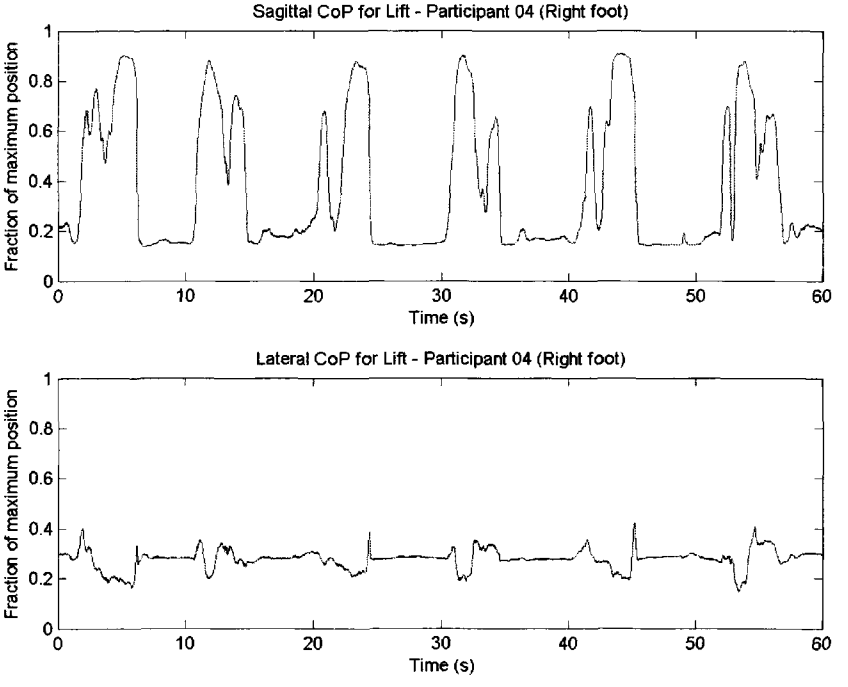

(b) Right Foot

Figure 4.18: CoP for lift Task - Participant 04.

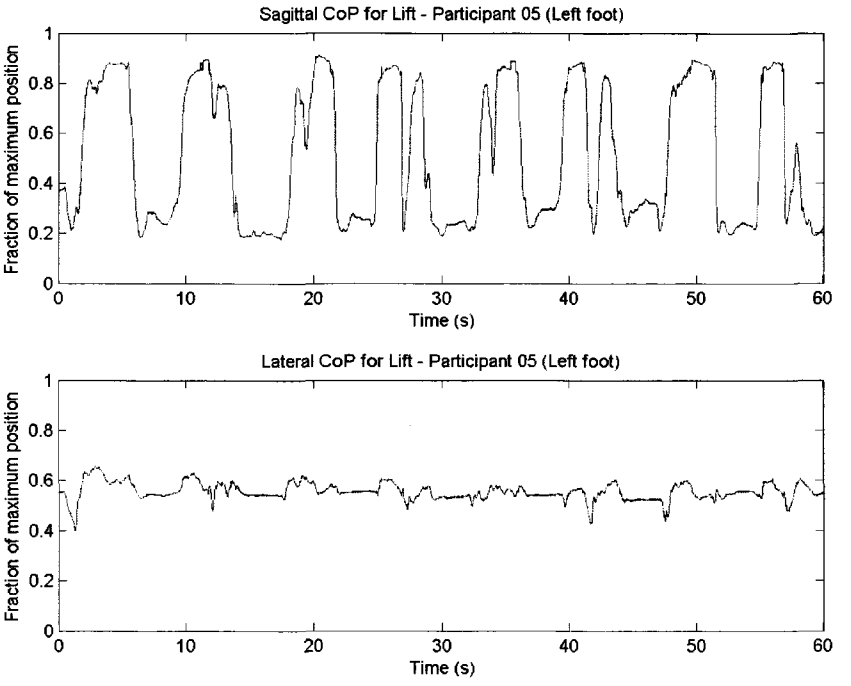

(a) Left Foot

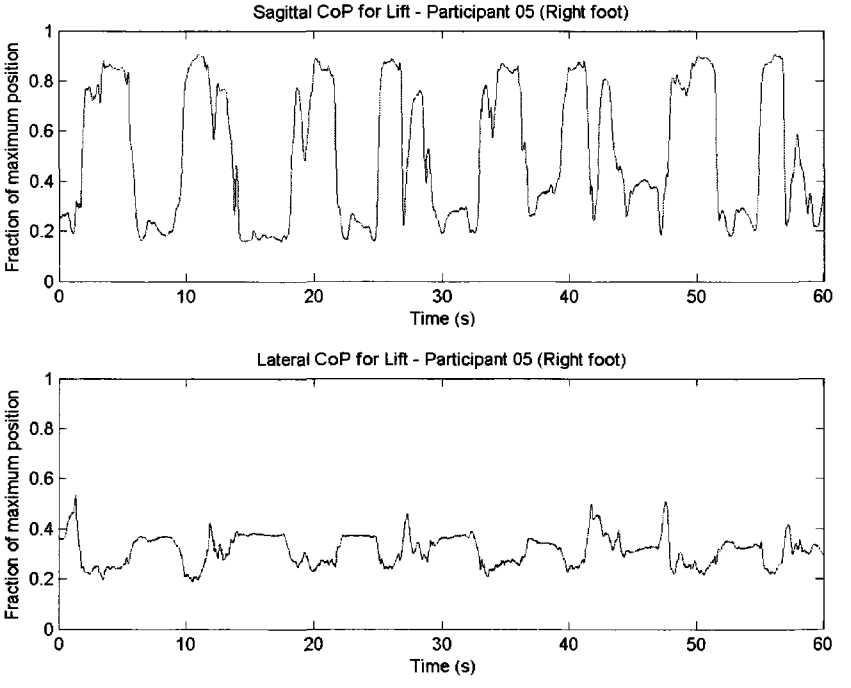

(b) Right Foot

Figure 4.19: CoP for lift Task - Participant 05.

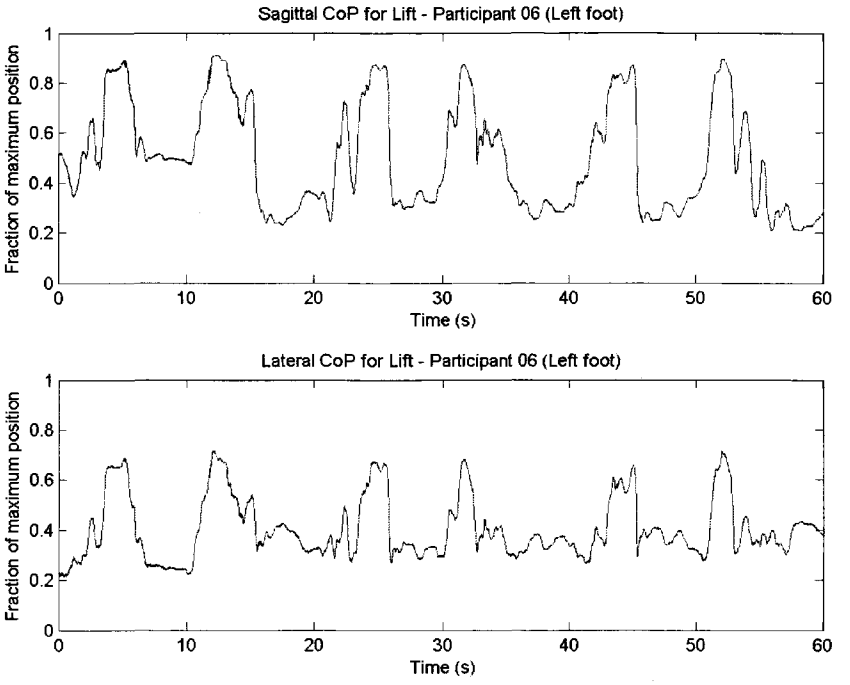

(a) Left Foot

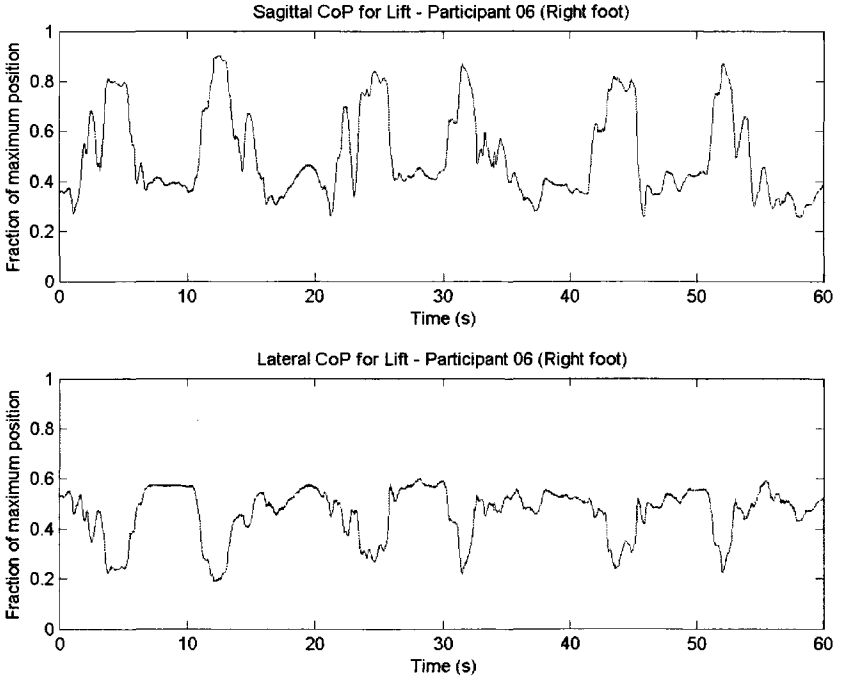

(b) Right Foot

Figure 4.20: CoP for lift task - Participant 06.

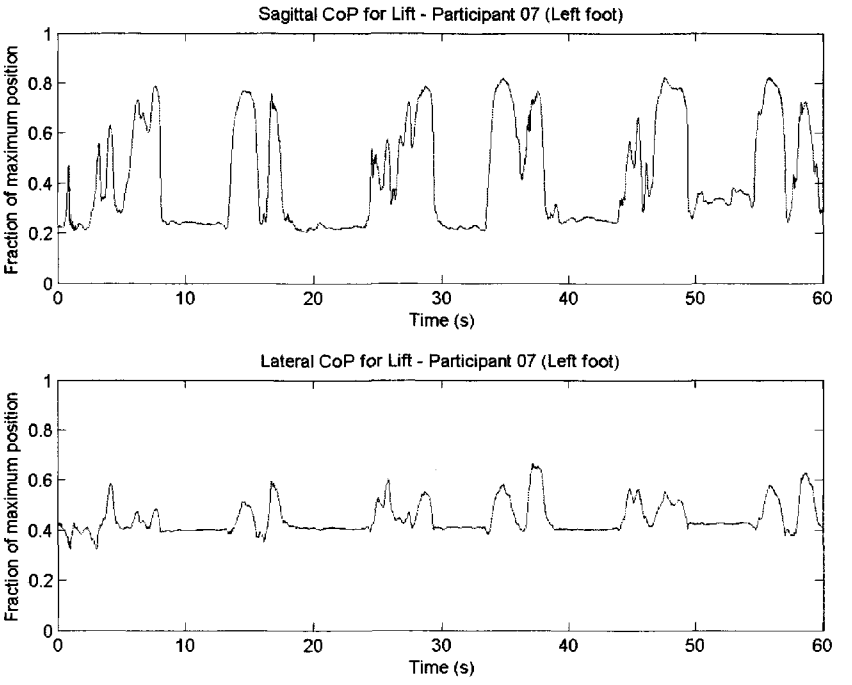

(a) Left Foot

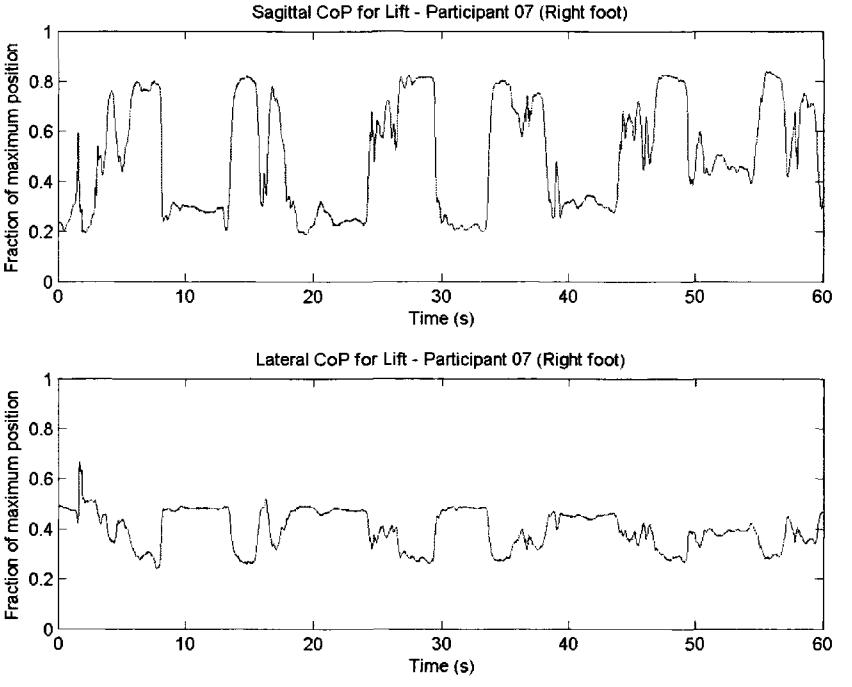

(b) Right Foot

Figure 4.21: CoP for lift task - Participant 07.

Stair Climbing Task

This analysis can not be performed due to the limitations discussed in Section 4.2.2. However, for the sake of completeness, the raw data is represented in the figures found in Appendix B.2.

Motion Platform Task

As seen in Figures 4.22 through 4.27, the motion platform task shows signs of even tighter control of the CoP than the sagittal lift/lower task. The sagittal component of CoP is maintained between 0.2 and 0.6 of the foot length for both feet of all participants in this task, while the lateral component is maintained between 0.3 and 0.6 of the foot width. Interestingly, with the exception of Participant 03, all participants showed signs of maintaining the lateral component of CoP of the left foot at approximately 0.4 of the foot width from its outer edge while maintaining that of the right at approximately 0.4 of the foot width from its inner edge. Considering the full span of values for the lateral component, this still represents only 12% of the total area under the BoS.

Unfortunately, it is difficult to determine whether this tighter grouping of CoP is representative of tighter kinematic thresholds for CoP in this type of task (one where the participant does not know what external perturbances will be applied and thus may maintain CoP further from the edges of the BoS to prevent sudden movement of CoP towards them) or if it is merely a case of the quiescent motion used not being drastic enough to push the CoP to its thresholds at all compared to the large moments experienced in the sagittal lift/lower task.

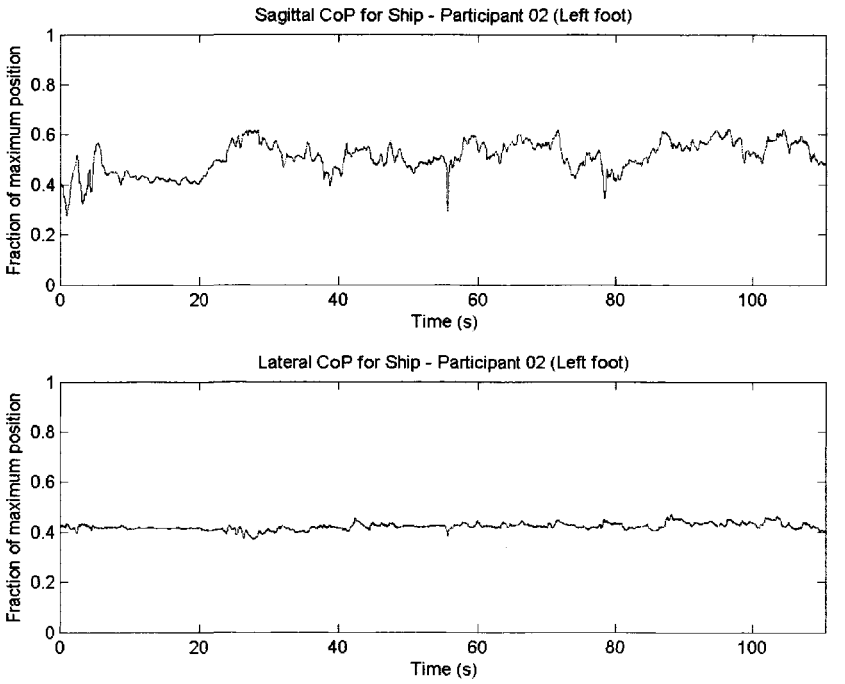

(a) Left Foot

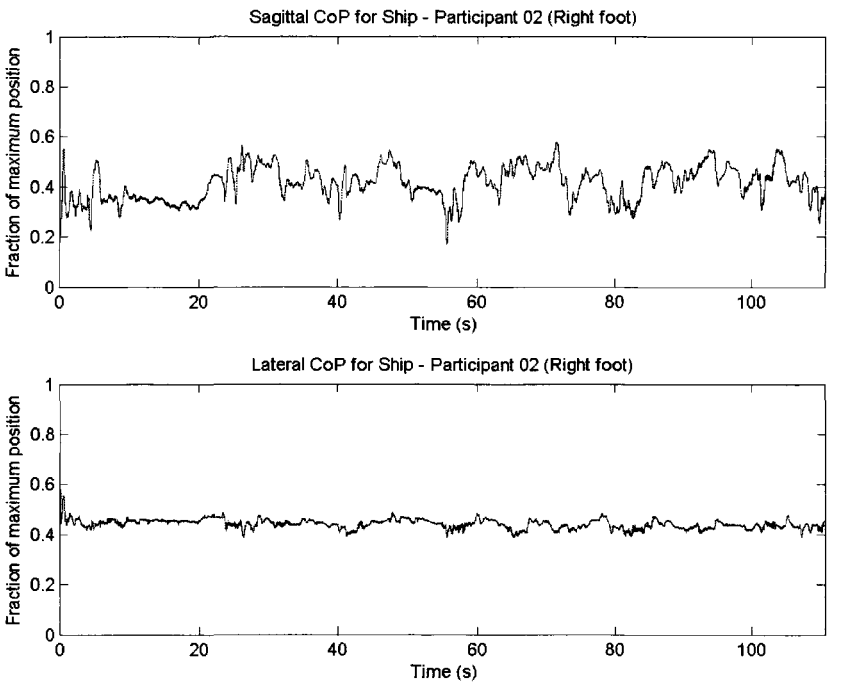

(b) Right Foot

Figure 4.22: CoP for ship task - Participant 02.

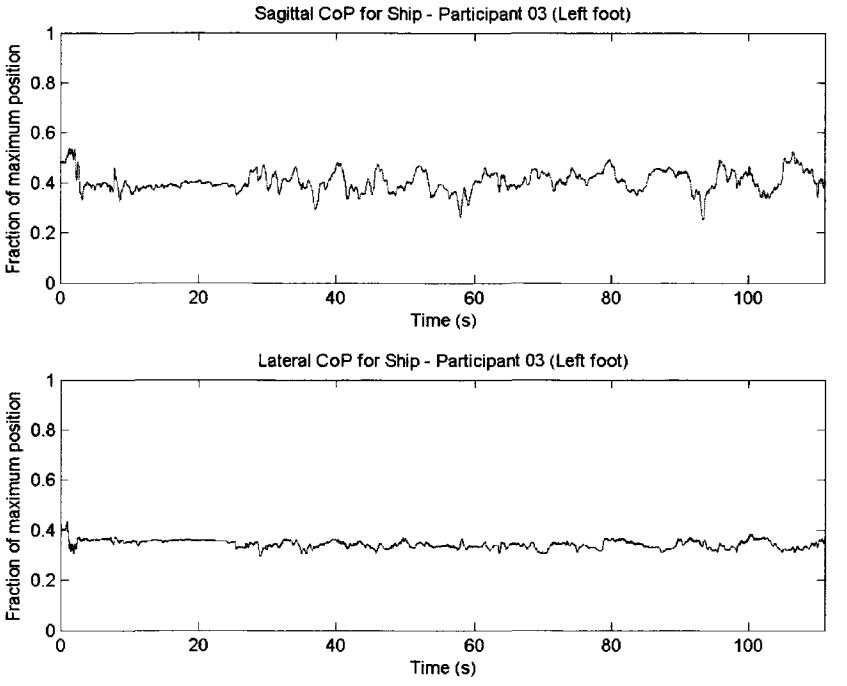

(a) Left Foot

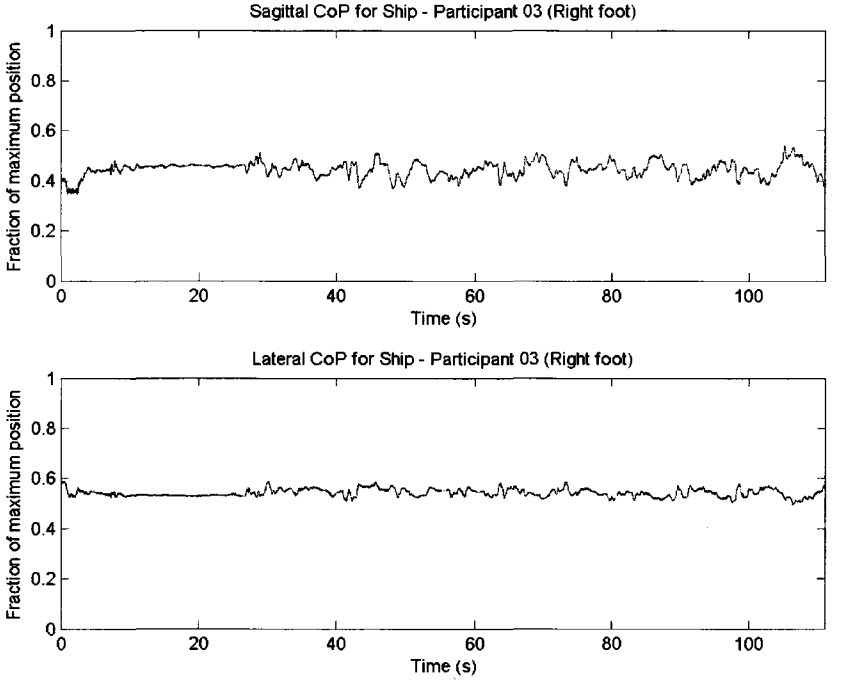

(b) Right Foot

Figure 4.23: CoP for ship task - Participant 03.

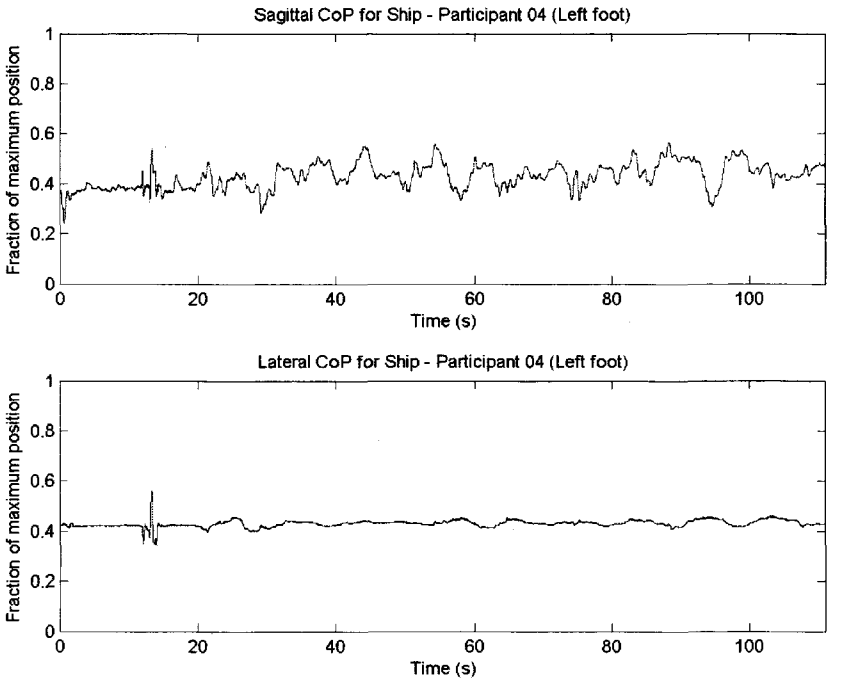

(a) Left Foot

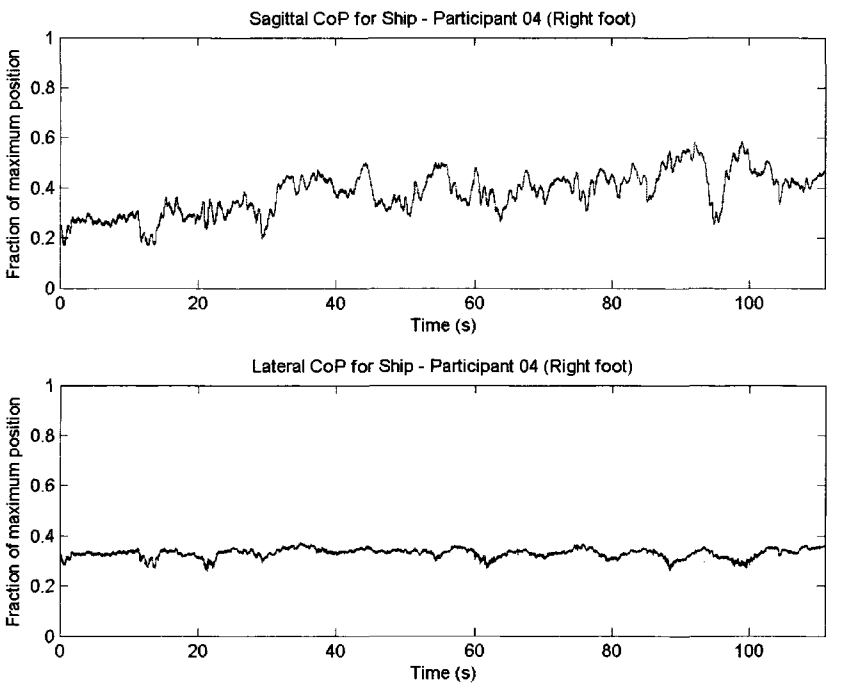

(b) Right Foot

Figure 4.24: CoP for ship task - Participant 04.

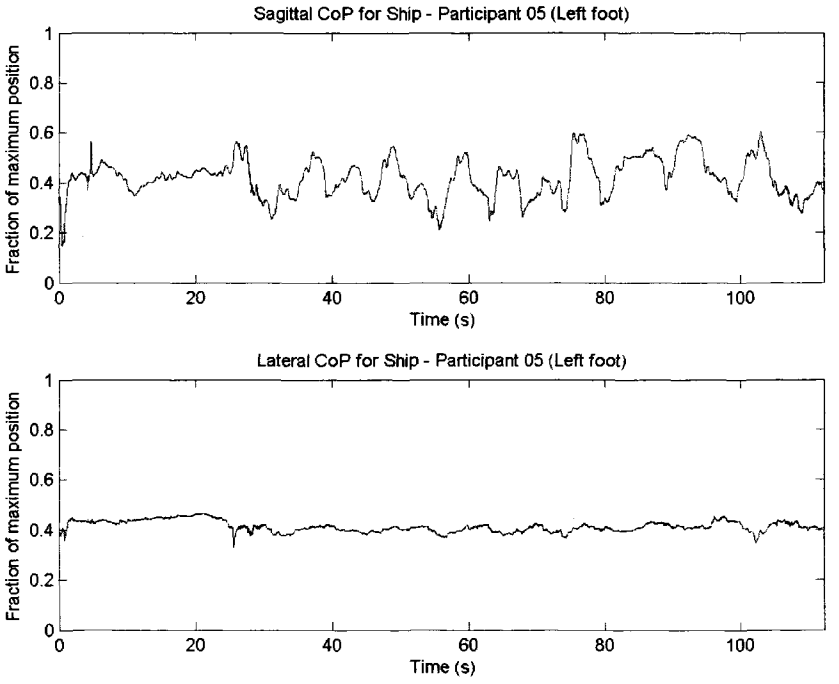

(a) Left Foot

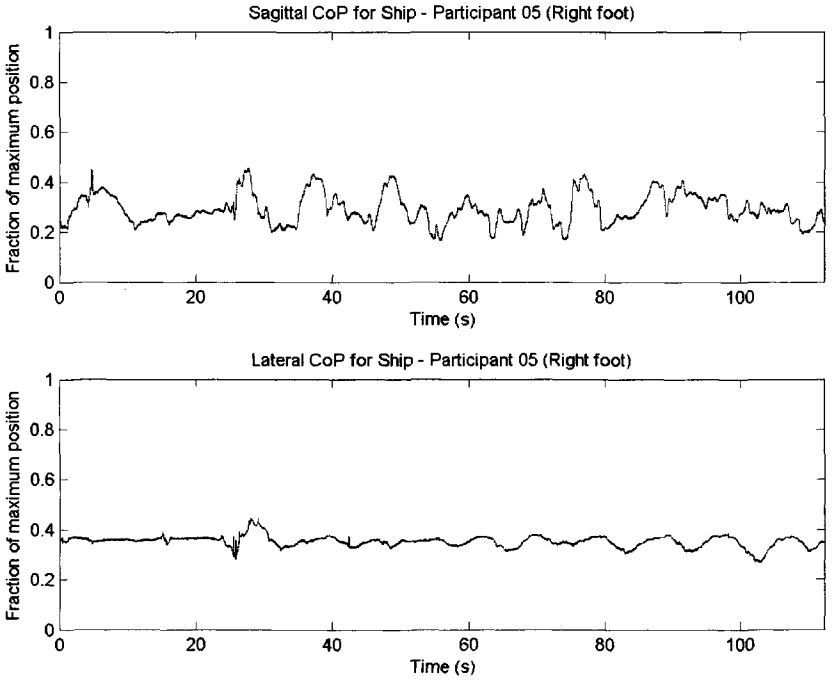

(b) Right Foot

Figure 4.25: CoP for ship task - Participant 05.

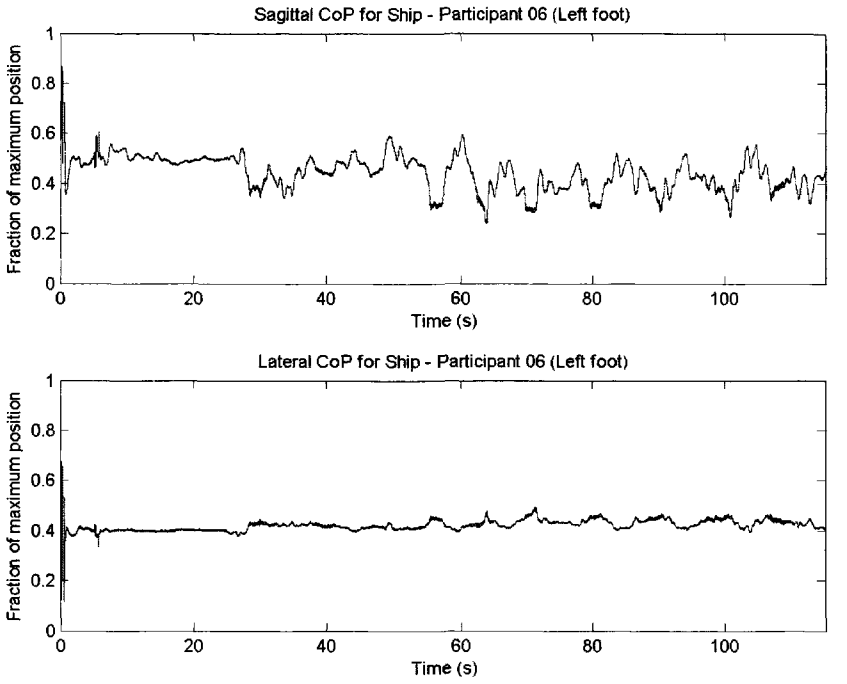

(a) Left Foot

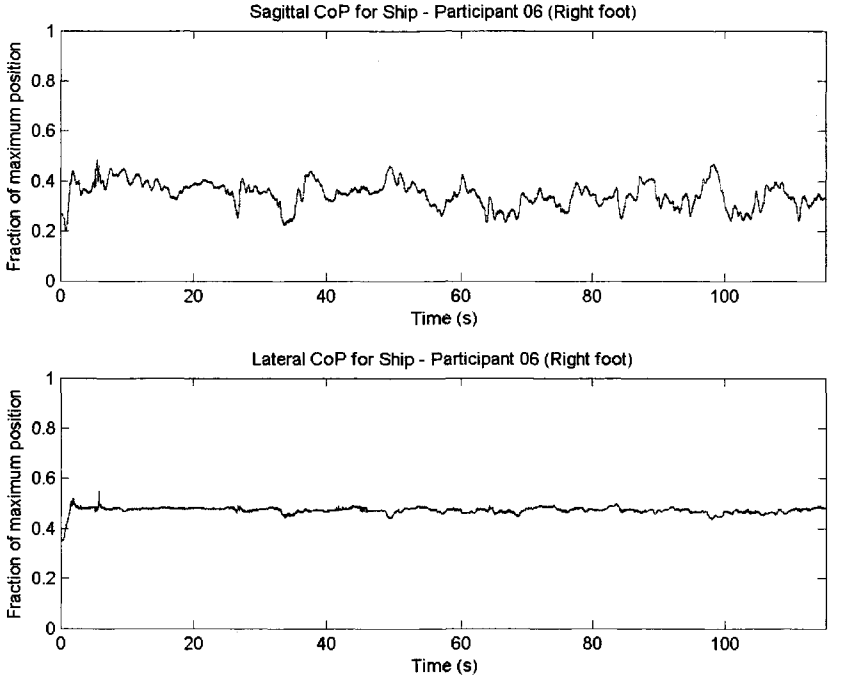

(b) Right Foot

Figure 4.26: CoP for ship task - Participant 06.

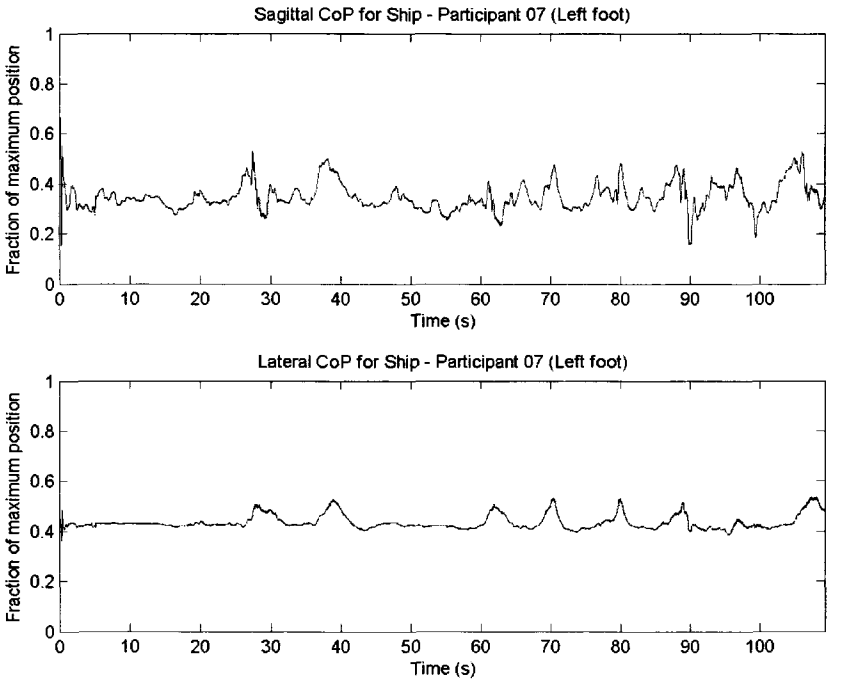

(a) Left Foot

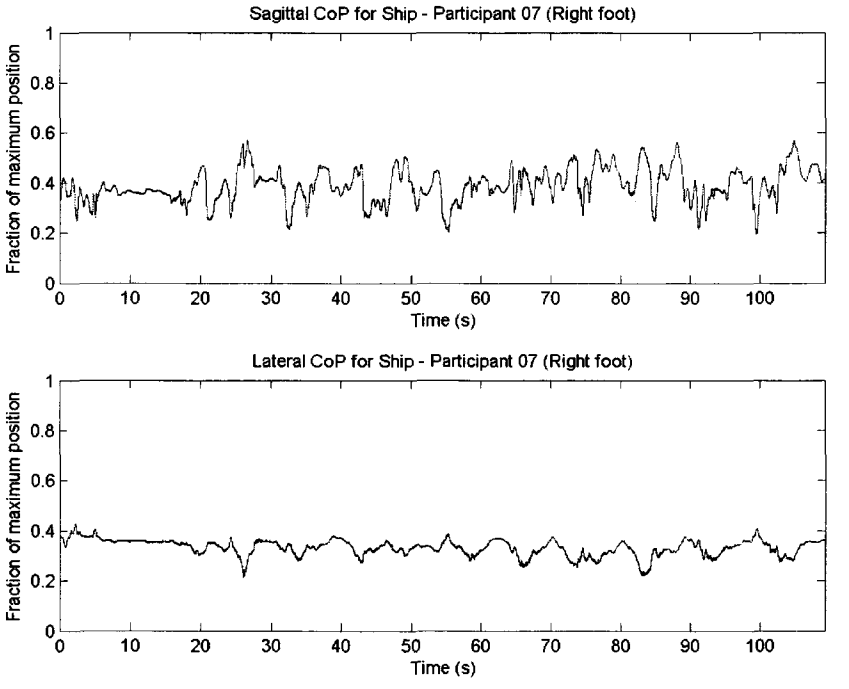

(b) Right Foot

Figure 4.27: CoP for ship task - Participant 07.

4.3.3 Conclusions

Several deficiencies have been identified with regards to Graham's [23] model, Equation (2.1), for predicting MIIs. The first such deficiency was the use of a rigid body to model a human performing complex, shipboard tasks. The human body has multiple DoF at each of its many joints and it was shown in Section 4.2 that tasks involving articulation of these joints significantly alter the relationship between CoM and CoP. These results provide strong support for the development of an articulated model for the prediction of MII, similar to the one proposed by Langlois *et al.* [1]. The second deficiency identified was the fact that the model allows the CoP to reach the absolute bounds of the BoS before predicting an MII. Langlois *et al.* [1] have already shown that a significant number of MIIs can occur that are not accounted for by the existing models. The current research may provide insights to support this fact; showing that CoP traverses an area that represents only a small fraction of the total BoS in all of the postural stability tasks that were investigated. However, it is important to note that further studies must be conducted to determine whether or not it is valid to infer that the area in which CoP is controlled within is similarly reduced when MIIs are actually induced. Finally, it has been shown that the fraction of the BoS that the CoP traverses varies from task to task and person to person. This supports the idea of developing a model that is based upon the physical properties of the system, as well as tuning parameters based on the individual's postural stability aptitude.

4.4 Most Active Muscles in Human Postural Stability Control and their Relative Amplitudes

4.4.1 Motivation

While it is true that CoM and CoP are two of the most important and frequently studied parameters associated with postural stability, they are not the only parameters of interest. Ultimately, both CoM and CoP are controlled through the actuation of muscles. Six of the most common muscles associated with postural stability were identified in Section 3.2.2.

What is of interest to the current research are the roles each of these muscles play in postural stability. Are they all equally involved? Are there delays in the activation of some muscles in relation to others? Are some muscles primarily responsible for the direct control of CoM, while others are primarily responsible for the direct control of CoP?

4.4.2 Results and Discussion

The abbreviations for muscle names, as well as the function of each muscle, are given in Table 3.1.

Quiet Standing Task

Tables 4.7 through 4.10 show the results of the cross-correlation analysis on the CoM and estimated muscle forces. The magnitude of correlation of the sagittal component of CoM with the left side muscles is fairly consistent across all muscles and participants; although, individual participants vary from having CoM lead muscle force to having it lag muscle force. Of particular interest is that the agonist-antagonist pairs show similar levels of correlation which indicates that they play fairly equal roles in the control of CoM. While lags vary widely between participants, they are fairly consistent across the muscles of individual participants and tend to be on the order of one to three seconds. That said, there are indications that individual participants favour one or two muscles for fast adjustments. For example, Participant 02 shows lags that are generally around two seconds while his RF has a substantially lower lag at 0.10 s.

Similar trends can be seen in the correlation of the sagittal component of CoM with the right side muscles. An interesting difference is the fact that there is significantly less lag in the correlations with the muscles of the right side. Once again, this can likely be attributed to all participants being right-side dominant. Participant 03, who suffers from drop foot in her left foot, shows the most pronounced change in lags between left and right side which seems easily explainable by her condition.

In the lateral direction, very similar results are seen.

Participant	RA		ES		BF		RF		G		TA	
	r-value	lag(s)	r-value	lag(s)	r-value	lag(s)	r-value	lag(s)	r-value	lag(s)	r-value	lag(s)
02	0.4103	2.06	0.3345	1.91	0.3941	2.26	-0.4059	0.10	0.4400	2.22	0.4277	2.07
03	-0.4782	-1.64	-0.6347	-0.11	-0.5272	-1.61	-0.5131	-1.63	-0.4648	-1.72	-0.4664	-1.63
04	-0.5393	-0.41	-0.3453	-2.28	-0.4354	-0.43	-0.4582	-0.37	-0.5295	-0.32	-0.5105	-0.41
05	-0.6335	-1.87	-0.5774	-0.17	-0.6149	-0.24	-0.6090	-1.91	-0.5837	-1.92	-0.5613	-1.92
07	0.4539	-1.08	-0.2372	3.80	0.7020	-0.54	0.7642	-1.13	0.7016	-0.79	0.6155	-1.53
mean	-0.1573	-0.59	-0.2920	0.63	-0.0963	-0.11	-0.2444	-0.99	-0.0873	-0.50	-0.0990	-0.68
std	0.5412	1.58	0.3864	2.30	0.6016	1.43	0.5688	0.84	0.6093	1.66	0.5714	1.64

Table 4.7: Cross-correlation analysis of sagittal CoM vs left side estimated muscle forces for quiet standing task.

Participant	RA		ES		BF		RF		G		TA	
	r-value	lag(s)	r-value	lag(s)	r-value	lag(s)	r-value	lag(s)	r-value	lag(s)	r-value	lag(s)
02	0.3681	2.20	0.2643	2.03	0.3107	2.32	-0.3818	0.31	0.4128	1.98	0.2888	2.47
03	-0.2724	-0.44	-0.3843	-0.39	-0.5578	-0.16	-0.5464	-0.26	0.7300	0.30	-0.4788	0.00
04	-0.5429	-0.15	-0.4389	-1.36	-0.4900	-1.23	-0.5925	-0.11	0.2981	0.75	-0.7021	-0.07
05	-0.4925	-1.56	-0.3374	-0.48	-0.7060	-0.19	-0.4804	-0.12	-0.5896	-0.19	-0.6601	0.00
07	0.4307	1.22	0.4759	-0.62	0.6619	-0.74	0.6253	-0.57	0.5641	-0.46	0.6466	-0.92
mean	-0.1018	0.25	-0.0841	-0.16	-0.1562	0.00	-0.2752	-0.15	0.2831	0.48	-0.1811	0.30
std	0.4692	1.47	0.4228	1.28	0.6046	1.37	0.5096	0.32	0.5141	0.96	0.6114	1.28

Table 4.8: Cross-correlation analysis of sagittal CoM vs right side estimated muscle forces for quiet standing task.

Participant	RA		ES		BF		RF		G		TA	
	r-value	lag(s)	r-value	lag(s)	r-value	lag(s)	r-value	lag(s)	r-value	lag(s)	r-value	lag(s)
02	0.5886	-0.47	0.3856	-0.29	0.4981	0.04	0.4670	-0.79	0.6709	-0.30	0.4376	-0.76
03	-0.4008	-1.96	-0.2507	-0.27	-0.3492	-1.92	-0.3526	-1.92	-0.4379	-1.97	-0.3991	-1.93
04	0.4559	-0.52	0.3290	-2.39	0.7538	-0.46	0.5649	-0.41	0.7807	-0.46	0.7044	-0.39
05	-0.7849	-1.91	-0.5392	-0.19	-0.5988	-1.89	-0.7589	-1.96	-0.7065	-1.98	-0.6932	-1.97
07	0.2192	0.55	0.1878	4.98	0.4473	4.85	0.3736	0.44	0.3640	4.78	0.3140	0.62
mean	0.0156	-0.86	0.0225	0.37	0.1502	0.12	0.0588	-0.93	0.1342	0.02	0.0727	-0.89
std	0.5869	1.07	0.4010	2.74	0.5882	2.78	0.5830	1.03	0.6695	2.78	0.5915	1.09

Table 4.9: Cross-correlation analysis of lateral CoM vs left side estimated muscle forces for quiet standing task.

Participant	RA		ES		BF		RF		G		TA	
	r-value	lag(s)	r-value	lag(s)	r-value	lag(s)	r-value	lag(s)	r-value	lag(s)	r-value	lag(s)
02	0.7448	-0.29	0.4422	-0.23	0.5324	0.00	0.4920	-0.99	0.5876	-0.17	0.5131	-0.04
03	-0.1938	-0.56	0.2140	1.14	-0.2594	-0.24	-0.3196	-0.58	0.2965	0.01	-0.2877	-0.10
04	0.7323	-0.19	0.6421	-1.73	0.5922	-1.36	0.7510	-0.15	0.5264	-0.37	0.8795	-0.20
05	-0.5673	-1.59	-0.3288	-0.54	-0.7454	-0.22	-0.4575	-0.17	-0.7683	-0.21	-0.8413	-0.02
07	0.6032	4.95	0.5631	5.00	0.3201	4.79	0.4443	4.96	0.4773	5.00	0.2375	0.66
mean	0.2638	0.46	0.3065	0.73	0.0880	0.59	0.1820	0.61	0.2239	0.85	0.1002	0.06
std	0.6054	2.57	0.3902	2.60	0.5746	2.40	0.5360	2.46	0.5652	2.32	0.6770	0.34

Table 4.10: Cross-correlation analysis of lateral CoM vs right side estimated muscle forces for quiet standing task.

Tables 4.11 through 4.14 show the same-side correlation analysis between CoP and estimated muscle force. The correlation between the sagittal CoP and estimated muscle force is very similar to that between the sagittal CoM and estimated muscle force which, given the high degree of correlation between sagittal CoM and CoP, is expected. In general, the lag between sagittal CoP and estimated muscle force is slightly lower than that with CoM. Participants 06 and 07 do not follow this general trend, instead showing substantially lower levels of correlation than the other participants.

In the lateral direction, there is much more variation of correlation coefficients between participants; however, the majority show less correlation between lateral CoP and estimated muscle force than was shown in the sagittal direction.

Participant	RA		ES		BF		RF		G		TA	
	r-value	lag(s)	r-value	lag(s)	r-value	lag(s)	r-value	lag(s)	r-value	lag(s)	r-value	lag(s)
02	0.4490	0.97	0.3436	0.83	0.4538	1.11	-0.4647	-1.01	0.4816	1.03	0.4919	1.03
03	-0.3807	1.24	-0.4630	2.63	-0.4464	3.12	0.4500	-1.84	-0.3788	3.16	-0.4416	3.03
04	0.3408	-0.17	-0.1498	3.38	0.6847	-0.24	0.4643	-0.12	0.7232	-0.02	0.6752	-0.11
05	0.4973	-2.01	-0.3585	0.87	-0.3876	0.86	0.5332	-2.05	-0.3874	0.18	0.4275	-2.05
06	-0.1364	-3.40	-0.0969	-4.11	-0.4989	0.38	-0.4865	0.42	0.2383	-0.51	0.4019	-0.05
07	-0.2233	-1.71	0.2532	0.17	-0.3308	-0.50	-0.3074	-0.95	-0.2828	-1.64	-0.2827	-1.50
mean	0.1540	-0.68	-0.1449	0.72	-0.0389	1.05	0.0993	-0.92	0.1354	0.77	0.3110	0.37
std	0.3905	1.99	0.3113	2.92	0.5625	1.27	0.5258	1.07	0.5034	1.45	0.4341	1.86

Table 4.11: Cross-correlation analysis of sagittal CoP vs estimated muscle forces for quiet standing task - left side.

Participant	RA		ES		BF		RF		G		TA	
	r-value	lag(s)	r-value	lag(s)	r-value	lag(s)	r-value	lag(s)	r-value	lag(s)	r-value	lag(s)
02	0.3059	1.07	0.1834	0.75	0.2103	1.38	-0.4504	-0.96	0.3427	0.76	0.1987	1.48
03	-0.3326	-0.12	-0.4556	-0.31	-0.6668	-0.05	-0.6557	-0.07	0.5004	0.72	-0.6221	0.42
04	-0.2966	3.87	-0.3587	3.23	-0.2669	3.66	-0.3377	-0.17	0.2900	0.20	-0.3175	-0.25
05	-0.3421	0.00	0.2470	5.00	-0.2493	1.19	0.2083	-5.00	0.2742	-0.40	0.3398	-0.10
06	0.1980	0.97	-0.2179	-1.17	-0.2396	0.28	-0.3019	0.22	0.3402	0.78	-0.1572	1.68
07	-0.3974	-0.36	-0.4473	-0.41	-0.5009	-0.50	-0.4252	-0.39	-0.3698	-0.05	-0.4337	-0.37
mean	-0.0935	1.16	-0.1204	1.50	-0.2425	1.29	-0.3075	-1.20	0.3495	0.41	-0.1117	0.65
std	0.3181	1.61	0.3186	2.56	0.3105	1.46	0.3196	2.17	0.0896	0.51	0.3889	0.89

Table 4.12: Cross-correlation analysis of sagittal CoP vs estimated muscle forces for quiet standing task - right side.

Participant	RA		ES		BF		RF		G		TA	
	r-value	lag(s)	r-value	lag(s)	r-value	lag(s)	r-value	lag(s)	r-value	lag(s)	r-value	lag(s)
02	0.1669	0.97	0.1669	3.21	0.1762	0.12	0.1925	3.64	0.2958	0.02	0.2902	1.07
03	0.3811	1.24	0.3811	0.32	-0.4279	-1.90	0.4682	-1.93	-0.3291	-1.32	0.3343	-0.12
04	0.4695	-0.17	0.4695	-0.65	0.2765	4.92	0.6122	0.00	0.2710	0.27	0.4379	3.87
05	-0.8710	-2.01	-0.8710	0.22	-0.7616	0.14	-0.8367	-1.47	-0.8015	-1.51	-0.7650	0.00
06	0.1836	-3.40	0.1836	0.59	0.1452	0.59	0.1230	0.77	-0.2356	0.17	-0.3267	0.97
07	-0.2755	-1.71	-0.2755	0.08	0.3425	-0.87	-0.4002	-1.71	-0.3602	-0.96	-0.3972	-0.36
mean	0.0660	-0.68	0.0660	0.74	-0.1183	0.77	0.1118	0.20	-0.1599	-0.47	-0.0059	1.16
std	0.5395	1.99	0.5395	1.46	0.4532	2.51	0.5665	2.21	0.4581	0.86	0.5195	1.61

Table 4.13: Cross-correlation analysis of lateral CoP vs estimated muscle forces for quiet standing task - left side.

Participant	RA		ES		BF		RF		G		TA	
	r-value	lag(s)	r-value	lag(s)	r-value	lag(s)	r-value	lag(s)	r-value	lag(s)	r-value	lag(s)
02	0.1901	0.40	0.1944	-2.20	-0.1373	2.86	0.3640	-1.89	-0.1327	2.55	-0.1423	4.39
03	0.2410	-0.21	0.2799	4.53	0.4302	5.17	0.4901	-0.45	-0.5307	0.81	0.4322	-0.05
04	-0.5061	3.82	-0.5524	3.18	-0.5024	3.66	-0.3390	3.98	-0.4419	3.54	-0.4043	3.98
05	-0.4118	0.00	-0.2980	1.05	-0.3482	1.20	-0.3993	1.23	0.5236	-0.33	0.5702	-0.07
06	0.2004	0.20	-0.1962	-1.61	-0.4063	-0.13	-0.4671	-0.20	0.2882	0.25	0.1820	0.00
07	0.2719	1.13	0.3510	1.13	0.4206	0.77	0.3515	1.13	0.3446	1.17	0.3950	-0.92
mean	-0.0573	0.84	-0.1145	0.99	-0.1950	2.52	-0.0703	0.54	-0.0587	1.36	0.1275	1.65
std	0.3687	1.68	0.3475	2.93	0.3686	2.02	0.4584	2.22	0.4567	1.62	0.4023	2.32

Table 4.14: Cross-correlation analysis of lateral CoP vs estimated muscle forces for quiet standing task - right side.

Tables 4.15 through 4.26 show the results of the cross-correlation analysis of the estimated muscle forces for the left and right sides of the body. For Participant 02, on the left side, RA shows fairly strong correlation to ES at zero lag. RA is strongly correlated with BF and leads it by 0.2 s and is only slightly less correlated with RF; however, in the case of RF it lags by 0.35 s. RA is most strongly correlated with G and TA and has nearly zero lag compared to them. ES shows slightly less correlation with the other muscles in comparison to RA, although it shows very similar lags. BF shows very high correlation with G and TA, more so even than RA does. BF also appears to lag all other muscles. RF shows moderate correlation with all other muscles and leads all but TA by approximately 0.5 s. G and TA show very high correlation with all other muscles. Participant 03 shows extremely high levels of correlation across all muscles and at fairly consistently small lags, with the exception of ES which lags all other muscles by approximately 1.5 s. Participant 04 has very little correlation between RA and ES compared to other participants and at a very high lag. Participant 05 has very low correlations between RA and ES in comparison to the other muscles.

On the right side, these trends are even more pronounced, with the majority of correlation coefficients being larger than 0.8. This again seems to fit well with the fact that all participants were right-foot dominant. As the quiet standing task should be void of any motion other than postural sway, the majority of muscle forces are being used to stabilize joints and control joint stiffness to counter postural sway. This likely explains the high degree of correlation across almost all muscles. The results of the correlation analysis also suggest that G and TA are good candidates for use as input in attempting to predict the muscle force in other muscles, or as possible parameters to postural stability models.

Muscle	RA		ES		BF		RF		G		TA	
	r-value	lag(s)	r-value	lag(s)	r-value	lag(s)	r-value	lag(s)	r-value	lag(s)	r-value	lag(s)
RA	1.0000	0.00	0.5999	0.00	0.6574	0.20	0.4700	-0.35	0.7909	0.03	0.7232	0.07
ES	0.5999	0.00	1.0000	0.00	0.5893	0.25	0.3700	-0.26	0.5682	0.04	0.5875	0.15
BF	0.6574	-0.20	0.5893	-0.25	1.0000	0.00	0.5862	-0.51	0.7905	-0.14	0.9569	-0.05
RF	0.4700	0.35	0.3700	0.26	0.5862	0.51	1.0000	0.00	0.5361	0.47	0.6480	0.14
G	0.7909	-0.03	0.5682	-0.04	0.7905	0.14	0.5361	-0.47	1.0000	0.00	0.7953	0.03
TA	0.7232	-0.07	0.5875	-0.15	0.9569	0.05	0.6480	-0.14	0.7953	-0.03	1.0000	0.00

Table 4.15: Cross-correlation analysis of left side estimated muscle forces for quiet standing task - Participant 02.

Muscle	RA		ES		BF		RF		G		TA	
	r-value	lag(s)	r-value	lag(s)	r-value	lag(s)	r-value	lag(s)	r-value	lag(s)	r-value	lag(s)
RA	1.0000	0.00	0.7674	1.57	0.9144	0.05	0.9240	0.03	0.9692	-0.02	0.9487	0.03
ES	0.7674	-1.57	1.0000	0.00	0.8567	-1.55	0.8756	-1.55	0.7378	-1.65	0.7539	-1.57
BF	0.9144	-0.05	0.8567	1.55	1.0000	0.00	0.9780	-0.01	0.8895	-0.07	0.9497	-0.02
RF	0.9240	-0.03	0.8756	1.55	0.9780	0.01	1.0000	0.00	0.8877	-0.06	0.9337	0.00
G	0.9692	0.02	0.7378	1.65	0.8895	0.07	0.8877	0.06	1.0000	0.00	0.9528	0.05
TA	0.9487	-0.03	0.7539	1.57	0.9497	0.02	0.9337	0.00	0.9528	-0.05	1.0000	0.00

Table 4.16: Cross-correlation analysis of left side estimated muscle forces for quiet standing task - Participant 03.

Muscle	RA		ES		BF		RF		G		TA	
	r-value	lag(s)	r-value	lag(s)	r-value	lag(s)	r-value	lag(s)	r-value	lag(s)	r-value	lag(s)
RA	1.0000	0.00	0.2714	-4.47	0.6519	0.00	0.7907	0.00	0.5764	0.16	0.6976	0.00
ES	0.2714	4.47	1.0000	0.00	0.3274	-0.32	0.2651	-0.31	0.3266	2.09	0.3455	0.70
BF	0.6519	0.00	0.3274	0.32	1.0000	0.00	0.7765	0.00	0.8182	0.15	0.8951	0.00
RF	0.7907	0.00	0.2651	0.31	0.7765	0.00	1.0000	0.00	0.6417	0.19	0.8548	0.00
G	0.5764	-0.16	0.3266	-2.09	0.8182	-0.15	0.6417	-0.19	1.0000	0.00	0.8461	-0.15
TA	0.6976	0.00	0.3455	-0.70	0.8951	0.00	0.8548	0.00	0.8461	0.15	1.0000	0.00

Table 4.17: Cross-correlation analysis of left side estimated muscle forces for quiet standing task - Participant 04.

Muscle	RA		ES		BF		RF		G		TA	
	r-value	lag(s)	r-value	lag(s)	r-value	lag(s)	r-value	lag(s)	r-value	lag(s)	r-value	lag(s)
RA	1.0000	0.00	0.7331	0.02	0.8505	0.01	0.9783	-0.01	0.9162	-0.06	0.9413	0.00
ES	0.7331	-0.02	1.0000	0.00	0.8785	-0.02	0.7142	-0.04	0.7892	-0.10	0.8502	-0.03
BF	0.8505	-0.01	0.8785	0.02	1.0000	0.00	0.8210	-0.04	0.9060	-0.11	0.9362	-0.03
RF	0.9783	0.01	0.7142	0.04	0.8210	0.04	1.0000	0.00	0.8947	-0.06	0.9266	0.00
G	0.9162	0.06	0.7892	0.10	0.9060	0.11	0.8947	0.06	1.0000	0.00	0.9433	0.00
TA	0.9413	0.00	0.8502	0.03	0.9362	0.03	0.9266	0.00	0.9433	0.00	1.0000	0.00

Table 4.18: Cross-correlation analysis of left side estimated muscle forces for quiet standing task - Participant 05.

Muscle	RA		ES		BF		RF		G		TA	
	r-value	lag(s)	r-value	lag(s)	r-value	lag(s)	r-value	lag(s)	r-value	lag(s)	r-value	lag(s)
RA	1.0000	0.00	0.1509	3.82	-0.1681	-0.51	-0.1196	-3.00	-0.1439	2.46	-0.1817	-0.23
ES	0.1509	-3.82	1.0000	0.00	0.2080	0.00	0.1534	0.13	0.1881	0.00	0.1964	0.27
BF	-0.1681	0.51	0.2080	0.00	1.0000	0.00	0.6602	0.05	0.3771	0.00	0.4907	0.22
RF	-0.1196	3.00	0.1534	-0.13	0.6602	-0.05	1.0000	0.00	0.4808	-0.25	0.6483	0.31
G	-0.1439	-2.46	0.1881	0.00	0.3771	0.00	0.4808	0.25	1.0000	0.00	0.6853	0.42
TA	-0.1817	0.23	0.1964	-0.27	0.4907	-0.22	0.6483	-0.31	0.6853	-0.42	1.0000	0.00

Table 4.19: Cross-correlation analysis of left side estimated muscle forces for quiet standing task - Participant 06.

Muscle	RA		ES		BF		RF		G		TA	
	r-value	lag(s)	r-value	lag(s)	r-value	lag(s)	r-value	lag(s)	r-value	lag(s)	r-value	lag(s)
RA	1.0000	0.00	0.3825	0.00	0.4824	0.00	0.5534	0.00	0.4697	0.27	0.4331	0.15
ES	0.3825	0.00	1.0000	0.00	-0.2577	-1.00	0.2547	0.00	-0.3819	-3.50	-0.2949	-1.78
BF	0.4824	0.00	-0.2577	1.00	1.0000	0.00	0.8177	0.00	0.7307	0.00	0.7580	0.13
RF	0.5534	0.00	0.2547	0.00	0.8177	0.00	1.0000	0.00	0.7615	0.00	0.7618	0.20
G	0.4697	-0.27	-0.3819	3.50	0.7307	0.00	0.7615	0.00	1.0000	0.00	0.6558	1.62
TA	0.4331	-0.15	-0.2949	1.78	0.7580	-0.13	0.7618	-0.20	0.6558	-1.62	1.0000	0.00

Table 4.20: Cross-correlation analysis of left side estimated muscle forces for quiet standing task - Participant 07.

Muscle	RA		ES		BF		RF		G		TA	
	r-value	lag(s)	r-value	lag(s)	r-value	lag(s)	r-value	lag(s)	r-value	lag(s)	r-value	lag(s)
RA	1.0000	0.00	0.6501	0.00	0.7611	0.29	0.4519	-0.61	0.8130	0.10	0.7297	0.27
ES	0.6501	0.00	1.0000	0.00	0.6241	0.17	0.5014	0.00	0.6209	0.04	0.5592	0.16
BF	0.7611	-0.29	0.6241	-0.17	1.0000	0.00	0.5972	-0.14	0.8492	-0.15	0.9779	-0.03
RF	0.4519	0.61	0.5014	0.00	0.5972	0.14	1.0000	0.00	0.4388	0.61	0.5933	0.09
G	0.8130	-0.10	0.6209	-0.04	0.8492	0.15	0.4388	-0.61	1.0000	0.00	0.7744	0.12
TA	0.7297	-0.27	0.5592	-0.16	0.9779	0.03	0.5933	-0.09	0.7744	-0.12	1.0000	0.00

Table 4.21: Cross-correlation analysis of right side estimated muscle forces for quiet standing task - Participant 02.

Muscle	RA		ES		BF		RF		G		TA	
	r-value	lag(s)	r-value	lag(s)	r-value	lag(s)	r-value	lag(s)	r-value	lag(s)	r-value	lag(s)
RA	1.0000	0.00	0.3248	0.00	0.4067	0.00	0.4115	0.00	-0.1864	-4.24	0.4148	0.50
ES	0.3248	0.00	1.0000	0.00	0.5257	0.09	0.4994	0.53	-0.2085	0.31	0.5316	0.95
BF	0.4067	0.00	0.5257	-0.09	1.0000	0.00	0.8298	0.00	-0.3487	0.22	0.8143	0.45
RF	0.4115	0.00	0.4994	-0.53	0.8298	0.00	1.0000	0.00	-0.2990	0.54	0.9414	0.38
G	-0.1864	4.24	-0.2085	-0.31	-0.3487	-0.22	-0.2990	-0.54	1.0000	0.00	-0.2452	-0.08
TA	0.4148	-0.50	0.5316	-0.95	0.8143	-0.45	0.9414	-0.38	-0.2452	0.08	1.0000	0.00

Table 4.22: Cross-correlation analysis of right side estimated muscle forces for quiet standing task - Participant 03.

Muscle	RA		ES		BF		RF		G		TA	
	r-value	lag(s)	r-value	lag(s)	r-value	lag(s)	r-value	lag(s)	r-value	lag(s)	r-value	lag(s)
RA	1.0000	0.00	0.8386	-0.98	0.8730	-0.14	0.7112	-0.03	0.6192	-0.34	0.8342	0.05
ES	0.8386	0.98	1.0000	0.00	0.8177	0.59	0.5432	1.60	0.5860	0.52	0.7264	1.42
BF	0.8730	0.14	0.8177	-0.59	1.0000	0.00	0.5508	0.00	0.6547	-0.11	0.6972	1.08
RF	0.7112	0.03	0.5432	-1.60	0.5508	0.00	1.0000	0.00	0.4826	0.00	0.8001	0.03
G	0.6192	0.34	0.5860	-0.52	0.6547	0.11	0.4826	0.00	1.0000	0.00	0.5154	0.31
TA	0.8342	-0.05	0.7264	-1.42	0.6972	-1.08	0.8001	-0.03	0.5154	-0.31	1.0000	0.00

Table 4.23: Cross-correlation analysis of right side estimated muscle forces for quiet standing task - Participant 04.

Muscle	RA		ES		BF		RF		G		TA	
	r-value	lag(s)	r-value	lag(s)	r-value	lag(s)	r-value	lag(s)	r-value	lag(s)	r-value	lag(s)
RA	1.0000	0.00	0.4413	0.00	0.6436	1.40	0.4574	0.77	0.6252	1.48	0.6034	1.69
ES	0.4413	0.00	1.0000	0.00	0.5757	0.26	0.4901	0.16	0.3998	0.30	0.3967	0.60
BF	0.6436	-1.40	0.5757	-0.26	1.0000	0.00	0.7246	0.00	0.8021	0.01	0.7988	0.22
RF	0.4574	-0.77	0.4901	-0.16	0.7246	0.00	1.0000	0.00	0.4812	0.00	0.5282	0.14
G	0.6252	-1.48	0.3998	-0.30	0.8021	-0.01	0.4812	0.00	1.0000	0.00	0.8781	0.23
TA	0.6034	-1.69	0.3967	-0.60	0.7988	-0.22	0.5282	-0.14	0.8781	-0.23	1.0000	0.00

Table 4.24: Cross-correlation analysis of right side estimated muscle forces for quiet standing task - Participant 05.

Muscle	RA		ES		BF		RF		G		TA	
	r-value	lag(s)	r-value	lag(s)	r-value	lag(s)	r-value	lag(s)	r-value	lag(s)	r-value	lag(s)
RA	1.0000	0.00	-0.1719	0.67	-0.1730	-0.29	0.3860	0.00	0.4572	0.00	-0.1511	4.03
ES	-0.1719	-0.67	1.0000	0.00	0.2117	1.56	0.2156	0.00	0.1623	0.00	-0.3142	0.26
BF	-0.1730	0.29	0.2117	-1.56	1.0000	0.00	0.3773	-0.07	0.1950	-0.97	-0.1463	1.51
RF	0.3860	0.00	0.2156	0.00	0.3773	0.07	1.0000	0.00	0.5209	0.00	-0.1753	0.27
G	0.4572	0.00	0.1623	0.00	0.1950	0.97	0.5209	0.00	1.0000	0.00	0.2267	0.00
TA	-0.1511	-4.03	-0.3142	-0.26	-0.1463	-1.51	-0.1753	-0.27	0.2267	0.00	1.0000	0.00

Table 4.25: Cross-correlation analysis of right side estimated muscle forces for quiet standing task - Participant 06.

Muscle	RA		ES		BF		RF		G		TA	
	r-value	lag(s)	r-value	lag(s)	r-value	lag(s)	r-value	lag(s)	r-value	lag(s)	r-value	lag(s)
RA	1.0000	0.00	0.8778	-0.01	0.7920	-0.24	0.8886	-0.03	0.7664	0.23	0.5452	-1.30
ES	0.8778	0.01	1.0000	0.00	0.7780	-0.14	0.8682	0.00	0.7598	0.22	0.6100	0.00
BF	0.7920	0.24	0.7780	0.14	1.0000	0.00	0.9430	0.12	0.8146	0.44	0.7598	0.00
RF	0.8886	0.03	0.8682	0.00	0.9430	-0.12	1.0000	0.00	0.8305	0.28	0.7016	0.00
G	0.7664	-0.23	0.7598	-0.22	0.8146	-0.44	0.8305	-0.28	1.0000	0.00	0.6096	-0.43
TA	0.5452	1.30	0.6100	0.00	0.7598	0.00	0.7016	0.00	0.6096	0.43	1.0000	0.00

Table 4.26: Cross-correlation analysis of right side estimated muscle forces for quiet standing task - Participant 07.

Tables 4.27 through 4.30 show the average and standard deviation of the cross-correlation analysis of the muscle forces across all participants for the quiet standing task.

Muscle	RA		ES		BF		RF		G		TA	
	r-value	lag(s)	r-value	lag(s)	r-value	lag(s)	r-value	lag(s)	r-value	lag(s)	r-value	lag(s)
RA	1.0000	0.0000	0.4842	0.1571	0.5647	-0.0402	0.5995	-0.5558	0.5964	0.4727	0.5937	0.0029
ES	0.4842	-0.1571	1.0000	0.0000	0.4337	-0.4408	0.4388	-0.3367	0.3713	-0.5206	0.4064	-0.3785
BF	0.5647	0.0402	0.4337	0.4408	1.0000	0.0000	0.7733	-0.0833	0.7520	-0.0273	0.8311	0.0419
RF	0.5995	0.5558	0.4388	0.3367	0.7733	0.0833	1.0000	0.0000	0.7004	0.0477	0.7955	0.1069
G	0.5964	-0.4727	0.3713	0.5206	0.7520	0.0273	0.7004	-0.0477	1.0000	0.0000	0.8131	0.3271
TA	0.5937	-0.0029	0.4064	0.3785	0.8311	-0.0419	0.7955	-0.1069	0.8131	-0.3271	1.0000	0.0000

Table 4.27: Cross-correlation analysis of left side estimated muscle forces for quiet standing task - Average across all Participants.

Muscle	RA		ES		BF		RF		G		TA	
	r-value	lag(s)	r-value	lag(s)	r-value	lag(s)	r-value	lag(s)	r-value	lag(s)	r-value	lag(s)
RA	0.0000	0.0000	0.2539	2.7177	0.3909	0.2411	0.4053	1.2078	0.4108	0.9800	0.4246	0.1264
ES	0.2539	2.7177	0.0000	0.0000	0.4339	0.6923	0.2887	0.6147	0.4360	1.8812	0.4219	1.0367
BF	0.3909	0.2411	0.4339	0.6923	0.0000	0.0000	0.1371	0.2104	0.1947	0.1055	0.1823	0.1080
RF	0.4053	1.2078	0.2887	0.6147	0.1371	0.2104	0.0000	0.0000	0.1762	0.2509	0.1299	0.1307
G	0.4108	0.9800	0.4360	1.8812	0.1947	0.1055	0.1762	0.2509	0.0000	0.0000	0.1256	0.6592
TA	0.4246	0.1264	0.4219	1.0367	0.1823	0.1080	0.1299	0.1307	0.1256	0.6592	0.0000	0.0000

Table 4.28: Cross-correlation analysis of left side estimated muscle forces for quiet standing task - Standard deviation across all Participants.

Muscle	RA		ES		BF		RF		G		TA	
	r-value	lag(s)	r-value	lag(s)	r-value	lag(s)	r-value	lag(s)	r-value	lag(s)	r-value	lag(s)
RA	1.0000	0.0000	0.4935	-0.0538	0.5506	0.1696	0.5511	0.0163	0.5158	-0.4619	0.4960	0.8727
ES	0.4935	0.0538	1.0000	0.0000	0.5888	0.4204	0.5197	0.3829	0.3867	0.2313	0.4183	0.5660
BF	0.5506	-0.1696	0.5888	-0.4204	1.0000	0.0000	0.6705	-0.0150	0.4945	-0.0915	0.6503	0.5381
RF	0.5511	-0.0163	0.5197	-0.3829	0.6705	0.0150	1.0000	0.0000	0.4092	0.2381	0.5649	0.1521
G	0.5158	0.4619	0.3867	-0.2313	0.4945	0.0915	0.4092	-0.2381	1.0000	0.0000	0.4598	0.0242
TA	0.4960	-0.8727	0.4183	-0.5660	0.6503	-0.5381	0.5649	-0.1521	0.4598	-0.0242	1.0000	0.0000

Table 4.29: Cross-correlation analysis of right side estimated muscle forces for quiet standing task - Average across all Participants.

Muscle	RA		ES		BF		RF		G		TA	
	r-value	lag(s)	r-value	lag(s)	r-value	lag(s)	r-value	lag(s)	r-value	lag(s)	r-value	lag(s)
RA	0.0000	0.0000	0.3912	0.5272	0.3898	0.6367	0.2024	0.4382	0.3661	1.9515	0.3488	1.8157
ES	0.3912	0.5272	0.0000	0.0000	0.2172	0.6058	0.2079	0.6323	0.3574	0.1912	0.3745	0.5416
BF	0.3898	0.6367	0.2172	0.6058	0.0000	0.0000	0.2041	0.0861	0.4794	0.4816	0.4013	0.6253
RF	0.2024	0.4382	0.2079	0.6323	0.2041	0.0861	0.0000	0.0000	0.3750	0.2825	0.3914	0.1457
G	0.3661	1.9515	0.3574	0.1912	0.4794	0.4816	0.3750	0.2825	0.0000	0.0000	0.4125	0.2643
TA	0.3488	1.8157	0.3745	0.5416	0.4013	0.6253	0.3914	0.1457	0.4125	0.2643	0.0000	0.0000

Table 4.30: Cross-correlation analysis of right side estimated muscle forces for quiet standing task - Standard deviation across all Participants.

Sagittal Lift/Lower Task

Tables 4.31 through 4.34 show the results of the cross-correlation analysis on the CoM and estimated muscle forces. In most cases, the correlation coefficients are very small in both the sagittal and lateral directions. There is substantially less correlation between the sagittal component of the CoM and estimated muscle force compared to the quiet standing task. This is likely due to the effect of the additional 10 kg mass that the participants had to hold. The muscles are acting to counter the forces and moments caused by adding this additional mass to the system in addition to any muscle force that is being generated to help control CoM. In general, the results show that there is a fairly even distribution of responsibility for control of the CoM across all of the muscles. Discussion of the lags associated with the correlations coefficients for the sagittal lift/lower task is not meaningful as no synchronization circuit was available to synchronize the signals.

Participant	RA		ES		BF		RF		G		TA	
	r-value	lag(s)	r-value	lag(s)	r-value	lag(s)	r-value	lag(s)	r-value	lag(s)	r-value	lag(s)
02	0.1966	3.18	0.1062	3.82	-0.1659	-6.00	0.1510	-1.31	-0.1787	-6.00	0.1064	3.37
03	0.1328	-6.00	0.1320	-6.00	0.1177	-6.00	0.1567	-6.00	0.1673	-6.00	0.1936	-6.00
05	0.2130	0.00	0.0858	0.00	0.1797	0.00	0.1937	0.00	0.2302	0.00	0.2131	0.00
mean	0.1808	-0.9392	0.1080	-0.7254	0.0438	-4.0000	0.1671	-2.4371	0.0729	-4.0000	0.1710	-0.8754
std	0.0424	4.6627	0.0231	4.9519	0.1843	3.4641	0.0232	3.1545	0.2201	3.4641	0.0568	4.7478

Table 4.31: Cross-correlation analysis of sagittal CoM vs left side estimated muscle forces for sagittal lift/lower task.

Participant	RA		ES		BF		RF		G		TA	
	r-value	lag(s)	r-value	lag(s)	r-value	lag(s)	r-value	lag(s)	r-value	lag(s)	r-value	lag(s)
02	0.3434	-3.63	0.2675	2.92	0.3306	2.57	0.2416	-5.28	0.2455	-5.98	-0.1885	-1.17
03	0.1090	-3.95	-0.0743	0.00	0.0830	-4.10	0.1145	-4.09	0.2709	-5.31	0.3422	-6.00
05	0.2097	-4.81	0.2970	-6.00	0.2003	-6.00	0.2154	-6.00	0.2488	-6.00	0.2624	-6.00
mean	0.2207	-4.13	0.1634	-1.03	0.2046	-2.51	0.1905	-5.12	0.2551	-5.76	0.1387	-4.39
std	0.1176	0.61	0.2064	4.55	0.1239	4.50	0.0671	0.96	0.0138	0.40	0.2862	2.79

Table 4.32: Cross-correlation analysis of sagittal CoM vs right side estimated muscle forces for sagittal lift/lower task.

Participant	RA		ES		BF		RF		G		TA	
	r-value	lag(s)	r-value	lag(s)	r-value	lag(s)	r-value	lag(s)	r-value	lag(s)	r-value	lag(s)
02	0.2498	0.00	0.1336	0.00	-0.2488	-6.00	0.2031	0.00	-0.2459	-6.00	0.1500	0.00
03	0.1385	-6.00	0.1377	-6.00	0.1229	-6.00	0.1622	-6.00	0.1724	-6.00	0.2001	-6.00
05	-0.2112	0.00	-0.0854	0.00	0.1818	-6.00	-0.1938	0.00	-0.2309	0.00	-0.2124	0.00
mean	0.0590	-2.00	0.0620	-2.00	0.0186	-6.00	0.0572	-2.00	-0.1015	-4.00	0.0459	-2.00
std	0.2406	3.46	0.1276	3.46	0.2335	0.00	0.2183	3.46	0.2373	3.46	0.2251	3.46

Table 4.33: Cross-correlation analysis of lateral CoM vs left side estimated muscle forces for sagittal lift/lower task.

Participant	RA		ES		BF		RF		G		TA	
	r-value	lag(s)	r-value	lag(s)	r-value	lag(s)	r-value	lag(s)	r-value	lag(s)	r-value	lag(s)
02	0.3388	-5.11	0.2075	0.00	0.2424	0.00	0.2100	-4.44	0.1363	-3.50	-0.1432	1.00
03	0.1117	-3.95	-0.0736	0.00	0.0861	-4.11	0.1179	-4.10	0.2747	-5.30	0.3449	-6.00
05	-0.2123	-4.54	-0.3022	-5.99	-0.2056	-6.00	-0.2199	-6.00	-0.2534	-6.00	-0.2677	-6.00
mean	0.0794	-4.54	-0.0561	-2.00	0.0410	-3.37	0.0360	-4.85	0.0526	-4.93	-0.0220	-3.67
std	0.2769	0.58	0.2553	3.46	0.2274	3.07	0.2263	1.01	0.2738	1.29	0.3238	4.04

Table 4.34: Cross-correlation analysis of lateral CoM vs right side estimated muscle forces for sagittal lift/lower task.

Tables 4.35 through 4.38 show the same-side correlation analysis between CoP and estimated muscle force. As was the case for CoM, the correlation coefficients between CoP and estimated muscle force for the sagittal lift/lower task are lower than in the quiet standing task. The main contributor to this difference is once again likely the 10 kg mass that the participants had to lift and lower in this task. The muscles would need to act to counter this external force and moment and a larger component of the muscle force signal would therefore be unrelated to the motion of the participants' own CoP. There are indications that a variety of lifting strategies are used amongst the participants. Some show much higher correlation between BF and RF and CoP while others show most of the control of CoP is related to G and TA. Still others have fairly balanced correlation coefficients.

Participant	RA		ES		BF		RF		G		TA	
	r-value	lag(s)	r-value	lag(s)	r-value	lag(s)	r-value	lag(s)	r-value	lag(s)	r-value	lag(s)
02	-0.2714	-1.13	0.1901	3.62	0.5575	3.16	0.4345	3.16	0.6265	-5.13	-0.2942	-0.91
03	-0.1967	0.61	-0.2320	0.57	-0.2154	0.55	-0.2118	0.63	-0.2358	0.54	-0.2126	1.45
04	0.1910	0.66	0.1892	0.65	0.2055	0.57	0.1946	0.66	0.1862	0.59	0.1988	0.66
05	0.3753	2.96	0.2657	3.01	0.5762	-4.34	0.4773	3.20	-0.3436	0.77	0.4090	3.91
06	-0.2845	0.13	-0.6487	-0.14	-0.4670	0.47	-0.2992	-4.97	-0.5832	0.14	0.3216	3.87
07	0.2770	4.55	0.3897	5.46	0.5737	5.12	0.5110	5.48	0.7661	-5.21	0.4019	6.00
mean	-0.0373	0.65	-0.0472	1.54	0.1314	0.08	0.1191	0.54	-0.0700	-0.62	0.0845	1.79
std	0.3015	1.48	0.3892	1.66	0.4645	2.72	0.3598	3.33	0.4787	2.53	0.3187	2.09

Table 4.35: Cross-correlation analysis of sagittal CoP vs estimated muscle forces for sagittal lift/lower task - left side.

Participant	RA		ES		BF		RF		G		TA	
	r-value	lag(s)	r-value	lag(s)	r-value	lag(s)	r-value	lag(s)	r-value	lag(s)	r-value	lag(s)
02	-0.2492	-2.94	-0.4068	-3.05	0.4616	2.04	-0.3377	-2.99	0.5817	1.87	0.4786	1.92
03	0.1744	0.44	-0.2219	5.01	0.1994	0.43	0.2025	0.39	0.2759	1.02	0.1928	0.32
04	0.1848	1.82	0.1727	1.36	0.1727	-3.24	0.1916	-3.09	0.1459	2.68	0.1722	-5.82
05	0.2443	-6.00	0.5176	-6.00	-0.4460	-3.08	0.3779	-6.00	-0.2956	-1.75	-0.2893	-1.76
06	0.3425	-1.11	-0.5738	-6.00	-0.5032	-6.00	0.2143	-2.63	-0.5366	-5.99	0.2204	-2.64
07	0.2461	-3.13	-0.1393	0.52	0.5162	-2.96	0.5092	-2.86	0.4346	-2.94	0.4072	-3.06
mean	0.1394	-1.56	-0.1024	-1.74	-0.0231	-1.97	0.1297	-2.87	0.0343	-0.43	0.1549	-1.60
std	0.2272	3.05	0.4442	4.83	0.4278	3.20	0.2722	2.27	0.4487	3.52	0.2776	2.96

Table 4.36: Cross-correlation analysis of sagittal CoP vs estimated muscle forces for sagittal lift/lower task - right side.

Participant	RA		ES		BF		RF		G		TA	
	r-value	lag(s)	r-value	lag(s)	r-value	lag(s)	r-value	lag(s)	r-value	lag(s)	r-value	lag(s)
02	-0.1940	-1.13	-0.1940	-5.35	-0.1411	-5.67	-0.2387	-5.68	-0.2259	3.28	0.1130	-2.94
03	-0.2442	0.61	-0.2442	-4.58	-0.2209	-4.55	-0.2299	-4.51	-0.2084	-4.57	-0.2263	0.44
04	-0.1972	0.66	-0.1972	0.68	-0.1951	0.56	-0.1848	0.66	-0.2120	0.70	-0.2131	1.82
05	0.2624	2.96	0.2624	-3.56	0.2678	-4.68	0.2991	-3.60	-0.2281	-6.00	0.3564	-6.00
06	0.2147	0.13	0.2147	-4.91	0.5412	-3.40	0.1928	6.00	0.5786	-4.39	0.3390	-1.11
07	0.2007	4.55	0.2007	-4.59	0.3611	-5.46	0.4779	-5.34	0.5345	-5.22	0.3199	-3.13
mean	-0.0316	0.65	-0.0316	-3.54	0.0504	-3.55	-0.0323	-1.43	-0.0592	-2.20	0.0738	-1.56
std	0.2480	1.48	0.2480	2.45	0.3386	2.43	0.2576	4.79	0.3566	3.98	0.2847	3.05

Table 4.37: Cross-correlation analysis of lateral CoP vs estimated muscle forces for sagittal lift/lower task - left side.

Participant	RA		ES		BF		RF		G		TA	
	r-value	lag(s)	r-value	lag(s)	r-value	lag(s)	r-value	lag(s)	r-value	lag(s)	r-value	lag(s)
02	-0.2705	-0.06	-0.3333	1.00	-0.4054	2.11	-0.3123	3.22	-0.5837	1.96	0.3767	5.89
03	0.2712	-4.44	-0.2460	4.71	0.2410	-0.61	0.2449	-0.69	-0.2692	4.85	0.3200	-0.71
04	-0.1125	-3.54	-0.1430	-3.38	0.1730	1.16	0.1391	1.30	0.1055	-4.98	0.1131	0.73
05	0.2466	-0.70	0.3296	-2.61	-0.3077	0.65	-0.2707	-6.00	0.2655	-0.74	0.2598	-3.45
06	0.3581	-5.92	0.5634	-6.00	0.4705	-6.00	0.1863	1.91	0.5459	-5.98	0.2195	-6.00
07	-0.2425	-3.18	0.2046	0.62	-0.5153	-2.93	-0.5124	-2.84	-0.3734	-2.88	-0.4096	-2.99
mean	0.0986	-2.93	0.0342	-1.26	0.0343	-0.54	-0.0025	-0.05	0.0128	-0.98	0.2578	-0.71
std	0.2738	2.49	0.3912	4.17	0.3750	3.21	0.2668	3.61	0.4450	4.57	0.1005	4.50

Table 4.38: Cross-correlation analysis of lateral CoP vs estimated muscle forces for sagittal lift/lower task - right side.

Tables 4.39 through 4.50 show the results of the cross-correlation analysis of the estimated muscle forces for the left and right sides of the body.

Participant 02 shows zero lag for all muscle to muscle correlations. The RF and TA have the largest correlation with all other muscles while their opposing muscles, the BF and G, show the least correlation with the other muscles. The RA and ES also have relatively high correlations with all muscles except the BF and G. This would indicate that, for Participant 02 in the sagittal lift/lower task, the RA, ES, RF, and TA are more active than the BF and G. It also indicates that all muscles are acting simultaneously during this task.

Participants 03 and 04 also show zero lag for all correlations; however, all muscles are extremely highly correlated ($r > 0.9$) with one another. This indicates that all muscles are equally utilized, and almost completely independent of any other influences.

Participant 05 shows much lower levels of correlation than the previous participants and lags up to 1.5 s. In this case RF and TA still show some of the highest correlations with the other muscles, but so does G. These results indicate that Participant 05 is using her legs for lifting and stabilizing and is not having to stabilize her core as much with the RA and ES as the previous participants. Interestingly, Participant 05 also had one of the lowest indices of postural stability in Section 4.1. Participant 06 shows similar results.

Participant 07 shows substantially different results than the others. In this case the ES, BF, and RF are the muscles that are most correlated with the others. He also shows some very substantial lags in some of the correlations. The significant difference between Participant 07 and the others is that he is much taller than the rest, at 6'4". This could have a large impact on the performance of this task as his reach would allow him to place the weight on the table with much less leaning forward than the other participants.

Muscle	RA		ES		BF		RF		G		TA	
	r-value	lag(s)	r-value	lag(s)	r-value	lag(s)	r-value	lag(s)	r-value	lag(s)	r-value	lag(s)
RA	1.0000	0.00	0.8525	0.00	0.6239	0.00	0.7426	0.00	0.5664	0.00	0.8567	0.00
ES	0.8525	0.00	1.0000	0.00	0.5385	0.00	0.7328	0.00	0.5021	0.00	0.9054	0.00
BF	0.6239	0.00	0.5385	0.00	1.0000	0.00	0.8136	0.00	0.5217	0.00	0.5508	0.00
RF	0.7426	0.00	0.7328	0.00	0.8136	0.00	1.0000	0.00	0.5145	0.00	0.7358	0.00
G	0.5664	0.00	0.5021	0.00	0.5217	0.00	0.5145	0.00	1.0000	0.00	0.6587	0.00
TA	0.8567	0.00	0.9054	0.00	0.5508	0.00	0.7358	0.00	0.6587	0.00	1.0000	0.00

Table 4.39: Cross-correlation analysis of left side estimated muscle forces for sagittal lift/lower task - Participant 02.

Muscle	RA		ES		BF		RF		G		TA	
	r-value	lag(s)	r-value	lag(s)	r-value	lag(s)	r-value	lag(s)	r-value	lag(s)	r-value	lag(s)
RA	1.0000	0.00	0.9605	0.00	0.9620	0.00	0.9755	0.00	0.9729	0.00	0.9218	0.00
ES	0.9605	0.00	1.0000	0.00	0.9940	0.00	0.9855	0.00	0.9876	0.00	0.8965	0.00
BF	0.9620	0.00	0.9940	0.00	1.0000	0.00	0.9866	0.00	0.9876	0.00	0.9039	0.00
RF	0.9755	0.00	0.9855	0.00	0.9866	0.00	1.0000	0.00	0.9882	0.00	0.9355	0.00
G	0.9729	0.00	0.9876	0.00	0.9876	0.00	0.9882	0.00	1.0000	0.00	0.9237	0.00
TA	0.9218	0.00	0.8965	0.00	0.9039	0.00	0.9355	0.00	0.9237	0.00	1.0000	0.00

Table 4.40: Cross-correlation analysis of left side estimated muscle forces for sagittal lift/lower task - Participant 03.

Muscle	RA		ES		BF		RF		G		TA	
	r-value	lag(s)	r-value	lag(s)	r-value	lag(s)	r-value	lag(s)	r-value	lag(s)	r-value	lag(s)
RA	1.0000	0.00	0.9997	0.00	0.9637	0.00	0.9837	0.00	0.9571	0.00	0.9891	0.00
ES	0.9997	0.00	1.0000	0.00	0.9635	0.00	0.9835	0.00	0.9571	0.00	0.9893	0.00
BF	0.9637	0.00	0.9635	0.00	1.0000	0.00	0.9767	0.00	0.9431	0.01	0.9575	0.00
RF	0.9837	0.00	0.9835	0.00	0.9767	0.00	1.0000	0.00	0.9422	0.00	0.9791	0.00
G	0.9571	0.00	0.9571	0.00	0.9431	-0.01	0.9422	0.00	1.0000	0.00	0.9458	0.00
TA	0.9891	0.00	0.9893	0.00	0.9575	0.00	0.9791	0.00	0.9458	0.00	1.0000	0.00

Table 4.41: Cross-correlation analysis of left side estimated muscle forces for sagittal lift/lower task - Participant 04.

Muscle	RA		ES		BF		RF		G		TA	
	r-value	lag(s)	r-value	lag(s)	r-value	lag(s)	r-value	lag(s)	r-value	lag(s)	r-value	lag(s)
RA	1.0000	0.00	0.3238	-0.44	0.3650	-0.14	0.6605	0.01	0.6781	0.02	0.5924	-0.16
ES	0.3238	0.44	1.0000	0.00	0.2901	-0.97	0.4123	0.51	0.3123	0.71	0.4853	0.39
BF	0.3650	0.14	0.2901	0.97	1.0000	0.00	0.5587	1.21	0.4397	1.65	0.4548	1.42
RF	0.6605	-0.01	0.4123	-0.51	0.5587	-1.21	1.0000	0.00	0.5293	0.27	0.7250	0.38
G	0.6781	-0.02	0.3123	-0.71	0.4397	-1.65	0.5293	-0.27	1.0000	0.00	0.6265	-0.26
TA	0.5924	0.16	0.4853	-0.39	0.4548	-1.42	0.7250	-0.38	0.6265	0.26	1.0000	0.00

Table 4.42: Cross-correlation analysis of left side estimated muscle forces for sagittal lift/lower task - Participant 05.

Muscle	RA		ES		BF		RF		G		TA	
	r-value	lag(s)	r-value	lag(s)	r-value	lag(s)	r-value	lag(s)	r-value	lag(s)	r-value	lag(s)
RA	1.0000	0.00	0.4895	0.00	0.4225	0.11	0.3215	-0.54	-0.3644	-5.59	0.3958	0.00
ES	0.4895	0.00	1.0000	0.00	0.6692	0.15	0.3229	-0.24	0.7254	0.13	0.4710	-0.13
BF	0.4225	-0.11	0.6692	-0.15	1.0000	0.00	0.5340	-0.14	0.5834	0.02	0.5327	-0.09
RF	0.3215	0.54	0.3229	0.24	0.5340	0.14	1.0000	0.00	0.3787	0.11	0.7441	0.08
G	-0.3644	5.59	0.7254	-0.13	0.5834	-0.02	0.3787	-0.11	1.0000	0.00	0.6513	-0.06
TA	0.3958	0.00	0.4710	0.13	0.5327	0.09	0.7441	-0.08	0.6513	0.06	1.0000	0.00

Table 4.43: Cross-correlation analysis of left side estimated muscle forces for sagittal lift/lower task - Participant 06.

Muscle	RA		ES		BF		RF		G		TA	
	r-value	lag(s)	r-value	lag(s)	r-value	lag(s)	r-value	lag(s)	r-value	lag(s)	r-value	lag(s)
RA	1.0000	0.00	0.2547	0.38	0.3170	0.00	0.2799	1.89	0.2975	0.00	0.2183	1.98
ES	0.2547	-0.38	1.0000	0.00	0.6956	-0.97	0.6839	-0.80	-0.4074	5.97	0.6640	-0.60
BF	0.3170	0.00	0.6956	0.97	1.0000	0.00	0.9367	0.12	0.4383	0.00	0.7928	0.36
RF	0.2799	-1.89	0.6839	0.80	0.9367	-0.12	1.0000	0.00	-0.3370	-5.85	0.8585	0.18
G	0.2975	0.00	-0.4074	-5.97	0.4383	0.00	-0.3370	5.85	1.0000	0.00	-0.3079	6.00
TA	0.2183	-1.98	0.6640	0.60	0.7928	-0.36	0.8585	-0.18	-0.3079	-6.00	1.0000	0.00

Table 4.44: Cross-correlation analysis of left side estimated muscle forces for sagittal lift/lower task - Participant 07.

Muscle	RA		ES		BF		RF		G		TA	
	r-value	lag(s)	r-value	lag(s)	r-value	lag(s)	r-value	lag(s)	r-value	lag(s)	r-value	lag(s)
RA	1.0000	0.00	0.4520	0.00	0.3548	1.11	0.4302	0.00	0.2028	2.24	-0.1922	-2.88
ES	0.4520	0.00	1.0000	0.00	0.6592	-0.12	0.5508	-0.02	0.3158	-1.38	-0.3631	4.29
BF	0.3548	-1.11	0.6592	0.12	1.0000	0.00	0.6170	-0.14	0.5836	0.00	-0.3873	4.31
RF	0.4302	0.00	0.5508	0.02	0.6170	0.14	1.0000	0.00	0.4378	-1.27	0.2881	-1.35
G	0.2028	-2.24	0.3158	1.38	0.5836	0.00	0.4378	1.27	1.0000	0.00	0.5054	0.01
TA	-0.1922	2.88	-0.3631	-4.29	-0.3873	-4.31	0.2881	1.35	0.5054	-0.01	1.0000	0.00

Table 4.45: Cross-correlation analysis of right side estimated muscle forces for sagittal lift/lower task - Participant 02.

Muscle	RA		ES		BF		RF		G		TA	
	r-value	lag(s)	r-value	lag(s)	r-value	lag(s)	r-value	lag(s)	r-value	lag(s)	r-value	lag(s)
RA	1.0000	0.00	0.9596	0.00	0.9696	0.00	0.9677	0.00	0.8274	0.00	0.6489	0.00
ES	0.9596	0.00	1.0000	0.00	0.9544	0.00	0.9335	0.00	0.8132	0.00	0.5809	0.00
BF	0.9696	0.00	0.9544	0.00	1.0000	0.00	0.9816	0.00	0.8960	0.00	0.7401	0.00
RF	0.9677	0.00	0.9335	0.00	0.9816	0.00	1.0000	0.00	0.8782	0.00	0.7299	0.00
G	0.8274	0.00	0.8132	0.00	0.8960	0.00	0.8782	0.00	1.0000	0.00	0.8115	0.00
TA	0.6489	0.00	0.5809	0.00	0.7401	0.00	0.7299	0.00	0.8115	0.00	1.0000	0.00

Table 4.46: Cross-correlation analysis of right side estimated muscle forces for sagittal lift/lower task - Participant 03.

Muscle	RA		ES		BF		RF		G		TA	
	r-value	lag(s)	r-value	lag(s)	r-value	lag(s)	r-value	lag(s)	r-value	lag(s)	r-value	lag(s)
RA	1.0000	0.00	0.5413	0.27	0.4590	-0.86	0.4643	-0.99	0.4407	0.00	0.4672	0.00
ES	0.5413	-0.27	1.0000	0.00	0.6081	-0.02	0.3455	-3.74	0.7491	0.06	0.7797	0.00
BF	0.4590	0.86	0.6081	0.02	1.0000	0.00	0.8251	0.01	0.4653	-1.93	0.5337	0.00
RF	0.4643	0.99	0.3455	3.74	0.8251	-0.01	1.0000	0.00	0.3387	-2.21	0.3760	0.00
G	0.4407	0.00	0.7491	-0.06	0.4653	1.93	0.3387	2.21	1.0000	0.00	0.7638	-0.12
TA	0.4672	0.00	0.7797	0.00	0.5337	0.00	0.3760	0.00	0.7638	0.12	1.0000	0.00

Table 4.47: Cross-correlation analysis of right side estimated muscle forces for sagittal lift/lower task - Participant 04.

Muscle	RA		ES		BF		RF		G		TA	
	r-value	lag(s)	r-value	lag(s)	r-value	lag(s)	r-value	lag(s)	r-value	lag(s)	r-value	lag(s)
RA	1.0000	0.00	0.5501	0.57	0.4580	0.04	0.5004	-0.30	0.7334	0.08	0.3945	0.20
ES	0.5501	-0.57	1.0000	0.00	0.6836	-0.27	0.6385	0.20	0.6466	-0.59	0.2972	1.29
BF	0.4580	-0.04	0.6836	0.27	1.0000	0.00	0.4795	1.10	0.6696	-0.03	0.4224	1.54
RF	0.5004	0.30	0.6385	-0.20	0.4795	-1.10	1.0000	0.00	0.5012	-1.12	0.2975	0.74
G	0.7334	-0.08	0.6466	0.59	0.6696	0.03	0.5012	1.12	1.0000	0.00	0.4355	0.04
TA	0.3945	-0.20	0.2972	-1.29	0.4224	-1.54	0.2975	-0.74	0.4355	-0.04	1.0000	0.00

Table 4.48: Cross-correlation analysis of right side estimated muscle forces for sagittal lift/lower task - Participant 05.

Muscle	RA		ES		BF		RF		G		TA	
	r-value	lag(s)	r-value	lag(s)	r-value	lag(s)	r-value	lag(s)	r-value	lag(s)	r-value	lag(s)
RA	1.0000	0.00	0.4764	0.00	0.4772	-1.42	0.3234	0.10	0.4533	-1.48	0.4463	0.03
ES	0.4764	0.00	1.0000	0.00	0.8409	0.06	0.2971	-0.40	0.9067	0.04	0.4544	-0.34
BF	0.4772	1.42	0.8409	-0.06	1.0000	0.00	0.5194	-0.13	0.8468	-0.01	0.6459	-0.22
RF	0.3234	-0.10	0.2971	0.40	0.5194	0.13	1.0000	0.00	0.4221	0.05	0.8855	-0.02
G	0.4533	1.48	0.9067	-0.04	0.8468	0.01	0.4221	-0.05	1.0000	0.00	0.5499	-0.13
TA	0.4463	-0.03	0.4544	0.34	0.6459	0.22	0.8855	0.02	0.5499	0.13	1.0000	0.00

Table 4.49: Cross-correlation analysis of right side estimated muscle forces for sagittal lift/lower task - Participant 06.

Muscle	RA		ES		BF		RF		G		TA	
	r-value	lag(s)	r-value	lag(s)	r-value	lag(s)	r-value	lag(s)	r-value	lag(s)	r-value	lag(s)
RA	1.0000	0.00	-0.1822	5.93	0.4051	0.73	0.3948	0.80	0.3237	0.00	0.3547	1.19
ES	-0.1822	-5.93	1.0000	0.00	0.2687	0.65	0.2659	0.71	0.2243	-2.27	0.3791	-1.81
BF	0.4051	-0.73	0.2687	-0.65	1.0000	0.00	0.9899	0.11	0.4945	-0.02	0.8800	0.31
RF	0.3948	-0.80	0.2659	-0.71	0.9899	-0.11	1.0000	0.00	0.4485	-0.18	0.8745	0.17
G	0.3237	0.00	0.2243	2.27	0.4945	0.02	0.4485	0.18	1.0000	0.00	0.4996	0.36
TA	0.3547	-1.19	0.3791	1.81	0.8800	-0.31	0.8745	-0.17	0.4996	-0.36	1.0000	0.00

Table 4.50: Cross-correlation analysis of right side estimated muscle forces for sagittal lift/lower task - Participant 07.

Tables 4.51 through 4.54 show the average and standard deviation of the results of the cross-correlation analysis on the estimated muscle forces across all participants for the sagittal lift/lower task.

Muscle	RA		ES		BF		RF		G		TA	
	r-value	lag(s)	r-value	lag(s)	r-value	lag(s)	r-value	lag(s)	r-value	lag(s)	r-value	lag(s)
RA	1.0000	0.0000	0.6468	-0.0098	0.6090	-0.0071	0.6606	0.2248	0.5179	-0.9275	0.6624	0.3027
ES	0.6468	0.0098	1.0000	0.0000	0.6918	-0.2996	0.6868	-0.0879	0.5128	1.1352	0.7353	-0.0571
BF	0.6090	0.0071	0.6918	0.2996	1.0000	0.0000	0.8010	0.1985	0.6523	0.2783	0.6988	0.2817
RF	0.6606	-0.2248	0.6868	0.0879	0.8010	-0.1985	1.0000	0.0000	0.5027	-0.9119	0.8297	0.1069
G	0.5179	0.9275	0.5128	-1.1352	0.6523	-0.2783	0.5027	0.9119	1.0000	0.0000	0.5830	0.9469
TA	0.6624	-0.3027	0.7353	0.0571	0.6988	-0.2817	0.8297	-0.1069	0.5830	-0.9469	1.0000	0.0000

Table 4.51: Cross-correlation analysis of left side estimated muscle forces for sagittal lift/lower task - Average across all Participants.

Muscle	RA		ES		BF		RF		G		TA	
	r-value	lag(s)	r-value	lag(s)	r-value	lag(s)	r-value	lag(s)	r-value	lag(s)	r-value	lag(s)
RA	0.0000	0.0000	0.3311	0.2609	0.2933	0.0779	0.3067	0.8416	0.5010	2.2823	0.3114	0.8249
ES	0.3311	0.2609	0.0000	0.0000	0.2648	0.5214	0.2783	0.4248	0.5206	2.3823	0.2266	0.3200
BF	0.2933	0.0779	0.2648	0.5214	0.0000	0.0000	0.2068	0.5010	0.2489	0.6708	0.2130	0.5788
RF	0.3067	0.8416	0.2783	0.4248	0.2068	0.5010	0.0000	0.0000	0.4796	2.4209	0.1109	0.1524
G	0.5010	2.2823	0.5206	2.3823	0.2489	0.6708	0.4796	2.4209	0.0000	0.0000	0.4591	2.4776
TA	0.3114	0.8249	0.2266	0.3200	0.2130	0.5788	0.1109	0.1524	0.4591	2.4776	0.0000	0.0000

Table 4.52: Cross-correlation analysis of left side estimated muscle forces for sagittal lift/lower task - Standard deviation across all Participants.

Muscle	RA		ES		BF		RF		G		TA	
	r-value	lag(s)	r-value	lag(s)	r-value	lag(s)	r-value	lag(s)	r-value	lag(s)	r-value	lag(s)
RA	1.0000	0.0000	0.4662	1.1281	0.5206	-0.0671	0.5135	-0.0675	0.4969	0.1406	0.3532	-0.2431
ES	0.4662	-1.1281	1.0000	0.0000	0.6691	0.0519	0.5052	-0.5415	0.6093	-0.6892	0.3547	0.5700
BF	0.5206	0.0671	0.6691	-0.0519	1.0000	0.0000	0.7354	0.1579	0.6593	-0.3317	0.4725	0.9913
RF	0.5135	0.0675	0.5052	0.5415	0.7354	-0.1579	1.0000	0.0000	0.5044	-0.7875	0.5752	-0.0775
G	0.4969	-0.1406	0.6093	0.6892	0.6593	0.3317	0.5044	0.7875	1.0000	0.0000	0.5943	0.0267
TA	0.3532	0.2431	0.3547	-0.5700	0.4725	-0.9913	0.5752	0.0775	0.5943	-0.0267	1.0000	0.0000

Table 4.53: Cross-correlation analysis of right side estimated muscle forces for sagittal lift/lower task - Average across all Participants.

Muscle	RA		ES		BF		RF		G		TA	
	r-value	lag(s)	r-value	lag(s)	r-value	lag(s)	r-value	lag(s)	r-value	lag(s)	r-value	lag(s)
RA	0.0000	0.0000	0.3679	2.3615	0.2245	0.9502	0.2307	0.5817	0.2395	1.1916	0.2857	1.3701
ES	0.3679	2.3615	0.0000	0.0000	0.2347	0.3144	0.2567	1.6065	0.2776	0.9535	0.3901	2.0728
BF	0.2245	0.9502	0.2347	0.3144	0.0000	0.0000	0.2278	0.4690	0.1799	0.7807	0.4502	1.7454
RF	0.2307	0.5817	0.2567	1.6065	0.2278	0.4690	0.0000	0.0000	0.1905	0.9000	0.2860	0.6871
G	0.2395	1.1916	0.2776	0.9535	0.1799	0.7807	0.1905	0.9000	0.0000	0.0000	0.1549	0.1790
TA	0.2857	1.3701	0.3901	2.0728	0.4502	1.7454	0.2860	0.6871	0.1549	0.1790	0.0000	0.0000

Table 4.54: Cross-correlation analysis of right side estimated muscle forces for sagittal lift/lower task - Standard deviation across all Participants.

Motion Platform Task

Tables 4.55 through 4.58 show the results of the cross-correlation analysis on the CoM and estimated muscle forces. In general, the correlation coefficients for this task are much lower than for the quiet standing task due to the large influence of the platform motion on CoM. However, the difference in coefficients with respect to the various muscles are still equally meaningful. With the exception of Participant 04, there is very little correlation between CoM and the estimated force of the RA and ES; indicating that in this type of task the participants are not using these muscles as much as the others for control of CoM. Participant 03 shows especially low values on her left side due to her foot drop condition; however, on her right side she shows signs of using her RF, G, and TA primarily for control of CoM. The large delay in G indicates that this muscle may be used to arrest the rate of change of CoM as it approaches its target.

Participant	RA		ES		BF		RF		G		TA	
	r-value	lag(s)	r-value	lag(s)	r-value	lag(s)	r-value	lag(s)	r-value	lag(s)	r-value	lag(s)
02	-0.1901	-0.78	0.1980	0.55	0.6540	0.59	-0.1528	-0.61	0.5402	0.39	0.6080	0.52
03	-0.0965	-1.69	-0.0965	-1.50	-0.0872	-1.62	-0.0952	-1.62	-0.1409	-2.46	-0.1826	-0.13
04	-0.3903	-0.47	-0.3384	-2.38	-0.4048	-0.32	-0.3545	-0.11	-0.2960	-2.31	-0.3768	-0.20
05	-0.1709	-1.80	-0.1843	-5.00	-0.2029	-0.66	-0.1507	-0.67	0.3746	1.18	-0.3602	-0.09
07	0.1058	0.91	0.1052	-1.30	0.1271	-2.28	0.1813	-3.43	0.2035	-1.10	0.2187	-3.75
mean	-0.1484	-0.7630	-0.0632	-1.9243	0.0172	-0.8583	-0.1144	-1.2883	0.1363	-0.8598	-0.0186	-0.7318
std	0.1790	1.0964	0.2168	2.0234	0.4047	1.1198	0.1925	1.3140	0.3493	1.6164	0.4245	1.7103

Table 4.55: Cross-correlation analysis of sagittal CoM vs left side estimated muscle forces for motion platform task.

Participant	RA		ES		BF		RF		G		TA	
	r-value	lag(s)	r-value	lag(s)	r-value	lag(s)	r-value	lag(s)	r-value	lag(s)	r-value	lag(s)
02	-0.1495	-0.83	0.0978	-2.60	0.2673	-2.65	-0.2216	-0.12	-0.1670	-1.49	0.2472	-2.71
03	-0.1860	-4.96	-0.2320	-2.67	-0.1125	-0.19	-0.2245	-0.25	-0.3689	2.93	-0.4880	-0.33
04	-0.4182	0.00	-0.5312	-1.35	-0.3703	-0.22	-0.3669	0.09	0.1743	-4.77	-0.3597	-0.06
05	-0.2081	-5.00	-0.0590	-0.43	-0.1768	-0.13	-0.2618	-0.20	0.3125	-1.60	-0.4569	-0.12
07	0.2392	-1.26	0.2350	-1.25	0.2445	-1.24	0.2555	-1.26	0.2601	-1.23	0.2101	-1.28
mean	-0.1445	-2.41	-0.0979	-1.66	-0.0296	-0.88	-0.1639	-0.35	0.0422	-1.23	-0.1695	-0.90
std	0.2387	2.39	0.2985	0.96	0.2774	1.09	0.2417	0.53	0.2961	2.74	0.3667	1.12

Table 4.56: Cross-correlation analysis of sagittal CoM vs right side estimated muscle forces for motion platform task.

Participant	RA		ES		BF		RF		G		TA	
	r-value	lag(s)	r-value	lag(s)	r-value	lag(s)	r-value	lag(s)	r-value	lag(s)	r-value	lag(s)
02	0.0975	-0.76	-0.0802	-3.97	-0.6088	0.18	-0.2322	1.88	-0.4151	0.32	-0.5526	0.23
03	-0.0395	-2.54	-0.0399	4.08	-0.0445	4.15	-0.0351	-2.54	-0.1738	-0.25	-0.0640	1.26
04	0.1635	-0.57	0.2099	-2.68	0.1847	-1.26	0.1856	-0.21	0.1659	-2.69	0.1588	-2.64
05	0.0985	-1.72	0.0579	3.84	0.0858	5.00	0.0841	0.21	-0.3553	0.18	0.1697	-1.84
07	-0.1474	-1.37	0.0674	-0.43	-0.1281	3.20	0.1967	-2.31	0.2374	2.37	-0.1774	2.53
mean	0.0345	-1.39	0.0430	0.17	-0.1022	2.25	0.0398	-0.60	-0.1082	-0.02	-0.0931	-0.09
std	0.1257	0.79	0.1126	3.69	0.3075	2.68	0.1785	1.85	0.2975	1.81	0.2965	2.14

Table 4.57: Cross-correlation analysis of lateral CoM vs left side estimated muscle forces for motion platform task.

Participant	RA		ES		BF		RF		G		TA	
	r-value	lag(s)	r-value	lag(s)	r-value	lag(s)	r-value	lag(s)	r-value	lag(s)	r-value	lag(s)
02	0.0822	-1.53	0.1179	1.60	-0.3893	-4.11	0.1037	-5.00	-0.0956	1.05	-0.3585	-4.14
03	-0.1618	-1.33	-0.3706	-0.18	-0.0472	-0.82	-0.1406	3.28	0.6148	0.01	0.3046	-1.56
04	0.2276	-0.12	0.2913	-1.39	0.1366	-2.68	0.1814	-0.01	0.2097	0.91	0.1598	-2.64
05	0.0685	-0.50	0.0748	1.90	0.0994	-4.72	0.0658	-2.37	0.6279	0.47	-0.2500	2.53
07	0.1913	-0.68	0.1961	-0.71	0.2004	-0.73	0.2276	-0.81	0.2070	-0.67	0.1970	-0.92
mean	0.0816	-0.83	0.0619	0.25	0.0000	-2.61	0.0876	-0.98	0.3127	0.36	0.0106	-1.34
std	0.1523	0.59	0.2554	1.44	0.2358	1.84	0.1425	3.05	0.3079	0.70	0.2948	2.49

Table 4.58: Cross-correlation analysis of lateral CoM vs right side estimated muscle forces for motion platform task.

Tables 4.59 through 4.62 show the same-side correlation analysis between CoP and estimated muscle force. These correlation coefficients are also significantly smaller than in the quiet standing task and again this is attributable to the large effect the platform orientation has on changes in CoP. In addition, the pressure sensors are not sensitive to shear loading - and may in fact become unreliable at recording accurate normal forces under too much shear loading. In general, however, the cross-correlation analysis still shows that the majority of control over CoP is being provided by the BF, RF, G, and TA with delays on the order of one second for most participants.

Participant	RA		ES		BF		RF		G		TA	
	r-value	lag(s)	r-value	lag(s)	r-value	lag(s)	r-value	lag(s)	r-value	lag(s)	r-value	lag(s)
02	-0.2235	-4.54	0.1911	-0.96	0.4438	-0.53	-0.1486	-0.87	0.3975	-0.81	0.4402	0.89
03	0.2448	-1.36	0.2652	-1.33	0.2516	-1.35	0.2502	-1.37	0.1840	-5.00	0.2459	-1.38
04	-0.3058	-0.23	-0.3270	0.02	-0.3122	-0.18	-0.2240	-0.13	-0.2589	-0.03	-0.2987	-0.18
05	-0.2177	-1.55	-0.1621	-1.52	-0.1876	-1.25	-0.2119	-1.49	0.3548	0.66	-0.4035	-0.80
06	0.2196	-5.00	0.2168	-2.93	-0.3263	0.41	-0.4301	-1.14	0.4855	0.74	0.1789	4.15
07	0.0881	-1.48	0.1049	2.52	0.1242	-1.29	0.1322	-4.08	0.3879	-0.88	-0.1599	-1.12
mean	-0.0565	-2.54	0.0368	-1.34	-0.0261	-0.58	-0.1529	-1.00	0.2326	-0.89	0.0326	0.54
std	0.2660	2.11	0.2647	1.07	0.3521	0.74	0.2490	0.54	0.2958	2.38	0.3650	2.19

Table 4.59: Cross-correlation analysis of sagittal CoP vs estimated muscle forces for motion platform task - left side.

Participant	RA		ES		BF		RF		G		TA	
	r-value	lag(s)	r-value	lag(s)	r-value	lag(s)	r-value	lag(s)	r-value	lag(s)	r-value	lag(s)
02	-0.1795	4.92	0.1598	-0.61	0.2155	-0.49	-0.2795	-0.91	-0.1773	-2.10	0.1942	-0.43
03	-0.1918	-3.66	-0.2523	-0.88	-0.3215	0.28	-0.2674	1.09	0.2511	-2.91	-0.5041	1.04
04	-0.3253	0.00	-0.5362	-2.94	-0.3090	-2.47	-0.2694	-2.00	0.1755	-2.24	-0.3087	-2.40
05	0.1053	1.17	0.1123	1.18	-0.0958	-0.28	-0.1205	-0.23	0.6278	-0.65	-0.4550	-0.62
06	0.1590	0.01	0.2033	4.65	-0.3179	-0.74	-0.5210	0.42	0.4119	0.50	0.1256	0.79
07	-0.1621	1.53	-0.1569	1.52	-0.1425	1.52	-0.1374	1.53	-0.1542	1.52	-0.1606	1.53
mean	-0.0865	0.49	-0.0626	0.28	-0.1657	-0.74	-0.2916	-0.33	0.2578	-1.48	-0.1896	-0.33
std	0.2085	3.07	0.3206	2.85	0.2335	1.04	0.1442	1.19	0.2986	1.38	0.3280	1.37

Table 4.60: Cross-correlation analysis of sagittal CoP vs estimated muscle forces for motion platform task - right side.

Participant	RA		ES		BF		RF		G		TA	
	r-value	lag(s)	r-value	lag(s)	r-value	lag(s)	r-value	lag(s)	r-value	lag(s)	r-value	lag(s)
02	-0.1152	-4.54	-0.1152	-0.92	-0.2074	5.00	-0.1569	-0.90	0.1161	-2.16	0.1571	4.92
03	0.3605	-1.36	0.3605	-2.07	0.3486	-2.07	0.3584	-2.07	0.3620	-2.08	0.3149	-3.66
04	-0.2507	-0.23	-0.2507	-2.32	-0.3400	5.00	-0.1784	5.00	-0.3130	-2.06	-0.2090	0.00
05	-0.1204	-1.55	-0.1204	1.11	0.1830	-1.07	-0.1146	-5.00	-0.2617	-1.03	-0.2406	1.17
06	-0.2390	-5.00	-0.2390	-4.42	-0.2445	0.00	0.3108	-1.17	-0.4537	0.39	-0.1627	0.01
07	-0.1336	-1.48	-0.1336	3.84	-0.0603	3.43	0.2105	-2.09	0.3050	2.52	-0.1833	1.53
mean	-0.0729	-2.54	-0.0729	-1.73	-0.0521	1.37	0.0438	-0.83	-0.1101	-1.39	-0.0281	0.49
std	0.2505	2.11	0.2505	2.03	0.2999	3.39	0.2669	3.64	0.3377	1.10	0.2490	3.07

Table 4.61: Cross-correlation analysis of lateral CoP vs estimated muscle forces for motion platform task - left side.

Participant	RA		ES		BF		RF		G		TA	
	r-value	lag(s)	r-value	lag(s)	r-value	lag(s)	r-value	lag(s)	r-value	lag(s)	r-value	lag(s)
02	0.1482	-1.54	0.1842	-0.57	0.1339	-2.84	0.2197	-4.79	0.1728	-5.00	0.1577	-2.84
03	0.1487	-2.00	0.2842	-0.81	0.2251	-0.83	0.1796	1.20	0.3483	4.40	0.5276	1.07
04	-0.1864	4.48	-0.1024	1.69	-0.2812	-2.67	-0.2583	-2.12	-0.2469	3.23	-0.2674	-2.43
05	0.0676	-1.35	0.1581	1.37	0.0869	5.00	0.1140	1.60	0.5139	-0.11	0.1537	5.00
06	-0.4616	-5.00	-0.2295	-4.97	-0.3020	-4.87	-0.4301	-0.01	-0.3186	-5.00	0.1592	0.28
07	0.1934	1.50	0.1723	1.51	0.1708	1.52	-0.1666	-4.48	0.1984	1.51	0.1701	1.49
mean	-0.0567	-1.08	0.0589	-0.66	-0.0275	-1.24	-0.0350	-0.82	0.0939	-0.50	0.1462	0.22
std	0.2648	3.44	0.2153	2.66	0.2463	3.77	0.2912	2.65	0.3653	4.43	0.2815	3.16

Table 4.62: Cross-correlation analysis of lateral CoP vs estimated muscle forces for motion platform task - right side.

Tables 4.63 through 4.74 show the results of the cross-correlation analysis of the estimated muscle forces for the left and right sides of the body.

Participant 02 shows very little lag between the various muscles and has the highest correlation coefficients in the RF, G, and TA.

Participant 03 once again shows extremely high levels of correlation across all muscles on her left side and lower correlations with RF, G, and TA on her right side. This is likely due to her foot drop condition in the left foot. Specifically, the high level of correlation across all muscles in the left side seems to indicate that the absence of neurological feedback in that foot is preventing efficient and independent control of the various muscles on that side of her body. It may also be that she is keeping her joints much stiffer to counter the slower, less certain reaction to change on that side of her body. This could also explain the lower correlations on the right side; since her left side is so much stiffer her CoM and CoP are not going to move as quickly and will require less active control from the right side.

Participant 04 shows signs of BF playing a larger role than in most of the other participants and G playing less of a role on his right side as well.

Participant 05 shows much higher RA, ES, and BF activity than most other participants. This indicates that she may have used a stiffening strategy for this task, increasing the stiffness of her ankles, knees, and hips to minimize changes to CoM in response to platform movement. Her right side G and TA show much lower correlation to the other muscles than typical. This may show that she is using a more complex strategy where she stiffens her her hips, knees, and ankle of the non-dominant leg while letting the ankle of her dominant leg remain less stiff to allow fast adjustments to CoP in response to unexpected changes in the support surface.

Participant 06 follows the trends for the most part, although his right side TA shows much lower correlation to the other muscles.

Participant 07 shows fairly typical correlation values for his left side with the exception of a higher BF than most participants, but has extremely high correlation coefficients for all muscles on his right side. This likely indicates that he is using a stiffening strategy on his dominant side while keeping his left side more in line with the more general strategy

seen in the other participants.

When considered with the results from the various other tasks, this fairly conclusively shows that RF, G, and TA are consistently the muscles most involved in postural stability tasks. This makes sense as these muscles directly control stiffness and articulation of the ankle, knee, and even hip to some degree in the case of RF.

Muscle	RA		ES		BF		RF		G		TA	
	r-value	lag(s)	r-value	lag(s)	r-value	lag(s)	r-value	lag(s)	r-value	lag(s)	r-value	lag(s)
RA	1.0000	0.00	0.5689	0.06	0.2690	4.92	0.5630	0.05	0.4461	0.00	0.3788	-0.03
ES	0.5689	-0.06	1.0000	0.00	0.3467	0.06	0.4589	-0.07	0.5458	0.00	0.5044	0.00
BF	0.2690	-4.92	0.3467	-0.06	1.0000	0.00	0.3339	0.04	0.7643	-0.05	0.9107	-0.05
RF	0.5630	-0.05	0.4589	0.07	0.3339	-0.04	1.0000	0.00	0.4270	0.01	0.4920	0.00
G	0.4461	0.00	0.5458	0.00	0.7643	0.05	0.4270	-0.01	1.0000	0.00	0.8080	0.00
TA	0.3788	0.03	0.5044	0.00	0.9107	0.05	0.4920	0.00	0.8080	0.00	1.0000	0.00

Table 4.63: Cross-correlation analysis of left side estimated muscle forces for motion platform task - Participant 02.

Muscle	RA		ES		BF		RF		G		TA	
	r-value	lag(s)	r-value	lag(s)	r-value	lag(s)	r-value	lag(s)	r-value	lag(s)	r-value	lag(s)
RA	1.0000	0.00	0.9873	0.00	0.9891	0.00	0.9982	0.00	0.8854	0.00	0.8643	0.00
ES	0.9873	0.00	1.0000	0.00	0.9839	0.00	0.9891	0.00	0.8704	0.00	0.8783	0.00
BF	0.9891	0.00	0.9839	0.00	1.0000	0.00	0.9908	0.00	0.9226	0.00	0.8978	0.00
RF	0.9982	0.00	0.9891	0.00	0.9908	0.00	1.0000	0.00	0.8872	0.00	0.8724	0.00
G	0.8854	0.00	0.8704	0.00	0.9226	0.00	0.8872	0.00	1.0000	0.00	0.8864	0.00
TA	0.8643	0.00	0.8783	0.00	0.8978	0.00	0.8724	0.00	0.8864	0.00	1.0000	0.00

Table 4.64: Cross-correlation analysis of left side estimated muscle forces for motion platform task - Participant 03.

Muscle	RA		ES		BF		RF		G		TA	
	r-value	lag(s)	r-value	lag(s)	r-value	lag(s)	r-value	lag(s)	r-value	lag(s)	r-value	lag(s)
RA	1.0000	0.00	0.5156	-0.15	0.8671	0.06	0.8409	0.06	0.8608	0.13	0.8326	0.02
ES	0.5156	0.15	1.0000	0.00	0.6070	0.02	0.4881	-0.08	0.5482	0.02	0.6280	-0.06
BF	0.8671	-0.06	0.6070	-0.02	1.0000	0.00	0.8475	-0.04	0.8932	0.01	0.9505	-0.02
RF	0.8409	-0.06	0.4881	0.08	0.8475	0.04	1.0000	0.00	0.8414	0.07	0.8295	0.00
G	0.8608	-0.13	0.5482	-0.02	0.8932	-0.01	0.8414	-0.07	1.0000	0.00	0.8893	-0.06
TA	0.8326	-0.02	0.6280	0.06	0.9505	0.02	0.8295	0.00	0.8893	0.06	1.0000	0.00

Table 4.65: Cross-correlation analysis of left side estimated muscle forces for motion platform task - Participant 04.

Muscle	RA		ES		BF		RF		G		TA	
	r-value	lag(s)	r-value	lag(s)	r-value	lag(s)	r-value	lag(s)	r-value	lag(s)	r-value	lag(s)
RA	1.0000	0.00	0.7996	0.01	0.7856	0.02	0.8992	0.00	0.6178	-0.06	0.5542	0.56
ES	0.7996	-0.01	1.0000	0.00	0.7689	0.02	0.8025	0.03	0.5868	-0.09	0.5937	0.07
BF	0.7856	-0.02	0.7689	-0.02	1.0000	0.00	0.7809	0.01	0.4799	-0.07	0.6676	0.09
RF	0.8992	0.00	0.8025	-0.03	0.7809	-0.01	1.0000	0.00	0.5450	-0.10	0.5760	0.05
G	0.6178	0.06	0.5868	0.09	0.4799	0.07	0.5450	0.10	1.0000	0.00	0.4035	0.14
TA	0.5542	-0.56	0.5937	-0.07	0.6676	-0.09	0.5760	-0.05	0.4035	-0.14	1.0000	0.00

Table 4.66: Cross-correlation analysis of left side estimated muscle forces for motion platform task - Participant 05.

Muscle	RA		ES		BF		RF		G		TA	
	r-value	lag(s)	r-value	lag(s)	r-value	lag(s)	r-value	lag(s)	r-value	lag(s)	r-value	lag(s)
RA	1.0000	0.00	0.2174	4.83	0.2613	0.00	0.1880	-0.01	0.3114	0.01	0.4381	4.83
ES	0.2174	-4.83	1.0000	0.00	-0.1481	-1.62	-0.2382	-1.48	0.3448	0.00	0.3551	0.04
BF	0.2613	0.00	-0.1481	1.62	1.0000	0.00	0.5236	0.01	-0.1794	3.92	0.3938	0.09
RF	0.1880	0.01	-0.2382	1.48	0.5236	-0.01	1.0000	0.00	-0.2984	3.11	0.3472	0.02
G	0.3114	-0.01	0.3448	0.00	-0.1794	-3.92	-0.2984	-3.11	1.0000	0.00	0.4302	0.04
TA	0.4381	-4.83	0.3551	-0.04	0.3938	-0.09	0.3472	-0.02	0.4302	-0.04	1.0000	0.00

Table 4.67: Cross-correlation analysis of left side estimated muscle forces for motion platform task - Participant 06.

Muscle	RA		ES		BF		RF		G		TA	
	r-value	lag(s)	r-value	lag(s)	r-value	lag(s)	r-value	lag(s)	r-value	lag(s)	r-value	lag(s)
RA	1.0000	0.00	-0.1365	-2.85	-0.3318	-1.40	-0.2647	-1.46	-0.2493	-1.37	-0.1970	-1.45
ES	-0.1365	2.85	1.0000	0.00	0.1351	-0.61	-0.1574	3.90	0.1250	0.99	-0.0964	4.04
BF	-0.3318	1.40	0.1351	0.61	1.0000	0.00	0.6704	0.00	0.5587	0.05	0.4606	0.00
RF	-0.2647	1.46	-0.1574	-3.90	0.6704	0.00	1.0000	0.00	0.5282	0.05	0.4990	0.05
G	-0.2493	1.37	0.1250	-0.99	0.5587	-0.05	0.5282	-0.05	1.0000	0.00	0.3472	-0.03
TA	-0.1970	1.45	-0.0964	-4.04	0.4606	0.00	0.4990	-0.05	0.3472	0.03	1.0000	0.00

Table 4.68: Cross-correlation analysis of left side estimated muscle forces for motion platform task - Participant 07.

Muscle	RA		ES		BF		RF		G		TA	
	r-value	lag(s)	r-value	lag(s)	r-value	lag(s)	r-value	lag(s)	r-value	lag(s)	r-value	lag(s)
RA	1.0000	0.00	0.3873	0.00	0.4238	0.03	0.6770	0.02	0.6164	-0.14	0.4211	-0.05
ES	0.3873	0.00	1.0000	0.00	0.4212	0.10	0.4144	0.31	0.3248	-0.96	0.3893	0.13
BF	0.4238	-0.03	0.4212	-0.10	1.0000	0.00	0.5860	0.10	0.5070	-0.15	0.9775	0.00
RF	0.6770	-0.02	0.4144	-0.31	0.5860	-0.10	1.0000	0.00	0.7031	-0.35	0.6008	-0.09
G	0.6164	0.14	0.3248	0.96	0.5070	0.15	0.7031	0.35	1.0000	0.00	0.5012	0.13
TA	0.4211	0.05	0.3893	-0.13	0.9775	0.00	0.6008	0.09	0.5012	-0.13	1.0000	0.00

Table 4.69: Cross-correlation analysis of right side estimated muscle forces for motion platform task - Participant 02.

Muscle	RA		ES		BF		RF		G		TA	
	r-value	lag(s)	r-value	lag(s)	r-value	lag(s)	r-value	lag(s)	r-value	lag(s)	r-value	lag(s)
RA	1.0000	0.00	0.3234	0.00	0.2489	0.09	0.5074	0.00	0.1657	-4.11	0.2389	2.66
ES	0.3234	0.00	1.0000	0.00	0.6262	-0.03	0.4804	0.00	-0.2311	0.96	-0.1919	-2.48
BF	0.2489	-0.09	0.6262	0.03	1.0000	0.00	0.4934	0.02	-0.1402	-2.60	-0.1352	-2.84
RF	0.5074	0.00	0.4804	0.00	0.4934	-0.02	1.0000	0.00	0.1409	-0.39	0.4360	0.04
G	0.1657	4.11	-0.2311	-0.96	-0.1402	2.60	0.1409	0.39	1.0000	0.00	0.2570	-1.09
TA	0.2389	-2.66	-0.1919	2.48	-0.1352	2.84	0.4360	-0.04	0.2570	1.09	1.0000	0.00

Table 4.70: Cross-correlation analysis of right side estimated muscle forces for motion platform task - Participant 03.

Muscle	RA		ES		BF		RF		G		TA	
	r-value	lag(s)	r-value	lag(s)	r-value	lag(s)	r-value	lag(s)	r-value	lag(s)	r-value	lag(s)
RA	1.0000	0.00	0.6069	-0.01	0.8904	-0.03	0.8103	0.20	0.4765	0.08	0.8993	0.07
ES	0.6069	0.01	1.0000	0.00	0.6110	-0.01	0.5598	0.53	0.3765	0.05	0.5816	0.14
BF	0.8904	0.03	0.6110	0.01	1.0000	0.00	0.8371	0.33	0.5138	0.08	0.8688	0.15
RF	0.8103	-0.20	0.5598	-0.53	0.8371	-0.33	1.0000	0.00	0.4482	-0.24	0.8404	-0.13
G	0.4765	-0.08	0.3765	-0.05	0.5138	-0.08	0.4482	0.24	1.0000	0.00	0.5122	0.05
TA	0.8993	-0.07	0.5816	-0.14	0.8688	-0.15	0.8404	0.13	0.5122	-0.05	1.0000	0.00

Table 4.71: Cross-correlation analysis of right side estimated muscle forces for motion platform task - Participant 04.

Muscle	RA		ES		BF		RF		G		TA	
	r-value	lag(s)	r-value	lag(s)	r-value	lag(s)	r-value	lag(s)	r-value	lag(s)	r-value	lag(s)
RA	1.0000	0.00	0.5040	4.56	0.6749	-0.01	0.6211	0.00	0.1960	-0.09	0.1767	-0.08
ES	0.5040	-4.56	1.0000	0.00	0.6312	0.03	0.7051	0.06	0.1743	0.00	0.1630	0.00
BF	0.6749	0.01	0.6312	-0.03	1.0000	0.00	0.8933	0.02	0.1254	4.55	0.3098	-0.08
RF	0.6211	0.00	0.7051	-0.06	0.8933	-0.02	1.0000	0.00	0.0908	-4.85	0.3130	-0.05
G	0.1960	0.09	0.1743	0.00	0.1254	-4.55	0.0908	4.85	1.0000	0.00	-0.0891	1.74
TA	0.1767	0.08	0.1630	0.00	0.3098	0.08	0.3130	0.05	-0.0891	-1.74	1.0000	0.00

Table 4.72: Cross-correlation analysis of right side estimated muscle forces for motion platform task - Participant 05.

Muscle	RA		ES		BF		RF		G		TA	
	r-value	lag(s)	r-value	lag(s)	r-value	lag(s)	r-value	lag(s)	r-value	lag(s)	r-value	lag(s)
RA	1.0000	0.00	0.2168	0.00	0.3818	0.14	0.3407	5.00	0.5705	0.00	0.1888	-4.50
ES	0.2168	0.00	1.0000	0.00	0.2476	0.00	0.2235	0.14	0.2323	-0.14	-0.1959	5.00
BF	0.3818	-0.14	0.2476	0.00	1.0000	0.00	0.5667	0.04	0.2434	-0.62	0.1550	0.00
RF	0.3407	-5.00	0.2235	-0.14	0.5667	-0.04	1.0000	0.00	0.3147	-5.00	-0.1733	0.17
G	0.5705	0.00	0.2323	0.14	0.2434	0.62	0.3147	5.00	1.0000	0.00	0.1346	0.00
TA	0.1888	4.50	-0.1959	-5.00	0.1550	0.00	-0.1733	-0.17	0.1346	0.00	1.0000	0.00

Table 4.73: Cross-correlation analysis of right side estimated muscle forces for motion platform task - Participant 06.

Muscle	RA		ES		BF		RF		G		TA	
	r-value	lag(s)	r-value	lag(s)	r-value	lag(s)	r-value	lag(s)	r-value	lag(s)	r-value	lag(s)
RA	1.0000	0.00	0.9957	0.00	0.9962	0.00	0.9942	0.00	0.9974	0.00	0.9856	0.00
ES	0.9957	0.00	1.0000	0.00	0.9968	0.00	0.9950	0.00	0.9946	0.00	0.9847	0.00
BF	0.9962	0.00	0.9968	0.00	1.0000	0.00	0.9983	0.00	0.9949	0.00	0.9861	0.00
RF	0.9942	0.00	0.9950	0.00	0.9983	0.00	1.0000	0.00	0.9939	0.00	0.9849	0.00
G	0.9974	0.00	0.9946	0.00	0.9949	0.00	0.9939	0.00	1.0000	0.00	0.9829	0.00
TA	0.9856	0.00	0.9847	0.00	0.9861	0.00	0.9849	0.00	0.9829	0.00	1.0000	0.00

Table 4.74: Cross-correlation analysis of right side estimated muscle forces for motion platform task - Participant 07.

Tables 4.75 through 4.78 show the average and standard deviation of the results of the cross-correlation analysis on the estimated muscle forces across all Participants for the sagittal lift/lower task.

Muscle	RA		ES		BF		RF		G		TA	
	r-value	lag(s)	r-value	lag(s)	r-value	lag(s)	r-value	lag(s)	r-value	lag(s)	r-value	lag(s)
RA	1.0000	0.0000	0.4921	0.3173	0.4734	0.6004	0.5374	-0.2269	0.4787	-0.2165	0.4785	0.6567
ES	0.4921	-0.3173	1.0000	0.0000	0.4489	-0.3531	0.3905	0.3823	0.5035	0.1538	0.4772	0.6790
BF	0.4734	-0.6004	0.4489	0.3531	1.0000	0.0000	0.6912	0.0033	0.5732	0.6421	0.7135	0.0167
RF	0.5374	0.2269	0.3905	-0.3823	0.6912	-0.0033	1.0000	0.0000	0.4884	0.5208	0.6027	0.0190
G	0.4787	0.2165	0.5035	-0.1538	0.5732	-0.6421	0.4884	-0.5208	1.0000	0.0000	0.6274	0.0148
TA	0.4785	-0.6567	0.4772	-0.6790	0.7135	-0.0167	0.6027	-0.0190	0.6274	-0.0148	1.0000	0.0000

Table 4.75: Cross-correlation analysis of left side estimated muscle forces for motion platform task - Average across all Participants.

Muscle	RA		ES		BF		RF		G		TA	
	r-value	lag(s)	r-value	lag(s)	r-value	lag(s)	r-value	lag(s)	r-value	lag(s)	r-value	lag(s)
RA	0.0000	0.0000	0.4042	2.4846	0.5007	2.1911	0.4902	0.6030	0.4218	0.5705	0.3867	2.1527
ES	0.4042	2.4846	0.0000	0.0000	0.4193	0.6703	0.4975	1.8187	0.2505	0.4121	0.3292	1.6447
BF	0.5007	2.1911	0.4193	0.6703	0.0000	0.0000	0.2360	0.0279	0.4090	1.6064	0.2438	0.0586
RF	0.4902	0.6030	0.4975	1.8187	0.2360	0.0279	0.0000	0.0000	0.4269	1.2673	0.2065	0.0244
G	0.4218	0.5705	0.2505	0.4121	0.4090	1.6064	0.4269	1.2673	0.0000	0.0000	0.2591	0.0676
TA	0.3867	2.1527	0.3292	1.6447	0.2438	0.0586	0.2065	0.0244	0.2591	0.0676	0.0000	0.0000

Table 4.76: Cross-correlation analysis of left side estimated muscle forces for motion platform task - Standard deviation across all Participants.

Muscle	RA		ES		BF		RF		G		TA	
	r-value	lag(s)	r-value	lag(s)	r-value	lag(s)	r-value	lag(s)	r-value	lag(s)	r-value	lag(s)
RA	1.0000	0.0000	0.5057	0.7579	0.6027	0.0348	0.6585	0.8698	0.5037	-0.7096	0.4850	-0.3173
ES	0.5057	-0.7579	1.0000	0.0000	0.5890	0.0165	0.5630	0.1740	0.3119	-0.0144	0.2885	0.4652
BF	0.6027	-0.0348	0.5890	-0.0165	1.0000	0.0000	0.7291	0.0842	0.3740	0.2110	0.5270	-0.4606
RF	0.6585	-0.8698	0.5630	-0.1740	0.7291	-0.0842	1.0000	0.0000	0.4486	-1.8027	0.5003	-0.0110
G	0.5037	0.7096	0.3119	0.0144	0.3740	-0.2110	0.4486	1.8027	1.0000	0.0000	0.3831	0.1385
TA	0.4850	0.3173	0.2885	-0.4652	0.5270	0.4606	0.5003	0.0110	0.3831	-0.1385	1.0000	0.0000

Table 4.77: Cross-correlation analysis of right side estimated muscle forces for motion platform task - Average across all Participants.

Muscle	RA		ES		BF		RF		G		TA	
	r-value	lag(s)	r-value	lag(s)	r-value	lag(s)	r-value	lag(s)	r-value	lag(s)	r-value	lag(s)
RA	0.0000	0.0000	0.2761	1.8602	0.2996	0.0657	0.2286	2.0248	0.3068	1.6681	0.3660	2.3127
ES	0.2761	1.8602	0.0000	0.0000	0.2509	0.0452	0.2650	0.2105	0.3976	0.6119	0.4608	2.4444
BF	0.2996	0.0657	0.2509	0.0452	0.0000	0.0000	0.2066	0.1245	0.3914	2.3496	0.4805	1.1680
RF	0.2286	2.0248	0.2650	0.2105	0.2066	0.1245	0.0000	0.0000	0.3472	2.4222	0.4132	0.1066
G	0.3068	1.6681	0.3976	0.6119	0.3914	2.3496	0.3472	2.4222	0.0000	0.0000	0.3718	0.9086
TA	0.3660	2.3127	0.4608	2.4444	0.4805	1.1680	0.4132	0.1066	0.3718	0.9086	0.0000	0.0000

Table 4.78: Cross-correlation analysis of right side estimated muscle forces for motion platform task - Standard deviation across all Participants.

4.4.3 Conclusions

Three main questions were posed regarding the muscles involved in postural stability. The first question asked whether all of the muscles of interest were equally involved in postural stability control. The analysis shows that the answer to this question is highly dependent on the nature of the task being performed, as well as the control strategies typically employed by the individual performing the task. In the case of tasks that involve large movements and lots of articulation of the joints, such as the sagittal lift/lower task, the muscle activity is much more strongly related to the planned movements than the postural stability parameters. However, in the case of relatively static tasks, the RF, G, and TA consistently show the greatest correlation to CoM, CoP, and other muscle forces. In the quiet standing task in particular, it was seen that agonist/antagonist muscle pairs share very similar degrees of correlation to the various postural stability parameters; suggesting that, in such static tasks, the main control strategy is to adjust the stiffness of the various joints through co-contraction of those muscles. The second question asked whether there were delays associated with the activation of the various muscles. Again, this was found to be highly dependent on the particular task and individual. In relatively static tasks such as the quiet standing task, the delays between CoM motion and muscle force are fairly constant for all muscles. There are, however, indications in the analysis that delays are lower in the dominant foot. On the other hand tasks that require large scale movements, such as the sagittal lift/lower task, show very little lag between the forces in the various muscles; indicating that the coordinated effort to control the large scale movements is fairly synchronous compared to the postural stability control system. The final question posed was whether some muscles could be associated with control of CoM while others could be associated with control of CoP. Due to the reasonably high levels of correlation between CoM and CoP themselves, this is particularly difficult to answer. In general, however, it can be said that the muscles higher up on the body have a more direct influence on CoM, while those lower on the body have a more direct influence on CoP. This makes sense, as the

higher muscles control articulation of joints with greater range of motion and greater influence on posture while the lower muscles control joints that can only cause minor changes in CoM but can directly control both the CoP and the force exerted by the feet on the ground.

Chapter 5

Conclusions and Recommendations

5.1 Quantitative Index for Evaluating Aptitude for Postural Stability

An index of postural stability aptitude was calculated using the standard deviation of the CoP over the course of a 30 second quiet standing task. While the index is useful in estimating the likely performance of an individual at general postural stability tasks, it does not provide a means to accurately predict the performance of a particular individual for a specific task. This is due to the wide variety of control strategies that can be employed to maintain stability while allowing differences in the various parameters associated with postural stability.

5.2 Systems Engineering Approach to Postural Stability

The current research, through correlation analysis of 18 postural stability parameters, has shown that it is not sufficient to study individual parameters in isolation. The interactions and relationships between those parameters are of utmost importance as seen, for example, in how the correlation between CoM and CoP changes depending on the task performed. While CoM has traditionally been seen as the parameter to be controlled, with CoP being the independent parameter used to control it, the current research shows that CoM and CoP both influence each other to different degrees depending on the individual and the task

performed. As well, the relationship between CoM, CoP, and muscle forces varies between individuals, tasks, and environmental influences.

5.3 Kinematic Threshold of CoP

The portion of the BoS in which the CoP is actively controlled represents a much smaller fraction of the overall BoS than is typically considered in postural stability research; between 12% and 28% in the tasks performed. Supposing that this area is similarly reduced when MII are actually induced, this may suggest that tradtional models used for prediction of MII, which are mostly based on rigid bodies and the full BoS area, may significantly underestimate the number of MIIs (without proper tuning). Alternatively, this may be further indication of the non-physical parameters affecting MII that were first proposed in [1]. Further study is required to determine the validity of assuming that the area in which the CoP is maintained is similarly reduced when MII are induced.

5.4 Postural Stability Models

The current research has shown, through correlation analysis and study of the motion of CoM and CoP, that treating the human body as a rigid body for the purposes of modelling postural stability can not be extended beyond the most static tasks. For complex tasks that involve large scale movements and joint articulations, CoM and CoP are too independent to use a rigid body. Performing such complex tasks has been shown to substantially alter the correlations between CoM, CoP, and muscle forces. Traditional models can neither account for this, nor the changes in the kinematics of the system when the person is not in an erect posture.

Additionally, the current research has shown that adjustment of joint stiffness, as well as independent control of CoM through joint articulations are two widely used strategies for postural stability control. To accurately model this an articulated model with variable stiffness, actuated joints would be needed.

5.5 Development of Postural Stability (Biomechanics) Research Capability

A substantial groundwork has been lain for the development of a postural stability (or more general biomechanics) research capability, within the Applied Dynamics Laboratory at Carleton University. Important elements of this capability include the MOOG motion platform, the Naturalpoint OptiTrack system, the Tekscan F-Scan pressure sensor system, and the CleveMed BioRadio system. In addition to these commercial systems, a substantial library of Matlab routines has been developed that can support future postural stability research.

5.6 Recommendations

5.6.1 Improvements to Motion Capture System

Many of the issues encountered in the current research were associated with occlusion of the retro reflective markers used by the motion capture systems (problems were encountered with both the Vicon and the OptiTrack systems). In the case of the Vicon system, most of the occlusions were caused by the participants' bodies themselves and as a result of the nature of the tasks performed. In the case of the tasks performed using the OptiTrack system, most of the occlusions were due to the safety railings and padding installed on the motion platform, as well as the small amount of physical space around the motion platform.

It is strongly advised that the motion platform be altered such that the area of "floor" of the platform is as large as possible while preventing collision with the actual floor at the maximum platform positions. This will provide a much larger capture volume that is further away from the obstructing safety railings. In addition, as future plans involve the attachment of three 42 inch LCD displays to add a visual component to the simulation capabilities of the platform, this will move the displays far enough away from the capture volume to significantly reduce the likelihood that they will contribute to marker occlusion.

It is also recommended that additional OptiTrack cameras be purchased and installed.

The current setup uses eight cameras installed on four tripods. Due to the need to have the capture volume include both the stationary and in-motion positions of the MOOG platform, it is very difficult to get good visibility of markers by multiple cameras with this setup. In comparison, the ElectronicArts motion capture studio in Vancouver, BC, uses 100 cameras. While this is partially necessary due to the much larger capture volume in the studio, they do not have to contend with the possibility of occlusions due to the safety railings that the Applied Dynamics Lab must. It is recommended that the lab be upgraded to either a 12 or 18 camera truss setup, as seen in Figures 5.1 and 5.2 respectively. The extra four to ten cameras would do a lot to help with marker occlusion problems and moving to a truss setup would eliminate problems of bumped tripods requiring re-aiming and recalibrating the system (or worse, unknown/unreported movement of the tripods causing incorrect data when a capture session is performed without knowledge of the need to re-aim the cameras).

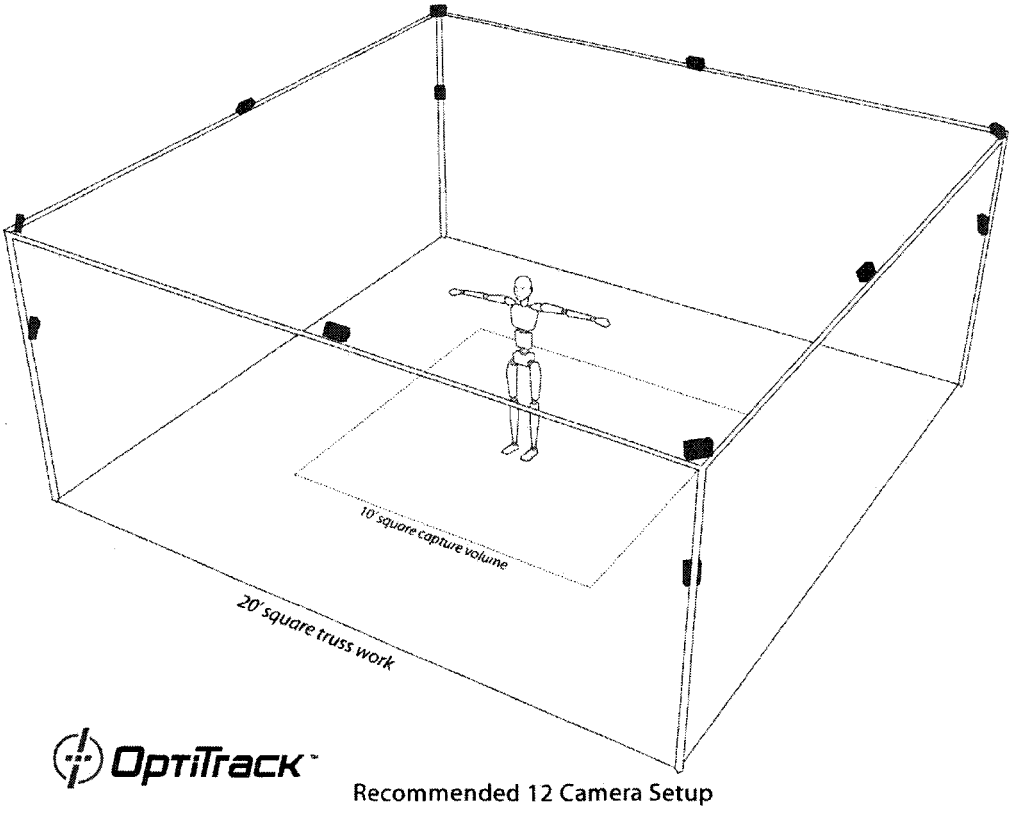

Figure 5.1: OptiTrack 12-camera Truss Setup (Copyright Naturalpoint).

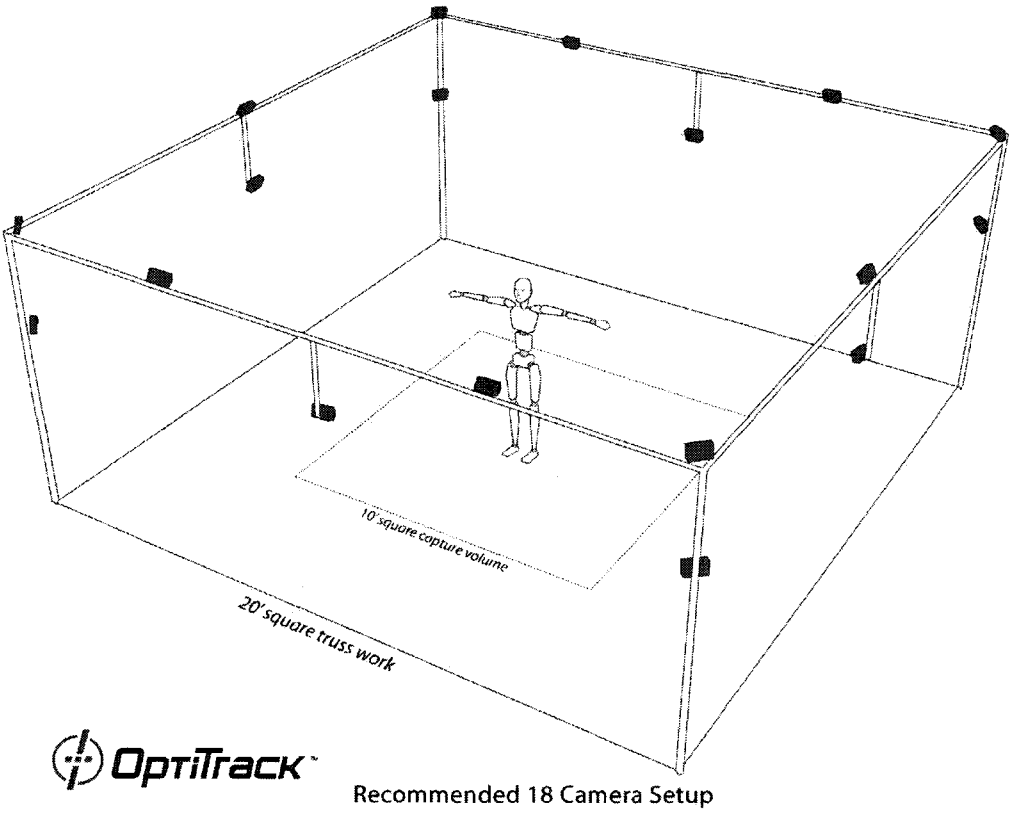

Figure 5.2: OptiTrack 18-camera Truss Setup (Copyright Naturalpoint).

5.6.2 Improvements to EMG System

The BioRadio devices proved to be somewhat limiting for the purposes of EMG recordings for research applications. The two largest limitations encountered were the available sample rate and the wireless technology used by the system.

The BioRadio supports sample rates up to 960 Hz for EMG; however, the author found that the functional limit is actually 800 Hz as any attempt to collect data at the 960 Hz setting resulted in almost 100% data packet loss. As discussed in the literature review, current findings indicate that a much higher range of frequencies in the EMG signal may hold important information about muscle force. From Potvin and Brown's work it is desirable to record EMG at 1024 Hz.

The wireless technology used by the BioRadio devices was, perhaps, the more serious limitation. Many issues with dropped data were encountered during preparation for the

research, and in the data collection sessions themselves. The participants' bodies occasionally blocked the signal. Evidence was seen that suggested a change in the orientation of the BioRadio antenna with respect to the base unit's antenna would result in minor changes in the recorded signal. Finally, at least one case was seen that suggested some of the dropped data may have been associated with another wireless signal in the room where the data collection was being performed (due to the fact that the majority of dropped frames were at a very precise interval).

It is recommended that the Applied Dynamics Lab be equipped with an EMG system capable of sample rates in excess of 1000 Hz and preferably a wired system. The advantages of a wireless system are outweighed by the problems experienced with data loss, and are rendered meaningless by the fact that the pressure sensor system is a wired system anyways.

5.7 Future Work

5.7.1 Comparison with ZRAM Strategy for Postural Stability of Biped Robots

The data collected and analysis tools developed in the current research can lead directly into the study of how human control strategies relate to the ZRAM strategy (or other control strategies) in biped robotics. Given the Matlab software developed for the calculation of CoM from the motion capture data, and the anthropometric data for radius of gyration of the applicable body segments as presented in [36], it should be possible to directly calculate the angular momentum about the CoM. Using this, and the pressure data from the F-Scan system, it should be possible to compare the various control strategies presented in [3] to the strategies used by humans.

5.7.2 Postural Stability Research

Each of the thesis objectives in the current research could easily be expanded to a full Master's thesis project. It is the author's belief that the current research has shown several areas that are interesting enough to warrant future work that could build upon the ideas

and software developed herein.

1. Perform similar experiments, where MIIs are induced in order to determine whether the reduction in the BoS observed in the current research infers a similar reduction in the kinematic thresholds of MII.

2. Can the fidelity of the inverted pendulum model [1] be improved using a reduced BoS according to the kinematic thresholds of MII as determined in the current research?

3. Can the index of postural stability aptitude be used as a tuning input to customize MII models to individual aptitudes?

4. Determine the differences in postural control strategies employed in anticipatory versus reactionary tasks. Specifically, the current research shows indications that CoM and CoP may be more tightly controlled in reactionary tasks; which could be useful for minimizing the risk of instability as a result of sudden, unexpected movements.

5. Explore the similarities and differences between human postural stability control and the ZRAM criteria for biped robotics control.

List of References

[1] R. Langlois, S. MacKinnon, and C. Duncan, "Modelling sea trial motion induced interruption data using an inverted pendulum articulated postural stability model," *International Journal of Maritime Engineering*, vol. 151, no. Part A1, 2009.

[2] A. Goswami, "Postural stability of biped robots and the foot-rotation indicator (fri) point," *The International Journal of Robotics Research*, vol. 18, pp. 523–533, June 1999.

[3] A. Goswami and V. Kallem, "Rate of change of angular momentum and balance maintenance of biped robots," in *Proceedings of the 2004 IEEE International Conference on Robotics and Autonomation*, pp. 3785–3790, 2004.

[4] C. A. Duncan, "Maintaining postural stability on moving surfaces: A preliminary investigation," Master's thesis, University of New Brinswick, 2007.

[5] H. Gray, *Anatomy of the human body.* http://www.bartleby.com/107/: Lea & Febiger, 1918.

[6] L. Rubenstein, "Falls in older people: epidemiology, risk factors, and strategies for prevention," *Age and Ageing*, vol. 35, no. S2, pp. ii37–ii41, 2006.

[7] "Guideline for the prevention of falls in older persons," in *Journal of the American Geriatrics Society*, vol. 49 of *Special Series: Clinical Practice*, pp. 664–672, American Geriatrics Society, 2001.

[8] H. Leung, W. Wong, F. Wu, and J. Guerin, "Perioperative and rehabilitation outcome after lower-limb amputation in elderly chinese patients in hong kong," *Journal of Orthopaedic Surgery*, vol. 12, no. 1, pp. 102–109, 2004.

[9] J. W. Blaszcyk and W. Klonowski, "Postural stability and fractal dynamics," *Acta Neurobiol. Exp.*, vol. 61, pp. 105–112, 2001.

[10] C. M. Hall and L. T. Brody, *Therapeutic Exercise: moving toward function.* 351 West Camden Street, Baltimore, Maryland: Lippincott Williams & Wilkins, 2005.

[11] M. B. Popovic, A. Goswami, and H. Herr, "Ground reference points in legged locomotion: Definitions, biological trajectories and control implications," *The International Journal of Robotics Research*, vol. 24, pp. 1013–1032, December 2005.

[12] M. Ava D. Segal, M. Michael S. Orendurff, P. Glenn K. Klute, C. Martin L. McDowell, R. Janice A. Pecoraro, M. Jane Shofer, and M. Joeseph M. Czerniecki, "Kinematic and kinetic comparisons of transfemoral amputee gait using c-leg and mauch sns prosthetic knees," *Journal of Rehabilitation Research and Development*, vol. 43, pp. 857–870, November/December 2006.

[13] J. Hoffer, M. Baru, S. Bedard, E. Calderon, G. Desmoulin, P. Dhawan, G. Jenne, J. Kerr, M. Whittaker, and T. Zwimpfer, "Initial results with fully implated neurostep fes system for foot drop," in *10th Annual Conference of the International FES Society*, 2005.

[14] J. K. Rankin, M. H. Woollacott, A. Shumway-Cook, and L. A. Brown, "Cognitive influence on postural stability: A neuromuscular analysis in young and older adults," *Journal of Gerontology*, vol. 55A, no. 3, pp. M112–M119, 2000.

[15] A. Bagchee, A. Bhattacharya, P. A. Succop, and R. Emerich, "Postural stability assessment during task performance," *Occupational Ergonomics*, vol. 1, no. 1, pp. 41–53, 1998.

[16] S. R. Lord, R. D. Clark, and I. W. Webster, "Postural stability and associated physiological factors in a population of aged persons," *Journal of Gerontology*, vol. 46, no. 3, pp. M69–M76, 1991.

[17] S. R. Lord, P. N. Sambrook, C. Gilbert, P. J. Kelly, T. Nguyen, I. W. Webster, and J. A. Eisman, "Postural stability, falls and fractures in the elderly: results from the dubbo osteroperosis epidemiology study," *Med J Aust.*, vol. 160, pp. 684–5,688–91, June 1994.

[18] Y. Pai, M. Rogers, J. Patton, T. Cain, and T. Hanke, "Static versus dynamic predictions of protective stepping following waistpull perturbations in young and older adults," *Journal of Biomechanics*, vol. 31, p. 11111118, 1998.

[19] P. Crossland and K. Rich, "Validating a model of the effects of ship motion on postural stability," in *Proceedings of the 1998 International Conference on Environmental Ergonomics*, pp. 385–388, 1998.

[20] N. Nawayseh and M. J. Griffin, "Effect of frequency, magnitude and direction of translational and rotational oscillation on the postural stability of standing people," *Journal of Sound and Vibration*, vol. 298, pp. 725–754, 2006.

[21] A. Baitis, T. Applebee, and T. McNamara, "Human factors considerations applied to operations of the ffg-8 and the lamps mkiii," *Naval Engineers Journal*, vol. 97, no. 4.

[22] Y. Pai, B. Maki, K. Iqbal, W. McIlroy, and S. Perry, "Thresholds of step initiation induced by support surface translation: a dynamic centre-of-mass model provides better prediction than static model," *Journal of Biomechanics*, vol. 33, p. 387392, 2000.

[23] R. Graham, A. Baitis, and W. Meyers, "On the development of seakeeping criteria," *Naval Engineers Journal*, 1992.

[24] J. Wedge and R. G. Langlois, "Simulating the effects of ship motion on postural stability using articulated dynamic models," in *Proceedings of the 2003 Spring Simulation Conference*, 2003.

[25] D. Gong, "The effect of the magnitude and the bandwidth of horizontal floor vibration on postural responses in standing posture," in *32nd UK Group Meeting on Human Responses to Vibration*, 1997.

[26] D. Gong, "Effect of narrow-band platform motions on induced postural responses in a standing posture," in *34th UK Group Meeting on Human Responses to Vibration*, 1999.

[27] W. McIlroy and B. Maki, "The control of lateral stability during rapid stepping reactions evoked by antero-posterior perturbation: does anticipatory control play a role?," *Gait and Posture*, vol. 9, p. 190198, 1999.

[28] W. McIlroy and B. Maki, "Early activation of arm muscles following external perturbation of upright stance," *Neuroscience Letters*, vol. 184, p. 177180, 1995.

[29] L. Kodde, H. Caberg, J. Mol, and C. Massen, "An application of mathematical models in posturography," *Journal of Biomedical Engineering*, vol. 4, p. 4448, 1982.

[30] P. Riley, R. Mann, and W. Hodge, "Modelling of the biomechanics of posture and balance," *Journal of Biomechanics*, vol. 23, p. 503506, 1990.

[31] T. Higuchi, "Approach to an irregular time series on the basis of the fractal theory," *Physica D*, vol. 31, pp. 277–283, 1988.

[32] M. P. Murray, A. A. Seireg, and S. B. Sepic, "Normal postural stability and steadiness: quantative assessment," *J Bone Joint Surg Am.*, vol. 57, pp. 510–516, 1975.

[33] H. Chaudry, T. Findley, K. S. Quigley, B. Bukiet, Z. Ji, T. Sims, and M. Maney, "Measures of postural stability," *Journal of Rehabilitation Research & Development*, vol. 41, no. 5, pp. 713–720, 2004.

[34] A. Shaepan and E. Willems, "Use of a multi-component force platform in stabilometric studies," *Newsletter Force Platform Group*, p. 111, 1982.

[35] D. Thomas and R. Whitney, "Postural movements during normal standing in man," *Journal of Anatomy*, vol. 93, p. 524541, 1959.

[36] D. A. Winter, *Biomechanics and Motor Control of Human Movement.* New Jersey: John Wiley and Sons Inc., 2005.

[37] J. Potvin and S. Brown, "Less is more: high pass filtering, to remove 99% of the surface emg signal power, improves emg-based biceps brachii muscle force estimates," *Journal of Electromyography and Kinesiology*, vol. 14, pp. 389–399, 2004.

[38] J. D. M. Drake and J. P. Callaghan, "Elimination of electrocardiogram contamination from electromyogram signals: An evaluation of currently used removal techniques," *Journal of Electromyography and Kinesiology*, vol. 16, pp. 175–187, 2006.

[39] D. Staudenmann, J. R. Potvin, I. Kingma, D. F. Stegeman, and J. H. van Dieen, "Effects of emg processing on biomechanical models of muscle joint systems: Sensitivity of trunk muscle moments, spinal forces, and stability," *Journal of Biomechanics*, vol. 40, pp. 900–909, 2007.

[40] H. Elftman, "The measurement of the external force in walking," *Science*, vol. 88, p. 152153, 1938.

[41] *MOOG FCS 6DOF2000E Motion System User's Manual.*

[42] "F-scan product page: http://www.tekscan.com/medical/system-fscan1.html." Website, November 2009. As accessed November 23, 2009.

[43] "Biocapture product page: http://www.clevemed.com/biocapture/overview.shtml." Website, November 2009. As accessed November 23, 2009.

[44] "Optitrack product page: http://naturalpoint.com/optitrack/." Website, November 2009. As accessed November 23, 2009.

[45] "Vicon product page: http://www.vicon.com/products/viconmx.html." Website, November 2009. As accessed November 23, 2009.

Appendix A

Matlab Scripts

A.1 Global Constants

```
% The base path to the exported pressure data files
BASEPATH = 'C:\\Users\joel\Documents\Tekscan\Research\Database\export\';

% The base path to the emg data files
EMG_BASEPATH = 'C:\\Users\joel\Documents\BioCapture Data\';

% The base path to the vicon data files
VICON_BASE_PATH = 'C:\\Users\joel\Documents\Vicon Data\';

% Value assigned by CleveMed to dropped data points
CLEVEMED_DROPPED_DATA_VALUE = 10000;

% Value assigned by F-Scan to dropped data points
FSCAN_DROPPED_DATA_VALUE = -1;

% Sample rate of CleveMed BioCapture system in Hz
EMG_SAMPLE_RATE = 800;
```

```
% Switch to turn on/off rectification of EMG signal when filtering
RECTIFY = 1;

% Anthropometric data associated with the body segments in Winter
% [weight_fraction com_distance_from_proximal_head]
BODY_SEGMENT_ANTH_DATA = [
    0.0060 0.506; % Hand
    0.0160 0.430; % Forearm
    0.0280 0.436; % Upper Arm
    0.0145 0.500; % Foot
    0.0465 0.433; % Lower Leg
    0.1000 0.433; % Thigh
    0.5780 0.660]; % Torso
```

A.2 Utility Scripts

A.2.1 Tekscan Header Parameters

```
% Returns value of parameter from F-Scan ascii file header
function value = getParameter(filename, parameter)
value = [];

fid = fopen(filename);

tline = fgetl(fid);
while(isempty(value))
    value = sscanf(tline, [parameter ' ' '%g']);
    tline = fgetl(fid);
end
```

```
fclose(fid);
```

A.2.2 Muscle Names

```
% Converts channel number to muscle name based on the channel order used
% when setting up the BioRadio for data collection.
function muscle = getmusclename(channel)
switch channel
    case 1
        muscle = 'Rectus Abdominis';
    case 2
        muscle = 'Erector Spinae';
    case 3
        muscle = 'Biceps Femoris';
    case 4
        muscle = 'Rectus Femoris';
    case 5
        muscle = 'Gastrocnemius';
    case 6
        muscle = 'Tibialis Anterior';
    case 7
        muscle = 'Noise';
end
```

A.2.3 Data Interpolation

```
% Performs cubic spline interpolation to fill in dropped data points.
% Can optionally return an array of those points so that
% artificial points can be identified when graphed.
function [filleddata,interpdata] = filldata(rawdata,droppedvalue,method)
```

```
if nargin < 3
    method = 'cubic';
end

[nrows, ncols] = size(rawdata);
tempdata = rawdata;

for i = 1:ncols
    % set up variables for interp1 routine
    % we'll be interpolating values at the
    % indexes where the dropped data points
    % are
    y = rawdata(:,i);
    x = 1:length(y);
    x = transpose(x);
    if isnan(droppedvalue)
        xi = find(isnan(y));
    else
        xi = find(y==droppedvalue);
    end

    % now remove the indexes of dropped data
    if isnan(droppedvalue)
        x = x(~isnan(y));
        y = y(~isnan(y));
    else
        x = x(y~=droppedvalue);
        y = y(y~=droppedvalue);
    end
```

```
    % do the interpolation
    yi = interp1(x,y,xi,method);

    % now insert the interpolated values back into the data
    for index = 1:length(xi)
        tempdata(xi(index),i) = yi(index);
    end
    interpdata(:,:,i) = [xi,yi];
end

filleddata = tempdata;
```

A.2.4 EMG Data Filling

```
% Fills in dropped EMG data points.  As the frequency content of the signal
% is of vital importance, simple interpolation will not suffice.  As such,
% an assumption is made that it is reasonable to assume that the frequency
% content of a gap in the EMG data will not significantly differ from the
% frequency content of the data immediately preceding the gap and following
% the gap.  The data is filled by splitting the gap in two and filling the
% first half with a copy of the data (of length = half the gap length)
% preceding the gap and filling the second half with a copy of the data
% following the gap.
function filled_data = fillemg(raw_data,dropped_value)

% Set the filled_data to the raw_data, we'll fill it in as we go
filled_data = raw_data;

% Find the indexes of all the dropped points within the raw data
```

```
dropped_indices = find(raw_data == dropped_value);

if isempty(dropped_indices)
    return
end

% Find the step size from one dropped index to the next.  Anything equal to
% 1 means sequential indices, anything grater means we have started a new
% gap in the data
step_size = diff(dropped_indices);

% Get the indices within the dropped_indices where gaps in the data start
gap_start_indices = find(step_size>1);

% The first index in dropped_indices is always a gap start.  Also, adjust
% the indices to account for diff reducing the vector length by 1.
gap_start_indices = [1; gap_start_indices + 1];

% Now, go through the list of start indices of dropped data
numgaps = length(gap_start_indices);
for i=1:numgaps
    % Local variables for the loop
    i_start = dropped_indices(gap_start_indices(i));
    % Last gap is a special case
    if i == numgaps
        i_end = max(dropped_indices);
    else
        i_end = dropped_indices(gap_start_indices(i+1) -1);
    end
```

```
    i_length = i_end - i_start;

    % Fill the first half of the gap with preceding data.  Need to
    % accomodate the possibility that we are too close to the start of the
    % data to fill a full half
    filler_start = max([1 i_start-i_length]);
    filler_end = i_start -1 ;
    filler_length = filler_end - filler_start;

    filler = filled_data(filler_start:filler_end);
    filled_data(i_start:i_start+filler_length) = filler;

    % Fill the second half of the gap with the following data.  Need to
    % accomodate the possibility that we are too close to the end of the
    % data to fill a full half
    filler_start = i_end + 1;
    filler_end = min([i_end + (i_length - filler_length) length(filled_data)]);
    filler_length = filler_end - filler_start;
    filler = filled_data(filler_start:filler_end);
    filled_data(i_end-filler_length:i_end) = filler;
end
```

A.3 Pressure Data Scripts

A.3.1 CoP Import

```
% Returns the CoP data in mm
function cop = importcop(copFilename)

constants;
```

```
imported_data = importdata(copFilename);

% Sagittal and lateral center of pressure position (in grid spaces) are in
% the third and fourth columns respectively.
cop = imported_data.data(:,3:4);

% Fill any missing data points
copx = filldata(cop(:,1),FSCAN_DROPPED_DATA_VALUE);
copy = filldata(cop(:,2),FSCAN_DROPPED_DATA_VALUE);
cop = [copx copy];

gridsize = getParameter(copFilename, 'ROW_SPACING');

% if we have a grid size of less than 1, the file units are meters,
% otherwise they are mm.  we want our units for the graphs to be mm
if(gridsize < 1)
    gridsize = gridsize*1000;
end

cop = cop*gridsize;
```

A.3.2 Find BoS

```
% Calculates the convex hull estimation of the BoS and returns this as a
% bitmask (filledmask).  Also returns a raw bitmask that has not been
% converted to convex hull (insolemask).
function [filledmask, insolemask] = getfootmask(pressurefile)

constants;
```

```
% Get the start and end frames from the header
startFrame = getParameter(pressurefile,'START_FRAME');
endFrame = getParameter(pressurefile,'END_FRAME');

% Get the number of sensor grid rows and columns from the header (this is
% almost always 60x21)
nRows = getParameter(pressurefile,'ROWS');
nCols = getParameter(pressurefile,'COLS');

fid = fopen(pressurefile);

% The data is stores as nCols floating point values.
format = repmat('%f',1,nCols);

% Seek to the point where we have read the line that starts with ASCII_DATA
% to get past all the header lines
tline = fgetl(fid);
while(~strcmp(tline,'ASCII_DATA @@'))
    tline = fgetl(fid);
end

% loop from start to end frame
% for each frame set the mask for cells that take a value other than 0.0
% or NaN.
pressures = textscan(fid, format, nRows, 'Headerlines', 2, 'delimiter', ...
    ',', 'TreatAsEmpty', 'B', 'CollectOutput', 1);
pressure = pressures{1};
pressure(isnan(pressure))=0;
```

```
insolemask = pressure&1;

% Now that the position in the file is set at the end of frame one, each
% additional frame will have a blank line plus the frame number at the
% start of it
for i=startFrame+1:endFrame
    pressures = textscan(fid, format, nRows, 'HeaderLines', 3, ...
        'delimiter', ',', 'TreatAsEmpty', 'B', 'CollectOutput', 1);
    pressure = pressures{1};
    pressure(isnan(pressure))=0;
    insolemask = pressure&1 | insolemask;
end

fclose(fid);

% now remove "false" zeros in the middle of the foot
filledmask = fillfoot2(insolemask);
```

A.3.3 Convert BoS to Convex Hull

```
% This converts the insolemask BoS mask to a convex hull estimation.  The
% basic algorithm makes three passes over the raw mask.
%
% The first pass looks for zeros that are not at the edges of the mask
% (defining a zero to be at the edge of the mask if more than two other
% zeros are encountered to the left, right, top, and bottom of that cell
% in the grid).
%
% The second pass looks for false ones that have been created by the first
% pass.  False ones are defined as cells with the value of one that have
```

```
% two or less other cells that are ones in the 3x3 sub-grid surrounding the
% cell.
%
% The final pass looks one more time for false zeros.  This time, a false
% zero is defined as a cell with the value of zero that has at least one
% other cell to its left AND right with a value of one, or at least one
% other cell to its top AND bottom that have a value of one.
function filledmask = fillfoot2(insolemask)
[m,n] = size(insolemask);
for i=1:m
    for j=1:n
        % Eliminate false 0's (those within the perimiter of the foot)
        if insolemask(i,j) == 0
            leftedge = sum(insolemask(i,1:j))>0;
            rightedge = sum(insolemask(i,j:n))>0;
            topedge = sum(insolemask(1:i,j))>0;
            bottomedge = sum(insolemask(i:m,j))>0;
            if leftedge + rightedge + topedge + bottomedge > 2
                insolemask(i,j) = 1;
            end
        end
    end
end

paddedmask = zeros(m+2,n+2);
paddedmask(2:m+1,2:n+1) = insolemask;
% Eliminate false 1's (those that are isolated)
for i=2:m+1
    for j=2:n+1
```

```
        sub = paddedmask(i-1:i+1,j-1:j+1);
        if sum(sum(sub)) <= 2
            insolemask(i-1,j-1) = 0;
        end
    end
end

for i=1:m
    for j=1:n
        % Eliminate false 0's (those within the perimiter of the foot)
        if insolemask(i,j) == 0
            leftedge = sum(insolemask(i,1:j))>0;
            rightedge = sum(insolemask(i,j:n))>0;
            topedge = sum(insolemask(1:i,j))>0;
            bottomedge = sum(insolemask(i:m,j))>0;
            if (leftedge && rightedge) || (topedge && bottomedge)
                insolemask(i,j) = 1;
            end
        end
    end
end

filledmask = insolemask;
```

A.3.4 Convert CoP Coordinate System

```
% Returns CoP converted to a coordinate system with the origin at the
% bottom left of the foot.
function cop = getcop(participant,task,hemisphere)
```

```
constants;

copfile = [BASEPATH  participant '_' task '_' hemisphere(1) '.asc'];

cop = importcop(copfile);

% Need to find the boundaries of the area under the foot so that they can
% be indicated on the CoP position plot
pressureFilename = [BASEPATH participant '_' task '_' hemisphere(1) '.asf'];
footmask = getfootmask(pressureFilename);

gridsize = getParameter(copfile,'ROW_SPACING');
% if we have a grid size of less than 1, the file units are meters,
% otherwise they are mm.  we want our units for the graphs to be mm
if(gridsize < 1)
    gridsize = gridsize*1000;
end

[I,J] = ind2sub(size(footmask),find(footmask));
maxSagittal = max(I)*gridsize;
minLateral = min(J)*gridsize;

% Convert to coord system with (0,0) at bottom left of foot boundary
cop = [(maxSagittal - cop(:,1)) (cop(:,2) - minLateral)];
```

A.3.5 Calculate Index of Postural Stability

```
% Calculates the postural stability index as the standard deviation of the
% CoP for the left and right feet.
function printStabilityIndex(participant)
```

```
constants;

endframe = getParameter([BASEPATH participant '_Balance_L.asc'], 'END_FRAME');

% We want only 30 seconds of quiet standing to eliminate movement during
% synch phase.
secondsperframe = getParameter([BASEPATH participant '_Balance_L.asc'], 'SECONDS_PER_FRA
startframe = max(1, endframe - floor(30/secondsperframe));

lcop = importcop([BASEPATH participant '_Balance_L.asc']);
rcop = importcop([BASEPATH participant '_Balance_R.asc']);

lcop = lcop(startframe:endframe);
rcop = rcop(startframe:endframe);

m_lcop = vectmag(lcop);
m_rcop = vectmag(rcop);

name = participant
lstd = std(m_lcop)
rstd = std(m_rcop)
```

A.3.6 Create CoP Plots

```
% Plots the center of pressure under the participant's feett.
function printCop(participant,task,doprint,startframe,endframe)

constants;
```

```
if nargin < 3
    doprint = 0;
end

for index=1:2
    if index == 1
        copfile = [BASEPATH  participant '_' task '_L.asc'];
        hemisphere = 'Left';
    else
        copfile = [BASEPATH  participant '_' task '_R.asc'];
        hemisphere = 'Right';
    end

    if nargin < 5
        endframe = getParameter(copfile,'END_FRAME');
    end

    if nargin < 4
        startframe = getParameter(copfile,'START_FRAME');
    end

    cop = importcop(copfile);
    cop = cop(startframe:endframe,:);

    % Need to find the boundaries of the area under the foot so that they
    % can be indicated on the CoP position plot
    pressureFilename = [BASEPATH participant '_' task '_' hemisphere(1) ...
        '.asf'];
    footmask = getfootmask(pressureFilename);
```

```
gridsize = getParameter(copfile,'ROW_SPACING');
% if we have a grid size of less than 1, the file units are meters,
% otherwise they are mm.  we want our units for the graphs to be mm
if(gridsize < 1)
    gridsize = gridsize*1000;
end
[I,J] = ind2sub(size(footmask),find(footmask));
minSagittal = min(I)*gridsize;
maxSagittal = max(I)*gridsize;
minLateral = min(J)*gridsize;
maxLateral = max(J)*gridsize;

% Convert to coord system with (0,0) at bottom left of foot boundary
newcop = [(maxSagittal - cop(:,1)) (cop(:,2) - minLateral)];

% Get the time values for the x-axis
time = (0:length(newcop)-1)*getParameter(copfile,'SECONDS_PER_FRAME');

% Try plotting position as percent of maximum
subplot(2,1,1)
plot(time,newcop(:,1)/(maxSagittal-minSagittal));
axis([min(time) max(time) 0 1.0]);
xlabel('Time (s)');
ylabel('Fraction of maximum position');
title(sprintf('Sagittal CoP for %s - participant %s (%s foot)', ...
    task,getParticipantID(participant),hemisphere));
subplot(2,1,2)
plot(time,newcop(:,2)/(maxLateral-minLateral));
```

```
    axis([min(time) max(time) 0 1.0]);
    xlabel('Time (s)');
    ylabel('Fraction of maximum position');
    title(sprintf('Lateral CoP for %s - participant %s (%s foot)', ...
        task,getParticipantID(participant),hemisphere));
    if doprint
         print('-dpng', sprintf('%s_CoP_%s(%s)',task, ...
             getParticipantID(participant),hemisphere))
    end
    figure
end
```

A.4 EMG Data Scripts

A.4.1 Power Spectrum Analysis

```
% Plots a welch power spectrum of the EMG data for the participant
% performing the task.
function plotpowerspectrum(participant,task,doprint)

constants;

if nargin < 3
    doprint = 0;
end

% set up a welch power spectrum estimator
h = spectrum.welch;
h.SegmentLength = 1024;
```

```
for num=1:2
    if num==1
        % get the data from file
        rawdata = importdata([EMG_BASEPATH lower(participant) '_' ...
            lower(task) '_task_left.csv']);
        hemisphere = 'Left';
    else
        rawdata = importdata([EMG_BASEPATH lower(participant) '_' ...
            task '_task_right.csv']);
        hemisphere = 'Right';
    end

    % loop over each of the channels in the data and plot
    % the raw power spectrum as well as the filtered power
    % spectrum
    for index=1:7
        filled_data = fillemg(rawdata(:,index), ...
            CLEVEMED_DROPPED_DATA_VALUE);
        unfiltered_hpsd = psd(h,filled_data-mean(filled_data),'FS', ...
            EMG_SAMPLE_RATE);

        if(~doprint)
            figure
        end
        plot(unfiltered_hpsd)
        title(sprintf(['Welch Power Spectral Density Estimate: %s' ...
            'Raw Data for participant %s (%s %s)'],task, ...
            getParticipantID(participant),hemisphere, ...
            getmusclename(index)));
```

```
        if doprint
            print('-dpng', sprintf('%s_Raw_Power_Density_%s(%s_%s)', ...
                task,getParticipantID(participant),hemisphere, ...
                getmusclename(index)))
        end
    end
end
```

A.4.2 Estimate Muscle Force

```
% Calculates the linear envelope force estimation for the emgdata
% Returns force estimate normalized to the maximum value in the filtered
% signal.
function estforce = estforce(emgdata)

constants;

% Use 6th order Butterworth
ORDER = 6;

% Calculate the Nyquist frequency
NYQUIST = EMG_SAMPLE_RATE/2;

% Use the standard lowpass cutoff of 500Hz or at the 0.99*Nyquist frequency,
% whichever is smaller as the butter routine can only take a maximum input
% of 1.0 = Freq/Nyquist and blows up at 1.0
RAW_LOWPASS = min([500 0.99*NYQUIST]);

% Use the standard highpass cutoff of 20Hz
HIGHPASS = 20;
```

```
% Low Pass Filter Raw sEMG signal
[b,a] = butter(ORDER,RAW_LOWPASS/NYQUIST,'low');
filtered_emg = filtfilt(b,a,emgdata);

% Now High Pass Filter
[b,a] = butter(ORDER,HIGHPASS/NYQUIST,'high');
filtered_emg = filtfilt(b,a,filtered_emg);

% Full wave rectify the signal
fwr = abs(filtered_emg);

% Now Low Pass Filter using 1st order Butterworth with
% cutoff at 1.0Hz: effectively determining linear envelope
[b,a] = butter(1,1/NYQUIST,'low');
lenvelope = filtfilt(b,a,fwr);

% Now linearly normalize the filtered fwr as a percentage
% of the maximum sEMG afer the previous step
lnorm_fwr = lenvelope/max(lenvelope);

estforce = lnorm_fwr;
```

A.4.3 Plot Normalize Muscle Forces

```
% Plots the normalized muscle force activity for the given participant
% performing the given task.
function [left_mean_force right_mean_force] = plotemg(participant, ...
    task,doprint)
```

```
constants;

if nargin < 3
    doprint = 0;
end

for num=1:2
    % get the data
    if num==1
        rawdata = importdata([EMG_BASEPATH lower(participant) '_' ...
            lower(task) '_task_left.csv']);
        hemisphere = 'Left';
    else
        rawdata = importdata([EMG_BASEPATH lower(participant) '_' ...
            lower(task) '_task_right.csv']);
        hemisphere = 'Right';
    end

    % we need to find the synch frame and then eliminate all data before it
    % and up to 5 seconds after it in order to eliminate muscle activity
    % associated with the synchronization step as well as to synchronize
    % the data to other sources
    if(length(rawdata(1,:)) == 8)
        synch_frame = find(rawdata(:,8) > 100000, 1, 'last');
        rawdata = rawdata(synch_frame:length(rawdata),:);
    end

    % set up the times for the x-axis
    time = ((1:length(rawdata))-1)/EMG_SAMPLE_RATE;
```

```
force_data = zeros(length(rawdata),6);

% loop over each of the channels in the data and plot
% the filled and filtered signal as well as the interpolated
% data points
for index=1:6
    filled_data = fillemg(rawdata(:,index), ...
        CLEVEMED_DROPPED_DATA_VALUE);
    force_data(:,index) = estforce(filled_data);
    plot(time,force_data(:,index))
    title(sprintf(['Estimated Force for %s Task or participant %s' ...
        '(%s %s)'],task,getParticipantID(participant),hemisphere, ...
        getmusclename(index)));
    xlabel('Time (s)')
    ylabel('Normalized muscle force')
    if doprint
        print('-dpng', sprintf('%s_Force_%s(%s_%s)',task, ...
            getParticipantID(participant),hemisphere, ...
            getmusclename(index)))
    end

end

% Remove the first and last two seconds of estimated force data due to
% the presence of transients in the filter response
force_data = force_data(2*EMG_SAMPLE_RATE:length(force_data)- ...
    2*EMG_SAMPLE_RATE,:);
mean_force = mean(force_data);
```

```
    min_force = min(force_data);
    std_force = std(force_data);

    bar(mean_force);
    set(gca,'XTick',1:numel({'RA', 'ES', 'BF', 'RF', 'G', 'TA'}));
    set(gca,'XTickLabel', {'RA', 'ES', 'BF', 'RF', 'G', 'TA'});
    title(sprintf(['Estimated Muscle Force: %s Task for participant' ...
        '%s (%s)'],task,getParticipantID(participant),hemisphere));
    ylabel('Normalized muscle force');
    xlabel('Muscle');
    hold on
    bar(min_force,'y');
    legend('Mean', 'Min');
    errorbar(1:6, mean_force, std_force, 'k.');
    axis([0 7 0 1.0]);
    hold off
    if doprint
        print('-dpng', sprintf('%s_Force_%s(%s)',task, ...
            getParticipantID(participant),hemisphere))
    end

    if num==1
        left_mean_force = mean_force;
    else
        right_mean_force = mean_force;
    end
end
```

A.4.4 Plot Aggregate Muscle Force Data

```
% Plots the aggregate force data across all participants for the given task
function plotAggregateForces(leftforces,rightforces,task,doprint)

if nargin < 4
    doprint = 0;
end

mean_force = mean(leftforces);
std_force = std(leftforces);

figure
subplot(2,1,1);
hold on
bar(mean_force);
set(gca,'XTick',1:numel({'RA', 'ES', 'BF', 'RF', 'G', 'TA'}));
set(gca,'XTickLabel', {'RA', 'ES', 'BF', 'RF', 'G', 'TA'});
title(sprintf(['Mean Estimated Muscle Force: %s Task for all' ...
    'participants (Left)'],task));
ylabel('Normalized muscle force');
xlabel('Muscle');
errorbar(1:6, mean_force, std_force, 'k.');
axis([0 7 0 1.0]);
hold off

mean_force = mean(rightforces);
std_force = std(rightforces);
```

```
subplot(2,1,2);
hold on
bar(mean_force);
set(gca,'XTick',1:numel({'RA', 'ES', 'BF', 'RF', 'G', 'TA'}));
set(gca,'XTickLabel', {'RA', 'ES', 'BF', 'RF', 'G', 'TA'});
title(sprintf(['Mean Estimated Muscle Force: %s Task for all' ...
    'participants (Right)'],task));
ylabel('Normalized muscle force');
xlabel('Muscle');
errorbar(1:6, mean_force, std_force, 'k.');
axis([0 7 0 1.0]);
hold off

if doprint
    print('-dpng', sprintf('%s_Force_All',task))
end
```

A.5 Motion Capture Data Scripts

A.5.1 Calculate CoM

```
% Determines whether to use Vicon or Arena import routines
function com = getcom(participant,task)

constants;

c3dfilename = [VICON_BASE_PATH participant ' ' task '.c3d'];

if (strcmp(task,'Lift') || strcmp(task,'Step'))
    com = getcom_Vicon(c3dfilename,participant,task);
```

```
    % Swap x and y, and reverse the sign on x to bring Vicon coordinate
    % system to be the same as the Arena coordinate system
    com = [-com(:,2) com(:,1) com(:,3)];
else
    com = getcom_Arena(c3dfilename);
end

% Calculates CoM from Vicon system.
function com = getcom_Vicon(c3dfilename,participant,task)

constants;

% Typo in one of the participants names
if(strcmp(participant,'Gil'))
    participant = 'Gill';
end

INTERP_METHOD = 'cubic';

itf = c3dserver;
openc3d(itf,0,c3dfilename);

% c3dserver functions will return positions for all frames of data, so
% don't need to loop (at least, not yet).
%
% Need to get positions of all markers identified as head or tail markers
% for the body segments of interest
rwrist = get3dtarget(itf,[participant ':' 'RWrist']);
rhanda = get3dtarget(itf,[participant ':' 'RHand_A']);
```

```
lwrist = get3dtarget(itf,[participant ':' 'LWrist']);
lhanda = get3dtarget(itf,[participant ':' 'LHand_A']);
relbow = get3dtarget(itf,[participant ':' 'RElbow']);
lelbow = get3dtarget(itf,[participant ':' 'LElbow']);
rshoulder = get3dtarget(itf,[participant ':' 'RShoulder']);
lshoulder = get3dtarget(itf,[participant ':' 'LShoulder']);
rheel = get3dtarget(itf,[participant ':' 'RHeel']);
rtoe = get3dtarget(itf,[participant ':' 'RToe']);
lheel = get3dtarget(itf,[participant ':' 'LHeel']);
ltoe = get3dtarget(itf,[participant ':' 'LToe']);
rknee = get3dtarget(itf,[participant ':' 'RKnee']);
rankle = get3dtarget(itf,[participant ':' 'RAnkle']);
lknee = get3dtarget(itf,[participant ':' 'LKnee']);
lankle= get3dtarget(itf,[participant ':' 'LAnkle']);
rhip = get3dtarget(itf,[participant ':' 'RFrontWaist']);
lhip = get3dtarget(itf,[participant ':' 'LFrontWaist']);
root = get3dtarget(itf,[participant ':' 'Root']);
topspine = get3dtarget(itf,[participant ':' 'TopSpine']);

closec3d(itf);

% Now, since the motion capture system may have dropped markers in some
% frames, we need to interpolate the data to avoid NaNs in further
% calculations
rwrist = filldata(rwrist,NaN,INTERP_METHOD);
rhanda = filldata(rhanda,NaN,INTERP_METHOD);
lwrist = filldata(lwrist,NaN,INTERP_METHOD);
lhanda = filldata(lhanda,NaN,INTERP_METHOD);
relbow = filldata(relbow,NaN,INTERP_METHOD);
```

```
lelbow = filldata(lelbow,NaN,INTERP_METHOD);
rshoulder = filldata(rshoulder,NaN,INTERP_METHOD);
lshoulder = filldata(lshoulder,NaN,INTERP_METHOD);
rheel = filldata(rheel,NaN,INTERP_METHOD);
rtoe = filldata(rtoe,NaN,INTERP_METHOD);
lheel = filldata(lheel,NaN,INTERP_METHOD);
ltoe = filldata(ltoe,NaN,INTERP_METHOD);
rknee = filldata(rknee,NaN,INTERP_METHOD);
rankle = filldata(rankle,NaN,INTERP_METHOD);
lknee = filldata(lknee,NaN,INTERP_METHOD);
lankle = filldata(lankle,NaN,INTERP_METHOD);
rhip = filldata(rhip,NaN,INTERP_METHOD);
lhip = filldata(lhip,NaN,INTERP_METHOD);
root = filldata(root,NaN,INTERP_METHOD);
topspine = filldata(topspine,NaN,INTERP_METHOD);

% Now calculate the CoM of each segment.  Vector equation is:
% head + (tail - head) * com_distance_from_proximal_head
rhand_com = rwrist + (rhanda - rwrist) * BODY_SEGMENT_ANTH_DATA(1,2);
lhand_com = lwrist + (lhanda - lwrist) * BODY_SEGMENT_ANTH_DATA(1,2);
rforearm_com = relbow + (rwrist - relbow) * BODY_SEGMENT_ANTH_DATA(2,2);
lforearm_com = lelbow + (lwrist - lelbow) * BODY_SEGMENT_ANTH_DATA(2,2);
rupperarm_com = rshoulder + (relbow - rshoulder) * ...
    BODY_SEGMENT_ANTH_DATA(3,2);
lupperarm_com = lshoulder + (lelbow - lshoulder) * ...
    BODY_SEGMENT_ANTH_DATA(3,2);
rfoot_com = rheel + (rtoe - rheel) * BODY_SEGMENT_ANTH_DATA(4,2);
lfoot_com = lheel + (ltoe - lheel) * BODY_SEGMENT_ANTH_DATA(4,2);
rlowerleg_com = rknee + (rankle - rknee) * BODY_SEGMENT_ANTH_DATA(5,2);
```

```
llowerleg_com = lknee + (lankle - lknee) * BODY_SEGMENT_ANTH_DATA(5,2);
rthigh_com = rhip + (rknee - rhip) * BODY_SEGMENT_ANTH_DATA(6,2);
lthigh_com = lhip + (lknee - lhip) * BODY_SEGMENT_ANTH_DATA(6,2);
torso_com = topspine + (root - topspine) * BODY_SEGMENT_ANTH_DATA(7,2);

% Now do a weighted summation of the segment coms using the
% weight_fractions
com = (rhand_com + lhand_com) * BODY_SEGMENT_ANTH_DATA(1,1);
com = com + (rforearm_com + lforearm_com) * BODY_SEGMENT_ANTH_DATA(2,1);
com = com + (rupperarm_com + lupperarm_com) * BODY_SEGMENT_ANTH_DATA(3,1);
com = com + (rfoot_com + lfoot_com) * BODY_SEGMENT_ANTH_DATA(4,1);
com = com + (rlowerleg_com + llowerleg_com) * BODY_SEGMENT_ANTH_DATA(5,1);
com = com + (rthigh_com + lthigh_com) * BODY_SEGMENT_ANTH_DATA(6,1);
com = com + torso_com * BODY_SEGMENT_ANTH_DATA(7,1);
com = com / sum(BODY_SEGMENT_ANTH_DATA(:,1));

% Get the transformation matrix so we can report CoM in body coordinates.
% For the lift task participants were oriented at -45degrees to the camera
% coordinate system and for the step task they were oriented at 135degrees.
if(strcmp(task,'Lift'))
    T = [cosd(-45) -sind(-45) 0;
         sind(-45) cosd(-45) 0;
         0 0 1];
else
    T = [cosd(135) -sind(135) 0;
         sind(135) cosd(135) 0;
         0 0 1];
end
```

```
% Convert com to body coordinates
com = com * T;

% Remove the mean value, which is basically the same as subtracting the
% translation off the coordiante system.  Consider only from 10s to 85s
% so that the values when the participant is moving to the task
% site and back are not skewing the mean.
com = [com(:,1)-mean(com(20*120:(length(com)-20*120),1)) ...
    com(:,2)-mean(com(20*120:(length(com)-20*120),2)) ...
    com(:,3)-mean(com(20*120:(length(com)-20*120),3))];

% Calculates CoM for the OptiTrack system.
function com = getcom_Arena(c3dfilename)

constants;

INTERP_METHOD = 'cubic';

itf = c3dserver;
openc3d(itf,0,c3dfilename);

% c3dserver functions will return positions for all frames of data, so
% don't need to loop (at least, not yet).
%
% Need to get positions of all markers identified as head or tail markers
% for the body segments of interest
rwrist = (get3dtarget(itf,'RHand2') + get3dtarget(itf,'RHand3'))/2;
rhanda = get3dtarget(itf,'RHand1');
lwrist = (get3dtarget(itf,'LHand2') + get3dtarget(itf,'RHand3'))/2;
```

```
lhanda = get3dtarget(itf,'LHand1');
relbow = get3dtarget(itf,'RUArm1');
lelbow = get3dtarget(itf,'LUArm1');
rshoulder = get3dtarget(itf,'RUArm3');
lshoulder = get3dtarget(itf,'LUArm3');
rheel = get3dtarget(itf,'RShin2');
rtoe = get3dtarget(itf,'RFoot1');
lheel = get3dtarget(itf,'LShin2');
ltoe = get3dtarget(itf,'LFoot1');
rknee = get3dtarget(itf,'RThigh2');
rankle = get3dtarget(itf,'RShin2');
lknee = get3dtarget(itf,'LThigh2');
lankle= get3dtarget(itf,'RShin2');
rhip = get3dtarget(itf,'Hip1');
lhip = get3dtarget(itf,'Hip2');
root = get3dtarget(itf,'Hip4');
topspine = get3dtarget(itf,'Chest1');

closec3d(itf);

% Now, since the motion capture system may have dropped markers in some
% frames, we need to interpolate the data to avoid NaNs in further
% calculations
rwrist = filldata(rwrist,NaN,INTERP_METHOD);
rhanda = filldata(rhanda,NaN,INTERP_METHOD);
lwrist = filldata(lwrist,NaN,INTERP_METHOD);
lhanda = filldata(lhanda,NaN,INTERP_METHOD);
relbow = filldata(relbow,NaN,INTERP_METHOD);
lelbow = filldata(lelbow,NaN,INTERP_METHOD);
```

```
rshoulder = filldata(rshoulder,NaN,INTERP_METHOD);
lshoulder = filldata(lshoulder,NaN,INTERP_METHOD);
rheel = filldata(rheel,NaN,INTERP_METHOD);
rtoe = filldata(rtoe,NaN,INTERP_METHOD);
lheel = filldata(lheel,NaN,INTERP_METHOD);
ltoe = filldata(ltoe,NaN,INTERP_METHOD);
rknee = filldata(rknee,NaN,INTERP_METHOD);
rankle = filldata(rankle,NaN,INTERP_METHOD);
lknee = filldata(lknee,NaN,INTERP_METHOD);
lankle = filldata(lankle,NaN,INTERP_METHOD);
rhip = filldata(rhip,NaN,INTERP_METHOD);
lhip = filldata(lhip,NaN,INTERP_METHOD);
root = filldata(root,NaN,INTERP_METHOD);
topspine = filldata(topspine,NaN,INTERP_METHOD);

% Now calculate the CoM of each segment.  Vector equation is:
% head + (tail - head) * com_distance_from_proximal_head
rhand_com = rwrist + (rhanda - rwrist) * BODY_SEGMENT_ANTH_DATA(1,2);
lhand_com = lwrist + (lhanda - lwrist) * BODY_SEGMENT_ANTH_DATA(1,2);
rforearm_com = relbow + (rwrist - relbow) * BODY_SEGMENT_ANTH_DATA(2,2);
lforearm_com = lelbow + (lwrist - lelbow) * BODY_SEGMENT_ANTH_DATA(2,2);
rupperarm_com = rshoulder + (relbow - rshoulder) * ...
    BODY_SEGMENT_ANTH_DATA(3,2);
lupperarm_com = lshoulder + (lelbow - lshoulder) * ...
    BODY_SEGMENT_ANTH_DATA(3,2);
rfoot_com = rheel + (rtoe - rheel) * BODY_SEGMENT_ANTH_DATA(4,2);
lfoot_com = lheel + (ltoe - lheel) * BODY_SEGMENT_ANTH_DATA(4,2);
rlowerleg_com = rknee + (rankle - rknee) * BODY_SEGMENT_ANTH_DATA(5,2);
llowerleg_com = lknee + (lankle - lknee) * BODY_SEGMENT_ANTH_DATA(5,2);
```

```
rthigh_com = rhip + (rknee - rhip) * BODY_SEGMENT_ANTH_DATA(6,2);
lthigh_com = lhip + (lknee - lhip) * BODY_SEGMENT_ANTH_DATA(6,2);
torso_com = topspine + (root - topspine) * BODY_SEGMENT_ANTH_DATA(7,2);

% Now do a weighted summation of the segment coms using the
% weight_fractions
com = (rhand_com + lhand_com) * BODY_SEGMENT_ANTH_DATA(1,1);
com = com + (rforearm_com + lforearm_com) * BODY_SEGMENT_ANTH_DATA(2,1);
com = com + (rupperarm_com + lupperarm_com) * BODY_SEGMENT_ANTH_DATA(3,1);
com = com + (rfoot_com + lfoot_com) * BODY_SEGMENT_ANTH_DATA(4,1);
com = com + (rlowerleg_com + llowerleg_com) * BODY_SEGMENT_ANTH_DATA(5,1);
com = com + (rthigh_com + lthigh_com) * BODY_SEGMENT_ANTH_DATA(6,1);
com = com + torso_com * BODY_SEGMENT_ANTH_DATA(7,1);
com = com / sum(BODY_SEGMENT_ANTH_DATA(:,1));
```

A.5.2 Plot CoM vs CoP

```
% Plots CoM vs CoP in both the lateral and sagittal directions for the
% given participant performing the given task.  comstartframe and
% copstartframe should be set to the synchronization frame numbers of the
% motion capture and pressure data respectively.
function plotcom(participant,task,doprint,comstartframe,copstartframe)

constants;

if(strcmp(task,'Lift') || strcmp(task,'Step'))
    sample_rate = 120;
else
    sample_rate = 100;
end
```

```
if nargin < 3
    doprint = 0;
end

if nargin < 4
    comstartframe = 1;
end

if nargin < 5
    copstartframe = 1;
end

com = getcom(participant,task);
com = com(comstartframe:length(com),:);
comtime = (0:length(com)-1) / sample_rate;
comtime = comtime';

leftcop = getcop(participant,task,'Left');
leftcop = leftcop(copstartframe:length(leftcop),:);
leftcoptime = (0:length(leftcop)-1) * getParameter([BASEPATH participant...
    '_' task '_L.asc'],'SECONDS_PER_FRAME');
leftcoptime = leftcoptime';
rightcop = getcop(participant,task,'Right');
rightcop = rightcop(copstartframe:length(rightcop),:);
rightcoptime = (0:length(rightcop)-1) * getParameter([BASEPATH ...
    participant '_' task '_R.asc'],'SECONDS_PER_FRAME');

figure
```

```
subplot(2,1,1)
plot(comtime, com(:,1), ':', leftcoptime, leftcop(:,2), '--', ...
    rightcoptime, rightcop(:,2), '-');
xlabel('Time (s)');
ylabel('Position (mm)');
legend('CoM','Left CoP','Right CoP','Location','Best','Orientation',...
    'horizontal');
title(sprintf('Lateral CoM and CoP Motion: %s Task for participant %s',...
    task,getParticipantID(participant)));

subplot(2,1,2)
plot(comtime, com(:,2), ':', leftcoptime, leftcop(:,1), '--', ...
    rightcoptime, rightcop(:,1), '-');
xlabel('Time (s)');
ylabel('Position (mm)');
legend('CoM','Left CoP','Right CoP','Location','Best','Orientation',...
    'horizontal');
title(sprintf('Sagittal CoM and CoP Motion: %s Task for participant %s',...
    task,getParticipantID(participant)));
if doprint
    print('-dpng', sprintf('CoMvCoP_%s_%s',task,...
        getParticipantID(participant)))
end
```

A.5.3 Cross-correlation Analysis

```
function printcorr(participant, task, comstartframe, copstartframe)

constants;
```

```
global rowid;

% Need to know the sample rates in Hz.
if(strcmp(task,'Lift') || strcmp(task,'Step'))
    comrate = 120;
else
    comrate = 100;
end
emgrate = EMG_SAMPLE_RATE;
coprate = floor(1 / getParameter([BASEPATH participant '_' task '_L.asc'], ...
    'SECONDS_PER_FRAME'));

leftcop = getcop(participant, task, 'Left');
rightcop = getcop(participant, task, 'Right');
if(strcmp(participant,'Bonnie') && strcmp(task,'Step'))
    leftemg = zeros(length(leftcop)/coprate*emgrate,6);
    rightemg = zeros(length(rightcop)/coprate*emgrate,6);
else
    leftemg = getemg(participant, task, 'Left');
    rightemg = getemg(participant, task, 'Right');
end
if(strcmp(participant,'Gil') && comrate == 120)
    com = zeros(length(leftcop)/coprate*comrate,3);
else
    com = getcom(participant, task);
end

% Synchronize the start frames.  EMG is synched by getemg.
com = double(com);
```

```
com = com(comstartframe:length(com),:);
leftcop = leftcop(copstartframe:length(leftcop),:);
rightcop = rightcop(copstartframe:length(rightcop),:);

% Need to get estimated force data
leftforces = estforce(leftemg(:,1:6));
rightforces = estforce(rightemg(:,1:6));

% Now all the data needs to cover the same period of time.  We'll have to
% use the lowest period available to make sure all data types are available
% for the full period.
period = floor(min([length(com)/comrate length(leftforces)/emgrate ...
    length(rightforces)/emgrate length(leftcop)/coprate]));
com = com(1:period*comrate,:);
leftforces = leftforces(1:period*emgrate,:);
rightforces = rightforces(1:period*emgrate,:);
leftcop = leftcop(1:period*coprate,:);
rightcop = rightcop(1:period*coprate,:);

% Now resample to the highest sample rate
highest = max([comrate coprate emgrate]);
com = resample(com, highest, comrate);
leftforces = resample(leftforces, highest, emgrate);
rightforces = resample(rightforces, highest, emgrate);
leftcop = resample(leftcop, highest, coprate);
rightcop = resample(rightcop, highest, coprate);

% Now perform the correlation analysis
rowid = 1;
```

```
% CoM sag vs lat
writexcorr(participant, task, highest, com(:,2), 'CoMsag', com(:,1), ...
    'CoMlat');
% Same side CoP sag vs lat
writexcorr(participant, task, highest, leftcop(:,1), 'LeftCoPsag', ...
    leftcop(:,2), 'LeftCoPlat');
writexcorr(participant, task, highest, rightcop(:,1), 'RightCoPsag', ...
    rightcop(:,2), 'RightCoPlat');
% Opposite foot CoP sag
writexcorr(participant, task, highest, leftcop(:,1), 'LeftCoPsag', ...
    rightcop(:,1), 'RightCoPsag');
% Opposite foot CoP lat
writexcorr(participant, task, highest, leftcop(:,2), 'LeftCoPlat', ...
    rightcop(:,2), 'RightCoPlat');
% Opposite foot CoP sag vs lat
writexcorr(participant, task, highest, leftcop(:,1), 'LeftCoPsag', ...
    rightcop(:,2), 'RightCoPlat');
writexcorr(participant, task, highest, leftcop(:,2), 'LeftCoPlat', ...
    rightcop(:,1), 'RightCoPsag');
% CoM vs CoP sag
writexcorr(participant, task, highest, com(:,2), 'CoMsag', ....
    leftcop(:,1), 'LeftCoPsag');
writexcorr(participant, task, highest, com(:,2), 'CoMsag', ...
    rightcop(:,1), 'RightCoPsag');
% CoM vs CoP lat
writexcorr(participant, task, highest, com(:,1), 'CoMlat', ...
    leftcop(:,2), 'LeftCoPlat');
writexcorr(participant, task, highest, com(:,1), 'CoMlat', ...
    rightcop(:,2), 'RightCoPlat');
```

```
% CoM sag vs muscles
writexcorr(participant, task, highest, com(:,2), 'CoMsag', ...
    leftforces(:,1), 'LeftRA');
writexcorr(participant, task, highest, com(:,2), 'CoMsag', ...
    leftforces(:,2), 'LeftES');
writexcorr(participant, task, highest, com(:,2), 'CoMsag', ...
    leftforces(:,3), 'LeftBF');
writexcorr(participant, task, highest, com(:,2), 'CoMsag', ...
    leftforces(:,4), 'LeftRF');
writexcorr(participant, task, highest, com(:,2), 'CoMsag', ...
    leftforces(:,5), 'LeftG');
writexcorr(participant, task, highest, com(:,2), 'CoMsag', ...
    leftforces(:,6), 'LeftTA');
writexcorr(participant, task, highest, com(:,2), 'CoMsag', ...
    rightforces(:,1), 'RightRA');
writexcorr(participant, task, highest, com(:,2), 'CoMsag', ...
    rightforces(:,2), 'RightES');
writexcorr(participant, task, highest, com(:,2), 'CoMsag', ...
    rightforces(:,3), 'RightBF');
writexcorr(participant, task, highest, com(:,2), 'CoMsag', ...
    rightforces(:,4), 'RighRF');
writexcorr(participant, task, highest, com(:,2), 'CoMsag', ...
    rightforces(:,5), 'RightG');
writexcorr(participant, task, highest, com(:,2), 'CoMsag', ...
    rightforces(:,6), 'RightTA');
% CoM lat vs muscles
writexcorr(participant, task, highest, com(:,1), 'CoMlat', ...
    leftforces(:,1), 'LeftRA');
writexcorr(participant, task, highest, com(:,1), 'CoMlat', ...
```

```
    leftforces(:,2), 'LeftES');
writexcorr(participant, task, highest, com(:,1), 'CoMlat', ...
    leftforces(:,3), 'LeftBF');
writexcorr(participant, task, highest, com(:,1), 'CoMlat', ...
    leftforces(:,4), 'LeftRF');
writexcorr(participant, task, highest, com(:,1), 'CoMlat', ...
    leftforces(:,5), 'LeftG');
writexcorr(participant, task, highest, com(:,1), 'CoMlat', ...
    leftforces(:,6), 'LeftTA');
writexcorr(participant, task, highest, com(:,1), 'CoMlat', ...
    rightforces(:,1), 'RightRA');
writexcorr(participant, task, highest, com(:,1), 'CoMlat', ...
    rightforces(:,2), 'RightES');
writexcorr(participant, task, highest, com(:,1), 'CoMlat', ...
    rightforces(:,3), 'RightBF');
writexcorr(participant, task, highest, com(:,1), 'CoMlat', ...
    rightforces(:,4), 'RighRF');
writexcorr(participant, task, highest, com(:,1), 'CoMlat', ...
    rightforces(:,5), 'RightG');
writexcorr(participant, task, highest, com(:,1), 'CoMlat', ...
    rightforces(:,6), 'RightTA');
% Left CoP sag vs muscles
writexcorr(participant, task, highest, leftcop(:,1), 'LeftCoPsag', ...
    leftforces(:,1), 'LeftRA');
writexcorr(participant, task, highest, leftcop(:,1), 'LeftCoPsag', ...
    leftforces(:,2), 'LeftES');
writexcorr(participant, task, highest, leftcop(:,1), 'LeftCoPsag', ...
    leftforces(:,3), 'LeftBF');
writexcorr(participant, task, highest, leftcop(:,1), 'LeftCoPsag', ...
```

```
    leftforces(:,4), 'LeftRF');
writexcorr(participant, task, highest, leftcop(:,1), 'LeftCoPsag', ...
    leftforces(:,5), 'LeftG');
writexcorr(participant, task, highest, leftcop(:,1), 'LeftCoPsag', ...
    leftforces(:,6), 'LeftTA');
% Left CoP lat vs muscles
writexcorr(participant, task, highest, leftcop(:,2), 'LeftCoPlat', ...
    leftforces(:,1), 'LeftRA');
writexcorr(participant, task, highest, leftcop(:,2), 'LeftCoPlat', ...
    leftforces(:,2), 'LeftES');
writexcorr(participant, task, highest, leftcop(:,2), 'LeftCoPlat', ...
    leftforces(:,3), 'LeftBF');
writexcorr(participant, task, highest, leftcop(:,2), 'LeftCoPlat', ...
    leftforces(:,4), 'LeftRF');
writexcorr(participant, task, highest, leftcop(:,2), 'LeftCoPlat', ...
    leftforces(:,5), 'LeftG');
writexcorr(participant, task, highest, leftcop(:,2), 'LeftCoPlat', ...
    leftforces(:,6), 'LeftTA');
% Right CoP sag vs muscles
writexcorr(participant, task, highest, rightcop(:,1), 'RightCoPsag', ...
    rightforces(:,1), 'RightRA');
writexcorr(participant, task, highest, rightcop(:,1), 'RightCoPsag', ...
    rightforces(:,2), 'RightES');
writexcorr(participant, task, highest, rightcop(:,1), 'RightCoPsag', ...
    rightforces(:,3), 'RightBF');
writexcorr(participant, task, highest, rightcop(:,1), 'RightCoPsag', ...
    rightforces(:,4), 'RighRF');
writexcorr(participant, task, highest, rightcop(:,1), 'RightCoPsag', ...
    rightforces(:,5), 'RightG');
```

```
writexcorr(participant, task, highest, rightcop(:,1), 'RightCoPsag', ...
    rightforces(:,6), 'RightTA');
% Right CoP lat vs muscles
writexcorr(participant, task, highest, rightcop(:,2), 'RightCoPlat', ...
    rightforces(:,1), 'RightRA');
writexcorr(participant, task, highest, rightcop(:,2), 'RightCoPlat', ...
    rightforces(:,2), 'RightES');
writexcorr(participant, task, highest, rightcop(:,2), 'RightCoPlat', ...
    rightforces(:,3), 'RightBF');
writexcorr(participant, task, highest, rightcop(:,2), 'RightCoPlat', ...
    rightforces(:,4), 'RighRF');
writexcorr(participant, task, highest, rightcop(:,2), 'RightCoPlat', ...
    rightforces(:,5), 'RightG');
writexcorr(participant, task, highest, rightcop(:,2), 'RightCoPlat', ...
    rightforces(:,6), 'RightTA');
% Left muscles
writexcorr(participant, task, highest, leftforces(:,1), 'LeftRA', ...
    leftforces(:,2), 'LeftES');
writexcorr(participant, task, highest, leftforces(:,1), 'LeftRA', ...
    leftforces(:,3), 'LeftBF');
writexcorr(participant, task, highest, leftforces(:,1), 'LeftRA', ...
    leftforces(:,4), 'LeftRF');
writexcorr(participant, task, highest, leftforces(:,1), 'LeftRA', ...
    leftforces(:,5), 'LeftG');
writexcorr(participant, task, highest, leftforces(:,1), 'LeftRA', ...
    leftforces(:,6), 'LeftTA');
writexcorr(participant, task, highest, leftforces(:,2), 'LeftES', ...
    leftforces(:,3), 'LeftBF');
writexcorr(participant, task, highest, leftforces(:,2), 'LeftES', ...
```

```
    leftforces(:,4), 'LeftRF');
writexcorr(participant, task, highest, leftforces(:,2), 'LeftES', ...
    leftforces(:,5), 'LeftG');
writexcorr(participant, task, highest, leftforces(:,2), 'LeftES', ...
    leftforces(:,6), 'LeftTA');
writexcorr(participant, task, highest, leftforces(:,3), 'LeftBF', ...
    leftforces(:,4), 'LeftRF');
writexcorr(participant, task, highest, leftforces(:,3), 'LeftBF', ...
    leftforces(:,5), 'LeftG');
writexcorr(participant, task, highest, leftforces(:,3), 'LeftBF', ...
    leftforces(:,6), 'LeftTA');
writexcorr(participant, task, highest, leftforces(:,4), 'LeftRF', ...
    leftforces(:,5), 'LeftG');
writexcorr(participant, task, highest, leftforces(:,4), 'LeftRF', ...
    leftforces(:,6), 'LeftTA');
writexcorr(participant, task, highest, leftforces(:,5), 'LeftG', ...
    leftforces(:,6), 'LeftTA');
% Right muscles
writexcorr(participant, task, highest, rightforces(:,1), 'RightRA', ...
    rightforces(:,2), 'RightES');
writexcorr(participant, task, highest, rightforces(:,1), 'RightRA', ...
    rightforces(:,3), 'RightBF');
writexcorr(participant, task, highest, rightforces(:,1), 'RightRA', ...
    rightforces(:,4), 'RightRF');
writexcorr(participant, task, highest, rightforces(:,1), 'RightRA', ...
    rightforces(:,5), 'RightG');
writexcorr(participant, task, highest, rightforces(:,1), 'RightRA', ...
    rightforces(:,6), 'RightTA');
writexcorr(participant, task, highest, rightforces(:,2), 'RightES', ...
```

```
    rightforces(:,3), 'RightBF');
writexcorr(participant, task, highest, rightforces(:,2), 'RightES', ...
    rightforces(:,4), 'RightRF');
writexcorr(participant, task, highest, rightforces(:,2), 'RightES', ...
    rightforces(:,5), 'RightG');
writexcorr(participant, task, highest, rightforces(:,2), 'RightES', ...
    rightforces(:,6), 'RightTA');
writexcorr(participant, task, highest, rightforces(:,3), 'RightBF', ...
    rightforces(:,4), 'RightRF');
writexcorr(participant, task, highest, rightforces(:,3), 'RightBF', ...
    rightforces(:,5), 'RightG');
writexcorr(participant, task, highest, rightforces(:,3), 'RightBF', ...
    rightforces(:,6), 'RightTA');
writexcorr(participant, task, highest, rightforces(:,4), 'RightRF', ...
    rightforces(:,5), 'RightG');
writexcorr(participant, task, highest, rightforces(:,4), 'RightRF', ...
    rightforces(:,6), 'RightTA');
writexcorr(participant, task, highest, rightforces(:,5), 'RightG', ...
    rightforces(:,6), 'RightTA');

function writexcorr(participant, task, samplerate, var1, var1title, ...
    var2, var2title)

global rowid;

rowid = rowid + 1;

if(strcmp(task,'Lift') || strcmp(task,'Step'))
    maxlag = samplerate * 10;
```

```
else
    maxlag = samplerate;
end

id = getParticipantID(participant);

[C,lags] = xcov(var1, var2, maxlag, 'coeff');
[r,i] = max(abs(C));
r = C(i);
lag = lags(i)/samplerate;
N = length(var1);
t = {sprintf('=C%d / sqrt((1-C%d^2)/(B%d-2))',rowid,rowid,rowid)};
tdist = {sprintf('=tdist(abs(E%d),B%d-2,2)',rowid,rowid)};
xlswrite([pwd '\xcorr_' task '.xls'], {'Correlation' 'N' 'r-value' ...
    'lag (s)' 't-value' 'p-value'}, ['Participant ' id], 'A1:F1');
xlswrite([pwd '\xcorr_' task '.xls'], {[var1title '_vs_' var2title]}, ...
    ['Participant ' id], sprintf('A%d',rowid));
xlswrite([pwd '\xcorr_' task '.xls'], N, ['Participant ' id], ...
    sprintf('B%d',rowid));
xlswrite([pwd '\xcorr_' task '.xls'], r, ['Participant ' id], ...
    sprintf('C%d',rowid));
xlswrite([pwd '\xcorr_' task '.xls'], lag, ['Participant ' id], ...
    sprintf('D%d',rowid));
xlswrite([pwd '\xcorr_' task '.xls'], t, ['Participant ' id], ...
    sprintf('E%d',rowid));
xlswrite([pwd '\xcorr_' task '.xls'], tdist, ['Participant ' id], ...
    sprintf('F%d',rowid));
```

Appendix B

Raw Results of the Stair Climbing Task

B.1 Relative Motion of CoM and CoP

Figures B.1 through B.6, which are included for the sake of completeness, show the CoM and CoP motion for all participants for the stair climbing task.

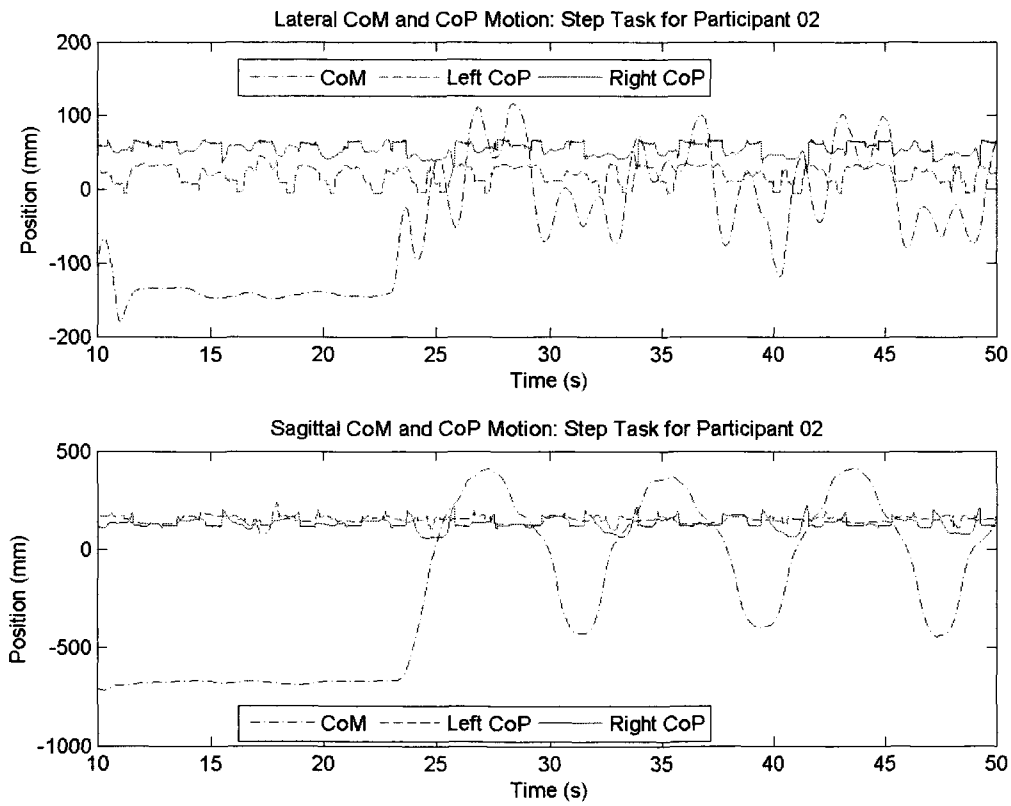

Figure B.1: Motion of CoM vs CoP for stair climbing task - Participant 02.

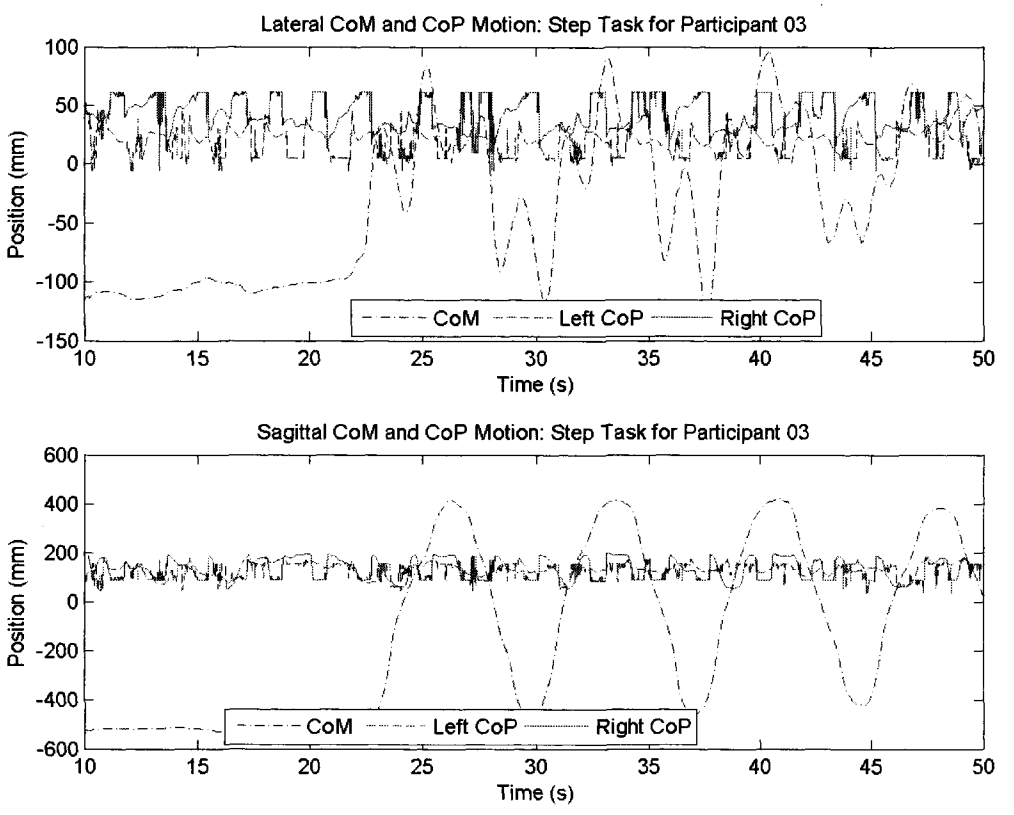

Figure B.2: Motion of CoM vs CoP for stair climbing task - Participant 03.

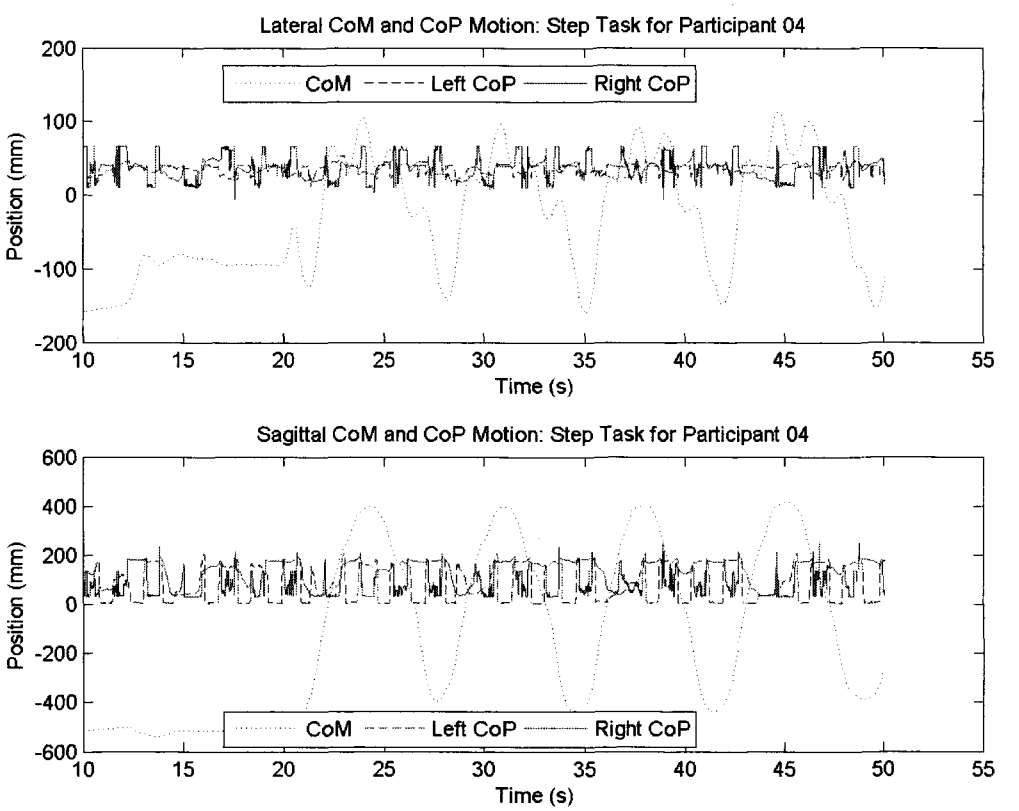

Figure B.3: Motion of CoM vs CoP for stair climbing task - Participant 04.

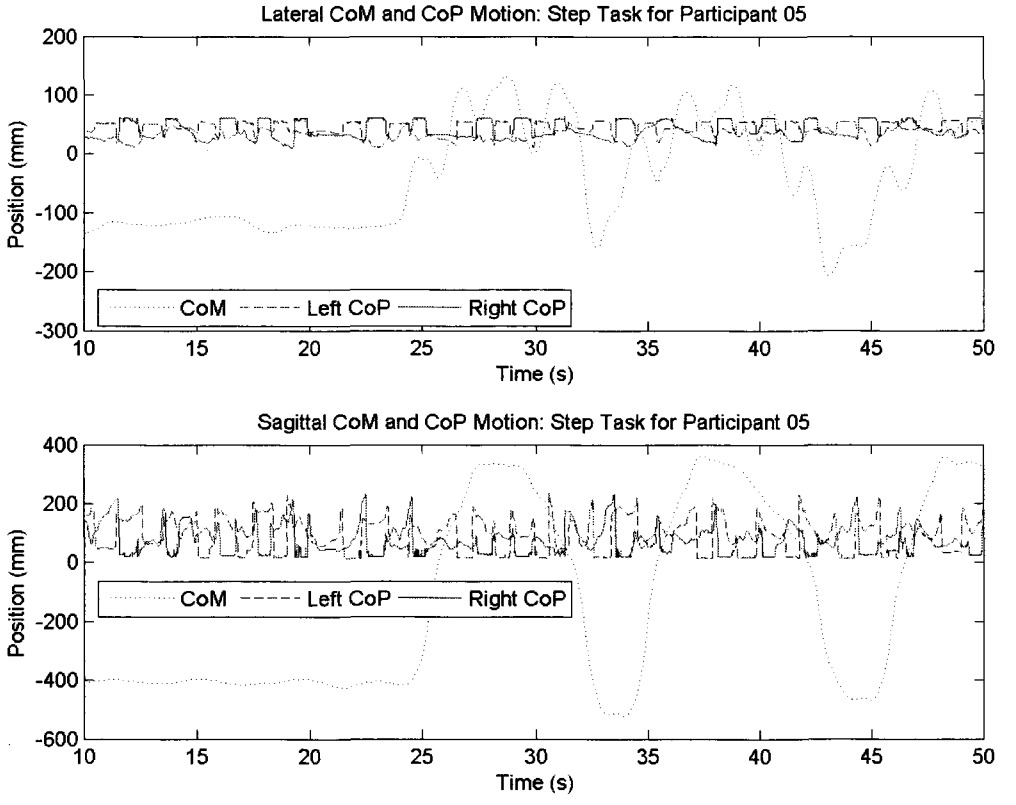

Figure B.4: Motion of CoM vs CoP for stair climbing task - Participant 05.

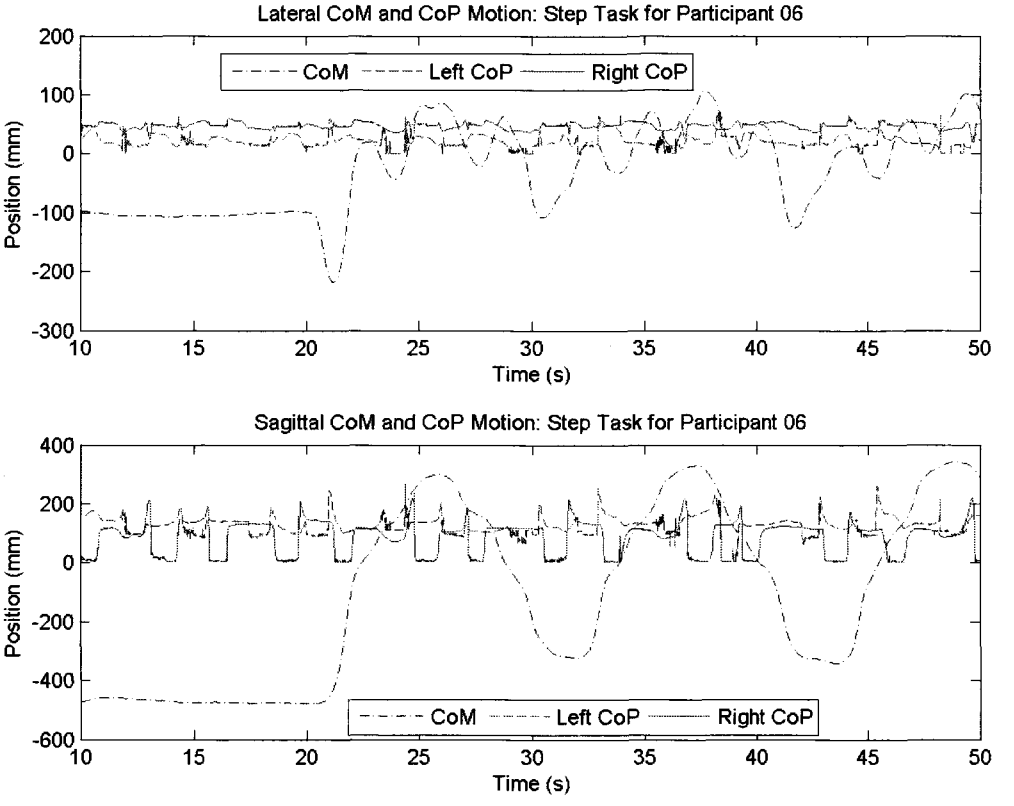

Figure B.5: Motion of CoM vs CoP for stair climbing task - Participant 06.

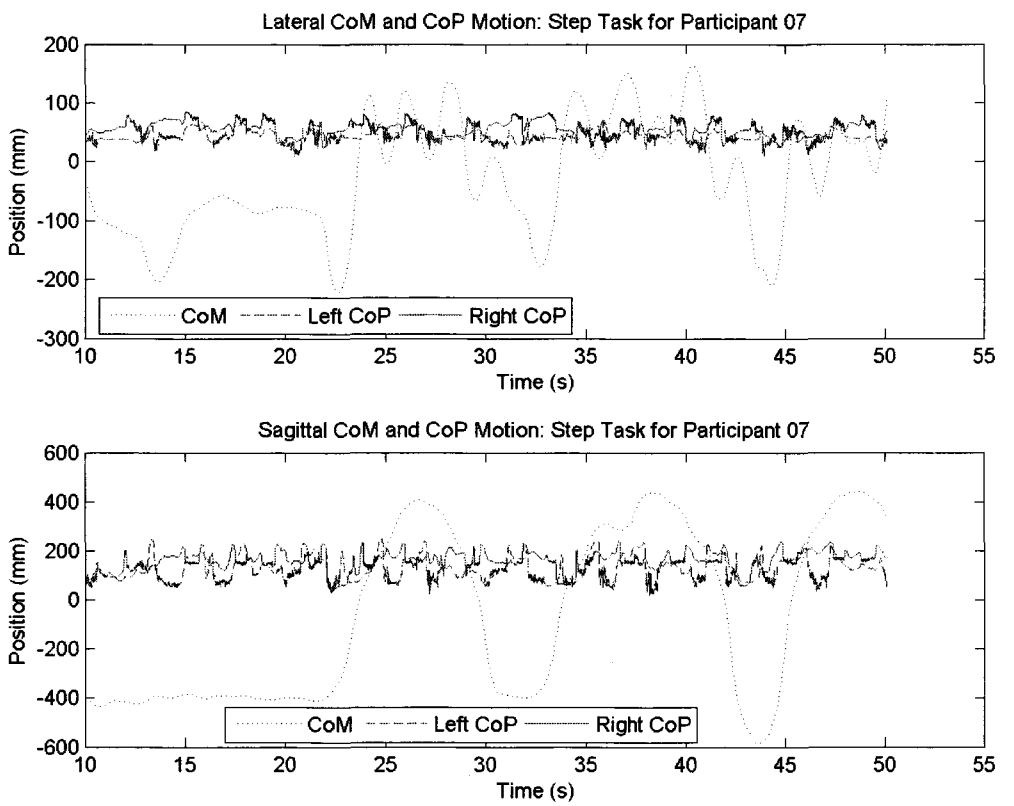

Figure B.6: Motion of CoM vs CoP for stair climbing task - Participant 07.

B.2 Kinematic Threshold of MII

Figures B.7 to B.12, which are included for completeness, show the sagittal and lateral components of CoP for both feet of all participants for the stair climbing task.

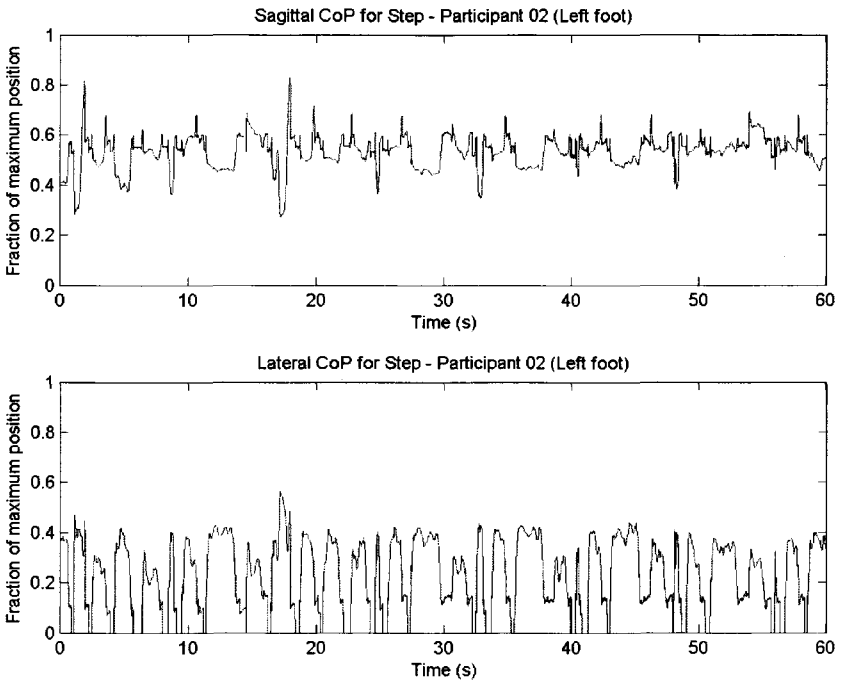

(a) Left Foot

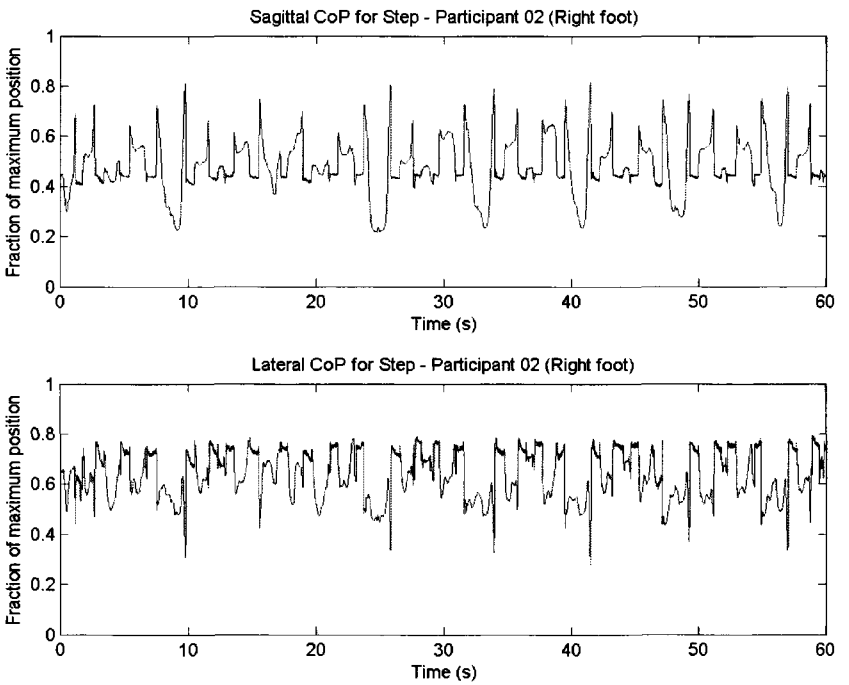

(b) Right Foot

Figure B.7: CoP for step task - Participant 02.

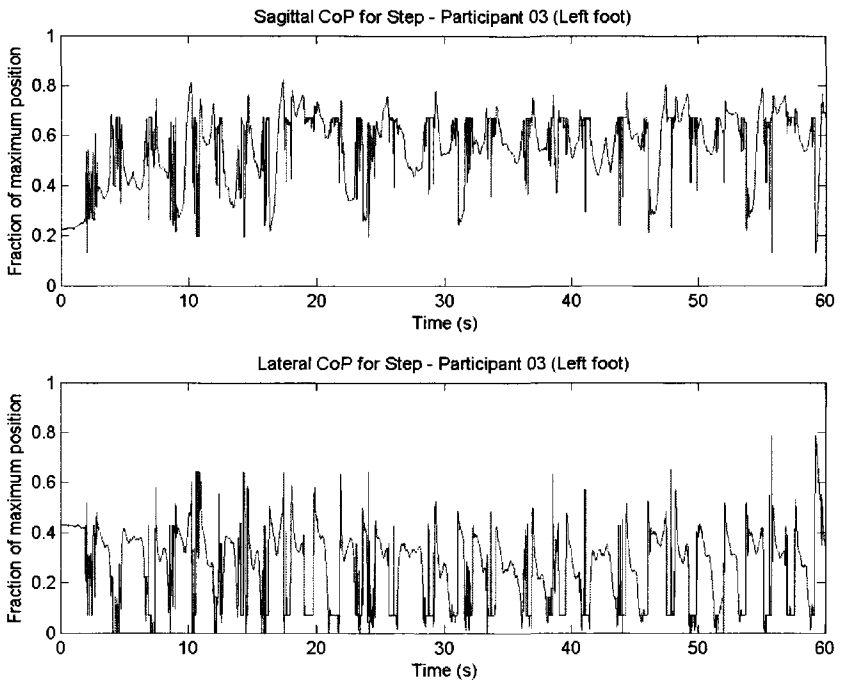

(a) Left Foot

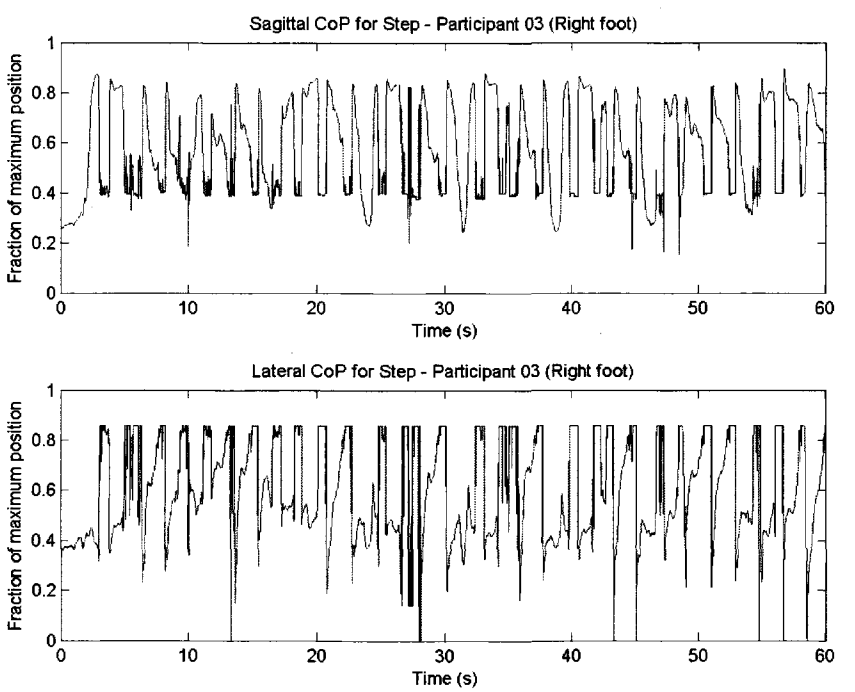

(b) Right Foot

Figure B.8: CoP for step task - Participant 03.

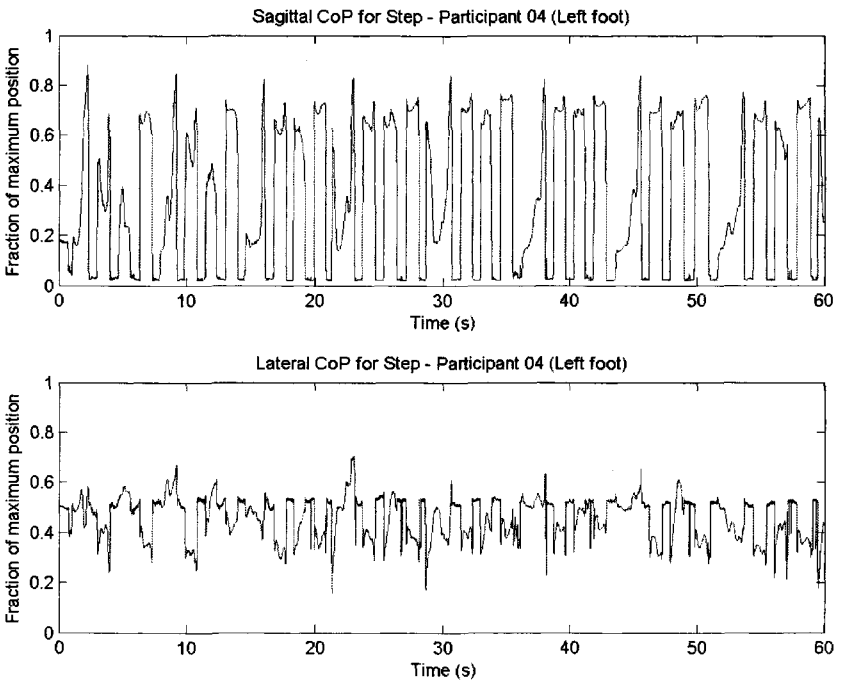

(a) Left Foot

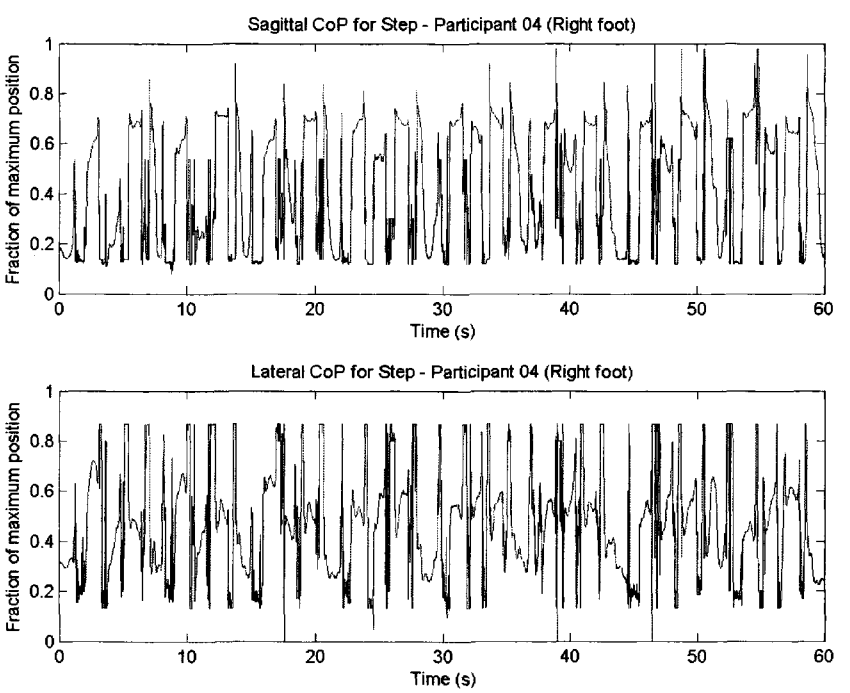

(b) Right Foot

Figure B.9: CoP for step task - Participant 04.

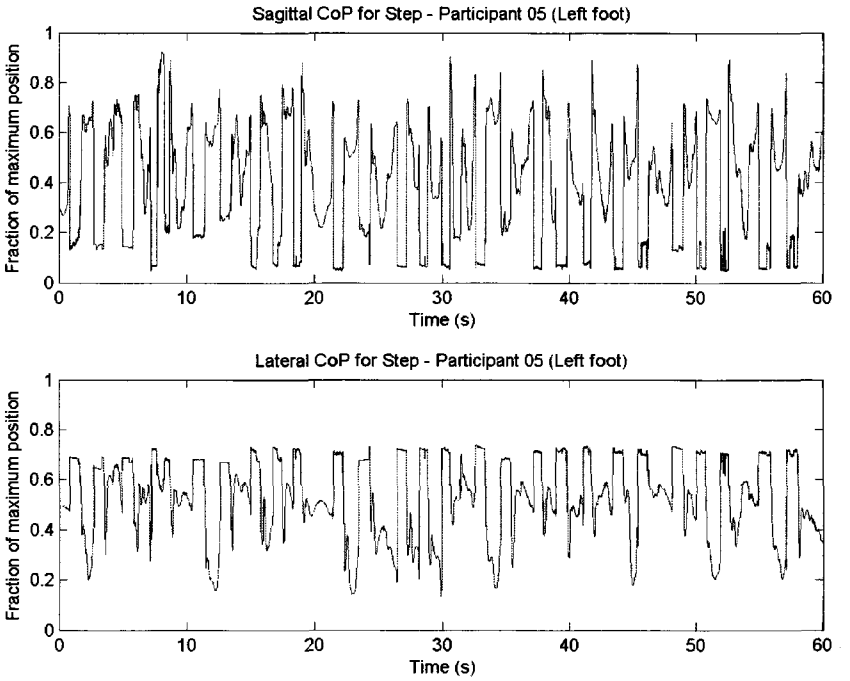

(a) Left Foot

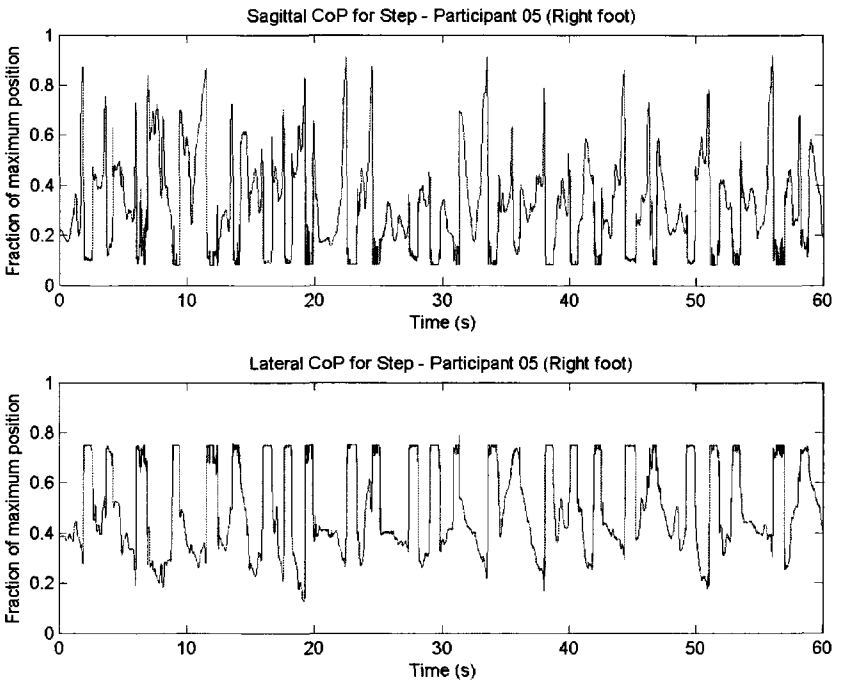

(b) Right Foot

Figure B.10: CoP for step task - Participant 05.

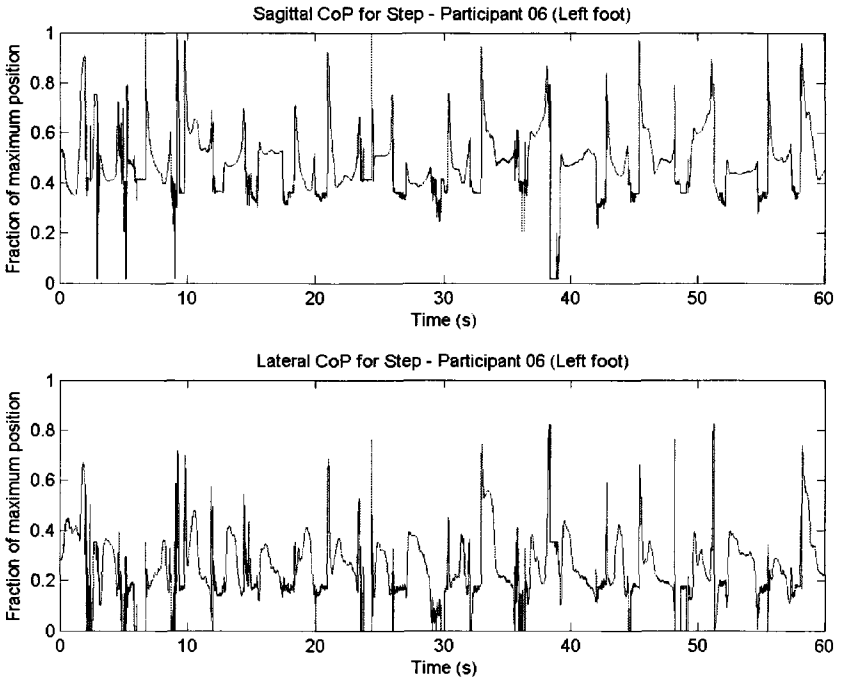

(a) Left Foot

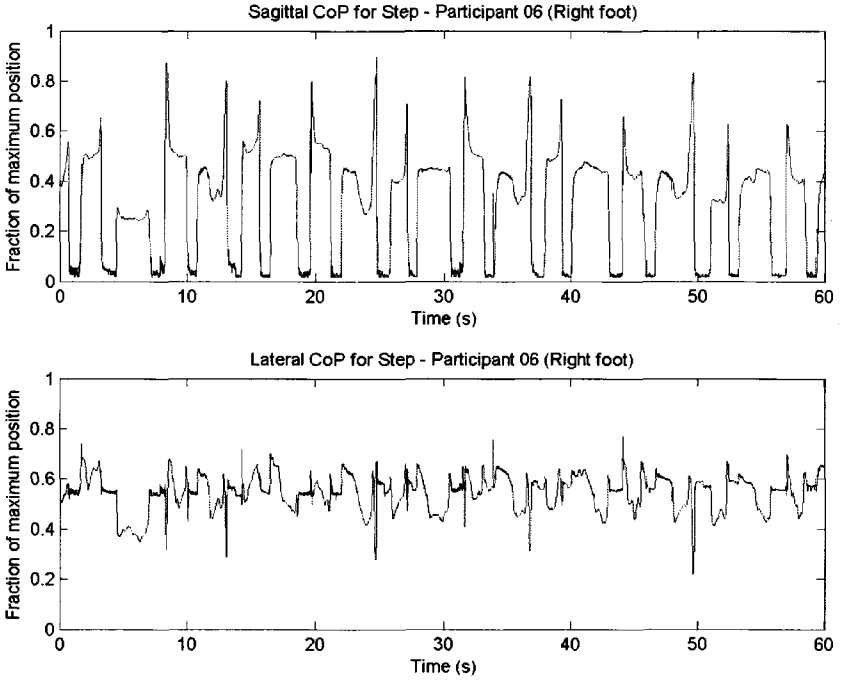

(b) Right Foot

Figure B.11: CoP for step task - Participant 06.

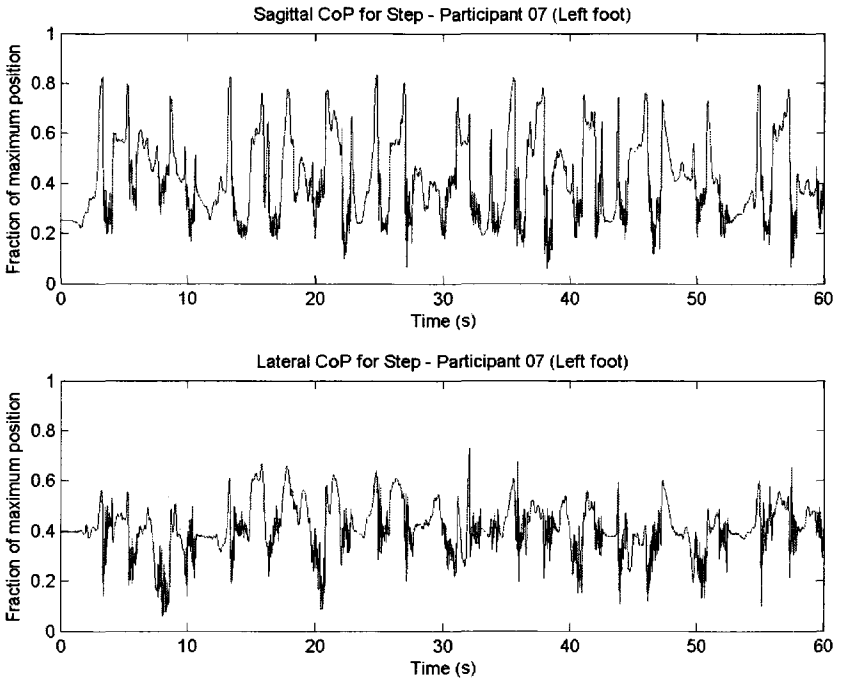

(a) Left Foot

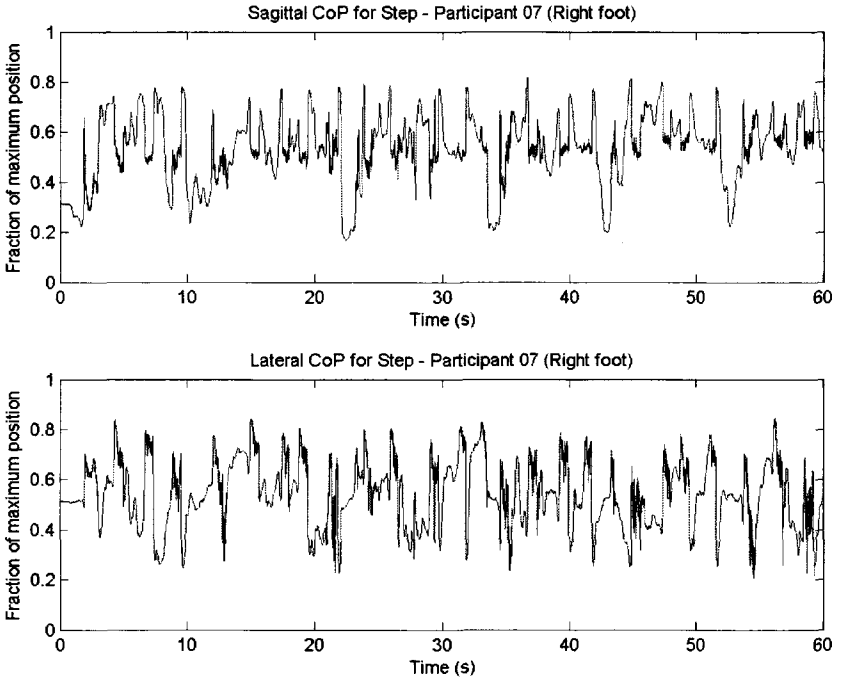

(b) Right Foot

Figure B.12: CoP for step task - Participant 07.